

WIMP dark matter candidates and searches – current status and future prospects

Leszek Roszkowski,^{a,b} Enrico Maria Sessolo^{c,a} and Sebastian Trojanowski^{d,a}

^a*National Centre for Nuclear Research,
Hoża 69, 00-681 Warsaw, Poland*

^b*Department of Physics and Astronomy, University of Sheffield,
Sheffield S3 7RH, United Kingdom*

^c*Institut für Physik, Technische Universität Dortmund,
D-44221 Dortmund, Germany*

^d*Department of Physics and Astronomy, University of California, Irvine,
California 92697, USA*

E-mail: leszek.roszkowski@ncbj.gov.pl, enrico.sessolo@ncbj.gov.pl,
sebastian.trojanowski@ncbj.gov.pl

ABSTRACT: We review several current aspects of dark matter theory and experiment. We overview the present experimental status, which includes current bounds and recent claims and hints of a possible signal in a wide range of experiments: direct detection in underground laboratories, gamma-ray, cosmic ray, X-ray, neutrino telescopes, and the LHC. We briefly review several possible particle candidates for a Weakly Interactive Massive Particle (WIMP) and dark matter that have recently been considered in the literature. We pay particular attention to the lightest neutralino of supersymmetry as it remains the best motivated candidate for dark matter and also shows excellent detection prospects. Finally we briefly review some alternative scenarios that can considerably alter properties and prospects for the detection of dark matter obtained within the standard thermal WIMP paradigm.

*UCI-HEP-TR-2017-09
DO-TH 17/15*

Contents

1	Introduction	2
1.1	Evidence for dark matter	3
2	WIMPs as dark matter	6
2.1	General properties	6
2.2	Production mechanisms	7
2.2.1	DM production from freeze-out	8
2.2.2	Other WIMP production mechanisms	10
2.3	Examples of WIMP candidates	12
3	Experimental situation	15
3.1	Direct detection: limits and anomalies	15
3.2	Gamma rays: limits and Galactic Center excess	20
3.3	Interlude: WIMP reconstruction from direct detection and gamma rays	27
3.4	Cosmic rays: limits and AMS02/Pamela	29
3.5	Neutrinos: limits and anomalies	30
3.6	X-rays: limits and the 3.5 keV line	32
3.7	LHC mono-X searches	32
4	The neutralino WIMP as DM	34
4.1	Brief review of supersymmetry and the neutralino as dark matter	34
4.2	Neutralino relic abundance	37
4.2.1	Coannihilations	37
4.2.2	Funnels	38
4.2.3	Other mass patterns	38
4.3	Simplest models defined at the GUT scale: the CMSSM and the NUHM	39
4.3.1	Implications of the Higgs boson for SUSY breaking scale	40
4.3.2	Neutralino DM in unified models in light of LHC and other recent data	41
4.3.3	Prospects for WIMP searches in GUT-constrained models	43
4.4	The pMSSM	44
4.5	Going beyond standard assumptions	47
4.5.1	Multi-component DM	48
4.5.2	Low reheating temperature	49
5	Summary and conclusions	50

1 Introduction

One of the most important quests of contemporary physics is to understand the nature of dark matter (DM) in the Universe. The long-held paradigm is that most DM is cold (CDM) and is made up of some weakly interacting massive particles (WIMPs). The WIMP solution to the DM problem remains attractive for a number of reasons. Firstly, WIMPs arise naturally in a large number of theoretically well-motivated models. Secondly, for reasonable ranges of WIMP mass and annihilation cross section the relic abundance of DM can be obtained through the robust mechanism of thermal freeze-out, possibly augmented with some other production mechanisms. Lastly, thermal WIMPs represent a promising target for DM experiments because a large fraction of their typical detection rates are within reach of current or planned detectors, making them testable by experiment.

We note that the concept of a WIMP as used in the literature is somewhat ambiguous. In general it encompasses a broad category of hypothetical candidates coming from specific theoretical scenarios, or their classes. In general it includes any non-baryonic massive particle (even with a very tiny mass) that interacts with any interaction that is either weak or sub-weak (e.g., axionic, gravitational). In a more commonly used sense, WIMP refers to a particle with mass in the range from about 2 GeV (the so-called Lee-Weinberg bound)¹ up to some 100 TeV (a rough unitarity bound [2]), whose interactions are set basically by the weak interaction coupling of the Standard Model, although strongly suppressed, as otherwise one would run into conflict with upper limits on its detection cross section.

In this topical review we will focus on the latter, “proper” WIMP category, and will cover the present status of some of the most popular and robust WIMP candidates and prospects for their detection. To this end we will also briefly survey the current experimental search situation, focusing in particular on several recent claims, or hints, of measuring a DM signal.

The field of dark matter is very broad and remains an arena of intense research both on the theoretical and experimental sides. Its various aspects have been covered in a number of review articles and here we mention but some of them. Observational evidence for dark matter can be found, e.g., in [3, 4]. Many WIMP particle candidates and prospects for their detection have been covered in several papers, starting from the early comprehensive review [5] (which, nearly thirty years later, still remains a very useful classic reference) and more recently in [6–9] and [10] which, although mostly devoted to non-standard WIMPs, like axinos and gravitinos, in the first chapter contains a summary of the current views on WIMPs from a particle physics perspective. References [11, 12] provide a recent succinct update on indirect detection aspects of WIMP searches.

The review is organized as follows. In the remainder of this Section we briefly summarize observational arguments for DM. Next, in Sec. 2 we present the case for the WIMP solution to the DM puzzle. We start by outlining some general properties of WIMPs (Subsec. 2.1), then discuss its production mechanisms in the early Universe (Subsec. 2.2) and finally (Subsec. 2.3) comment on several specific WIMP candidates that have recently been discussed in the literature – the purpose of this is to provide a broader perspective on the

¹The bound was actually derived by more authors. For more references, see [1].

current speculations about particle candidates for DM. In Sec. 3 we turn to the experimental searches and briefly review the current situation both in direct detection (DD) in underground searches (Subsec. 3.1) and (Subsecs 3.2 – 3.6) in several modes of indirect detection (ID), focusing in particular on some recent claims of DM detection. Finally, in Subsec. 3.7, we summarize the searches for DM-like particles at the LHC. We devote Sec. 4 to the arguably most popular WIMP candidate, the lightest neutralino of supersymmetry (SUSY) by reviewing and updating its properties and prospect for detection in light of recent progress in DM searches and also of SUSY searches and Higgs boson discovery at the LHC. While most of the Section deals with well known SUSY frameworks and standard assumptions, we conclude it by presenting some recent works on relaxing them and discuss ensuing implications. In Sec. 5 we provide a summary and outlook.

1.1 Evidence for dark matter

Over the last decades observational evidence for the existence of large amounts of DM in the Universe has been steadily mounting, and is well now described in several reviews [3, 4]. Here we merely briefly summarize some of the better known arguments.

The first claim about the existence of DM is usually attributed to Zwicky’s original paper on the Coma Cluster [13].² The cluster consists of more than a thousand galaxies. Careful analysis of the movement along their gravitational orbits led to the conclusion that there should be a large amount of non-luminous matter contained in the cluster. Zwicky referred to it as “dunkle Materie” (dark matter) and apparently thought it was just ordinary matter in a non-shining form.

One of the most widely recognized arguments for the existence of DM is based on galaxy rotation curves, i.e., the relation between orbital velocity and radial distance of visible stars or gas from the center of a galaxy. It was first noted in the late 1930s that the outer parts of the M31 disc were moving with unexpectedly high velocities [18], an observation that was then confirmed more than thirty years later [19, 20]. According to these observations the velocities of distant stars in M31 remain roughly constant over a wide range of distances from the center of the galaxy, in contradiction with expectations based on the distribution of visible matter in the galaxy. Similar results were later obtained [21] for various other spiral galaxies.

The existence of DM is also supported by data coming from gravitational lensing. Gravitational lensing, or the bending of light in a strong gravitational field (for a review see, e.g., [22]), is most easily observed when light passes through a very massive and/or dense object, like a galaxy cluster or the central region of a galaxy. Light rays can bend around the object, or lens, leading to a distortion of the image of the light source, as can be seen in Fig. 1(a). This effect is commonly known as strong lensing. The size and shape of the image can be used to determine the distribution of mass in the lens which can then be compared with the visible mass.

When the lens is not as massive as in the case of strong lensing, or when light travels far from the core of the galaxy or cluster, the effect is much weaker. However, it can still

²Earlier speculations were made by Kapteyn [14], Oort [15] and Jeans [16]. For a historical development, see [17].

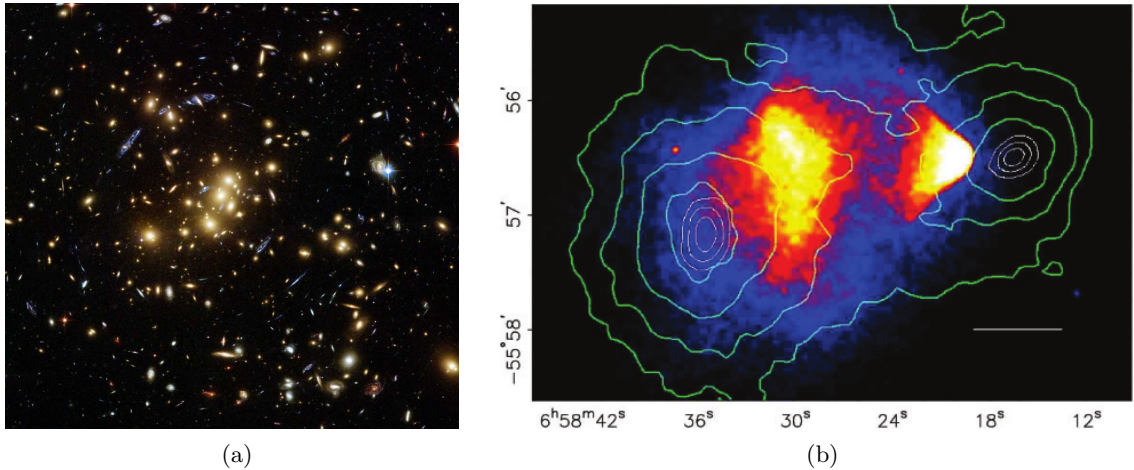


Figure 1: (a) Strong gravitational lensing around galaxy cluster CL0024+17. Taken from Ref. [22]. (b) Bullet Cluster mass density contours (green) and the distribution of baryonic matter. Taken from Ref. [23].

be analyzed even in the case of individual stars. Microlensing effects of this kind were proposed [24, 25] to look for DM in the Milky Way in form of Massive Compact Halo Objects (MACHOs), which should cause an occasional brightening of stars from nearby galaxies. This strategy led to an exclusion of MACHOs with masses in the range 0.6×10^{-7} to $15M_{\odot}$ as the dominant form of DM in the Galaxy [26].

Perhaps the most spectacular argument for the existence of dark matter in clusters can be found in the Bullet Cluster. It consists of two clusters of galaxies which have undergone a head-on collision [23]. The hot-gas clouds (observed through their X-ray emission) that contain the majority of the baryonic mass in both clusters have been decelerated in the collision while the movement of the galaxies and the dark matter halos in clusters remained almost intact. Analysis of the gravitational lensing effect shows that the center of mass for both clusters is clearly separated from the gas clouds, as can be seen in Fig. 1(b). One can thus infer the presence of a large amount of additional mass in both clusters. The Bullet Cluster is the first known example of a system where the dark matter and the baryonic component have been separated from each other.

Studies of weak gravitational lensing of large scale structures (LSS) provide further evidence for DM. In this context the effect is usually called cosmic shear. It causes systematic distortions of the positions of distant galaxies, though the impact is very subtle ($\sim 0.1\% - 1\%$). Tangential shear is usually analyzed in terms of two-point (or even three-point) correlation functions that on the other hand can be related to the DM mass density correlation functions. The latter quantity is a Fourier transform of the matter power spectrum and can be used to determine the matter density (both ordinary and dark) of the Universe; see, e.g., [27].

Last but not least, a crucial role in determining the DM abundance in the Universe is played by studies of cosmic microwave background (CMB) radiation. The CMB radiation seen today originates from the decoupling and recombination epoch. Small inhomogeneities

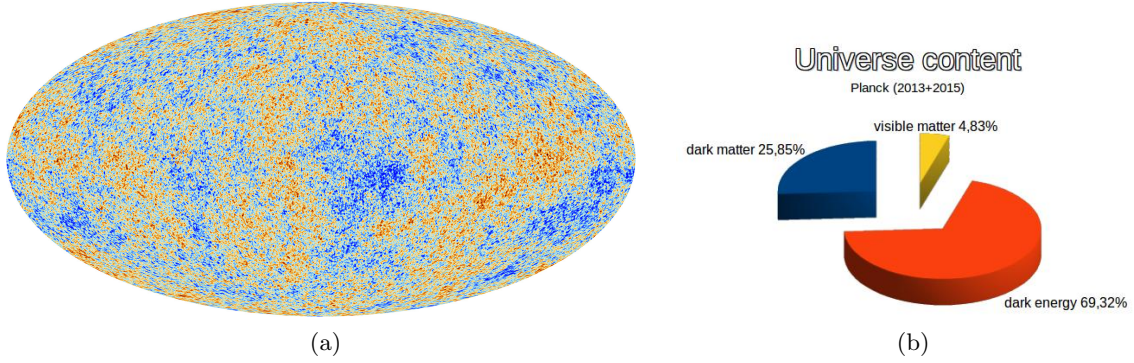


Figure 2: (a) Temperature anisotropy of the CMB after the first results released by the Planck Collaboration [29]. (b) Total mass-energy distribution in the Universe.

in the distribution of its temperature correspond to fluctuations of the matter density in the early Universe that subsequently gave rise to the observed large structures. The power spectrum of temperature anisotropies (see Fig. 2(a)) when expanded in terms of spherical harmonics depends on cosmological parameters can then be obtained by fitting the resulting spectrum, with some underlying assumption of cosmological model, e.g., the Λ CDM model.

The current values [28] of the relic abundance, that is the ratio of the density to the critical density, of baryonic matter Ω_b , and the corresponding quantity for the non-baryonic DM component, Ω_{DM} that were obtained by WMAP and more recently by PLANCK by fitting the six-parameter Λ CDM model are:

$$\Omega_b h^2 = 0.02226(23), \quad (1.1)$$

$$\Omega_{\text{DM}} h^2 = 0.1186(20), \quad (1.2)$$

where $h = H_0/100 \text{ km Mpc s} = 0.678(9)$ [28] is the reduced Hubble constant, with H_0 denoting the Hubble constant today.

The remaining dominant contribution, $\Omega_\Lambda \approx 0.692$, accounts for the so-called dark energy (for a recent review see, e.g., [30, 31]). A schematic cartoon showing different contributions to the mass-energy content of the Universe is shown in Fig. 2(b).

Further information about the amount of matter and dark energy components of the Universe can be derived from analyses of baryon acoustic oscillations (BAO, periodic fluctuations in the density of baryonic matter that originated from the opposite effects of gravitational attraction and radiation pressure), supernovae type Ia, or from the Lyman- α forests (neutral hydrogen clouds seen in absorption in quasar spectra). In the case of elliptical galaxies and galaxy clusters another important piece of evidence for the existence of DM comes from the X-ray emission from hot gas (for further discussion see, e.g., [4]).

2 WIMPs as dark matter

2.1 General properties

One clear conclusion about DM that one can draw from observational evidence is that DM is made up of some particles should be electrically neutral.³ DM should interact with ordinary matter preferably only weakly (or sub-weakly), where weak can be taken to mean interacting via the weak nuclear force or just having a (sub)weak but non negligible coupling to the Standard Model particles.

Dark matter self-interactions cannot be too strong in order to be compatible with constraints on structure formation and observations of galaxy cluster systems such as the Bullet Cluster with current limits of order $\sigma/m < 0.7\text{cm}^2/\text{g}$ [36]. Note, however, that this limit can be satisfied even for strongly interacting dark matter (SIMP) with $\alpha_\chi \sim 1$ in the dark sector and the correct relic density obtained thanks to DM mass-dependent $3 \rightarrow 2$ processes [37]. Moreover, to be in agreement with CMB data, most of the DM should be non-baryonic in nature.

It has been suggested that DM could be made up of primordial black holes (PBHs) [38] which, if formed before the period of Big Bang Nucleosynthesis (BBN) would not violate determinations of ordinary matter abundance, thus weakening the argument for the need of non-baryonic DM today. The idea of PBHs as DM has recently been revived with a suggestion that the first detection of gravitational waves by LIGO [39] could be potentially explained in terms of two coalescing PBHs [40]. However, there are many limits on PBHs as DM; see [41, 42].

One simple classification of DM particles is based on how relativistic they are around the time when they fall out of thermal equilibrium in the early Universe, i.e., when they decouple from thermal plasma. Hot dark matter (HDM) in the mass range of up to a few tens of eV, which was still relativistic at the time of decoupling, due to large mean free path did not cluster to form clumps as small as galaxies, and does it reproduce the observed Universe in numerical simulations of LSS formation (see, e.g., [43]). It is incompatible with data from the LSS [44–46] and deep-field observations [47, 48], which constrain the allowed average velocity of the DM particles from above. For these reasons, HDM can only contribute a small fraction, determined by the properties of the CMB, of the total DM density. A familiar (and known to exist) example of possible HDM is neutrinos with a tiny mass.

In contrast, cold dark matter (CDM) behaves very differently. Non-baryonic CDM decoupled from thermal plasma at freeze-out and its density perturbations started growing linearly at the onset of the epoch of matter dominance. This provided early potential wells (seeds), thus triggering and catalyzing the growth of the density perturbations of baryonic matter after it decoupled from radiation some time later. This is the basic reason why CDM generally proves successful in reproducing observations in numerical simulations

³One should not forget that in principle the DM puzzle could be explained in terms of something else than particles but such approaches suffer from problems. This includes modifying gravity (MOND) [32] which still needs to invoke DM in order to explain all data [33], or cosmic fluid [34] which is also increasingly challenged by observations, see, e.g., [35].

of LSS, despite well known problems with potentially predicting too few substructures (missing satellites problem) [49, 50] or too dense regions towards the center of the largest DM subhalos obtained in simulations when comparing to the brightest observed dwarf satellite galaxies (too-big-to-fail problem) [51, 52] (for recent review see, e.g., [53]). Cold DM, as opposed to warm or hot DM is also preferred by the properties of the CMB.

Warm dark matter (WDM), in the mass range of a few keV, is a possible form of DM which is intermediate between HDM and CDM. It was still relativistic at the time of decoupling but fluctuations corresponding to sufficiently large halos would not be damped by free streaming. It has been considered as a possible way of ameliorating some apparent problems of CDM, because it reduces the power spectrum on small scales, thus reducing the missing satellite problem of CDM [54] although this has been disputed. It has been claimed, however, that WDM leads to some other problems [55]: the cutoff in the power spectrum $P(k)$ at large wavelength k implied by WDM will also inhibit the formation of small dark matter halos at high redshift. But such small halos are presumably where the first stars form, which produce metals rather uniformly throughout the early Universe as indicated by observations of the Lyman-alpha forests. An almost sterile neutrino with the mass of a few keV is a popular candidate for WDM. One has to note, though, that such sterile neutrinos are produced in the early Universe being not in thermal equilibrium, hence their effect on the structure formation needs to be studied in detail before drawing robust conclusions (for a recent review see [56]).

An array of these and related arguments have led to establishing a popular (and sensible) paradigm that the dominant fraction of DM is probably cold and that it should be not only (sub)weakly interacting but also non-relativistic and massive, or in short, it is made up of WIMPs. Finally, the DM particles should be either absolutely stable, or extremely long lived (for instance, a recent analysis finds a lower bound of 160 Gyr [57]). This is as much as we can be fairly confident about the nature of DM.

Non-WIMP DM candidates (for a recent review see [10]) have also been vastly explored in the literature. Among them one can distinguish an ultralight axion that emerges from the solution to the strong CP problem. Axion DM can closely resemble CDM when axions, upon thermalization, form a Bose-Einstein condensate with the energy density determined by the mechanism of bosonic coherent motions. Another interesting scenario is to consider extremely weakly interacting massive particles (EWIMPs) as DM candidates. Such weak interactions can naturally appear, e.g., if they are described by non-renormalizable operators suppressed by some high energy scale, e.g., the Planck mass, $M_P \approx 10^{18}$ GeV, as it is in the case of gravitino DM [58–63] or the Peccei-Quinn scale, $f_a \approx 10^{11} - 10^{12}$ GeV, for the axino DM [64, 65].

2.2 Production mechanisms

One property of CDM that is now very precisely established is its cosmological relic abundance – compare Eq. (1.2) – and the fact that it has been derived from the properties of CMB at the time of recombination or from baryonic acoustic oscillations at the earlier time after (dark) matter dominance started suggest that DM was indeed produced in the early Universe. Big Bang nucleosynthesis also place limits on the production of DM from decays

during the BBN epoch [66–68]. It is generally assumed that the bulk of dark matter in the Universe was produced between the end of inflation (actually, reheating) and some time before BBN.

Several mechanisms for generating sufficient amounts of DM in the early Universe have been identified and will be briefly reviewed below.

2.2.1 DM production from freeze-out

The most robust mechanism for generating the WIMP DM relic abundance is the so-called freeze-out mechanism. In the very early and hot Universe SM species and DM were in thermal equilibrium, with DM particle production from annihilations balancing each other out. As the Universe expanded and cooled, WIMPs eventually froze out of equilibrium with the thermal plasma. This decoupling happened when the WIMP annihilation rate became roughly less than the expansion rate of the Universe $\Gamma_{\text{ann}} \lesssim H \sim T_f^2/\bar{M}_P$, where T_f stands for the freeze-out temperature (the index f indicates that quantities are evaluated at the freeze-out time) and \bar{M}_P is the reduced Planck mass. After freeze-out the WIMP yield, $Y_\chi = n_\chi/s$, where n_χ (denoting here generic WIMPs with the symbol χ) is the number density of DM particles and $s \sim T^3$ is the entropy density, remained mostly constant.

Given the annihilation rate, $\Gamma_{\text{ann}} = n_\chi \langle \sigma_{\text{ann}} v \rangle$, one can rewrite the formula for today’s value of the DM relic abundance in terms of the thermally averaged product of annihilation cross section σ_{ann} and the Møller velocity, $v_{\text{Møll}} = \sqrt{(\vec{v}_1 - \vec{v}_2)^2 - (\vec{v}_1 \times \vec{v}_2)^2}$, at freeze-out [69],

$$\Omega_\chi h^2 \simeq \frac{m_\chi n_\chi(T_0)}{\rho_c} h^2 = \frac{T_0^3}{\rho_c} \frac{x_f}{\bar{M}_P} \frac{1}{\langle \sigma_{\text{ann}} v_{\text{Møll}} \rangle_f} h^2, \quad (2.1)$$

where $T_0 \approx 2.35 \times 10^{-13}$ GeV [70] is the temperature of the Universe at present, $\rho_c \approx 8 \times 10^{-47} h^2 \text{ GeV}^4$ [70] is the critical energy density, $x = m_\chi/T$ and $\vec{v}_{1,2}$ are the velocities of both annihilating DM particles. Note that Møller velocity is equal to the relative velocity of two DM particles $|\vec{v}_1 - \vec{v}_2|$ in the center-of-mass frame.

The value of x_f can be roughly estimated by assuming that around freeze-out the number density of WIMP DM is equal to the non-relativistic equilibrium number density $n_\chi \approx n_{\chi,\text{eq}} \simeq g_\chi (m_\chi T/2\pi)^{3/2} \exp(-m_\chi/T)$, where g_χ is the number of degrees of freedom for the DM particles. Using $\Omega_\chi h^2 \approx 0.12$ one then obtains

$$x_f^{3/2} e^{-x_f} \approx \frac{10^{-8} \text{ GeV}}{m_\chi}. \quad (2.2)$$

This leads to $x_f \approx 30$ for $m_\chi \approx 100 \text{ GeV} - 10 \text{ TeV}$. More careful analysis shows that the appropriate value is closer to $x_f \approx 25$ [71].

Finally we put the estimated value of x_f back into Eq. (2.1) and find

$$\langle \sigma_{\text{ann}} v \rangle_f \approx 3 \times 10^{-26} \text{ cm}^3/\text{s}, \quad (2.3)$$

for which the correct value of the WIMP DM relic density is obtained (see [72] for a more detailed study). For typical velocities $v \approx 0.1 c$ one obtains a cross section of weak strength for WIMP with mass around the electroweak scale. In the early days, this coincidence was found so remarkable that it was coined as the “WIMP miracle”.

However, subsequent developments showed that the situation may well be much more complex. A critique of the “WIMP miracle” can be found in Ref. [10]. Here we merely mention that in specific well motivated cases the relic abundance can often be different from 0.12 by several orders of magnitude. For instance, for the neutralino DM of SUSY one typically finds $\Omega_\chi h^2$ well in excess of the correct value, as will be discussed in Sec. 4. It is also important to note that WIMP DM particle mass is not necessarily confined to the electroweak scale. An argument based on unitarity gives a generous upper bound on thermal relic mass of the order of 100 TeV [2]. Furthermore, on dimensional grounds, and for simplicity assuming that WIMP mass m_χ is the only relevant scale, one expects

$$\sigma_{\text{ann}} \propto \frac{g^4}{m_\chi^2}, \quad (2.4)$$

where g is a coupling constant responsible for the WIMP annihilation process. One can see that Eq. (2.3) can be then satisfied for a wide range of masses (from 10 MeV to 10 TeV) and a wide range of coupling constant values (from gravitational to strong) as long as their ratio is kept fixed [10, 73]. Even more freedom can be achieved in a more realistic scenario in which DM-SM mediator mass and its coupling constants to the SM appear in the annihilation cross section.

In a precise treatment, which takes into account the dynamics of freeze-out, the DM yield after freeze-out is found by solving the respective set of Boltzmann equations:⁴

$$\frac{d\rho_R}{dt} = -4H\rho_R + \langle\sigma_{\text{ann}}v\rangle\langle E\rangle(n_\chi^2 - n_{\chi,\text{eq}}^2), \quad (2.5)$$

$$\frac{dn_\chi}{dt} = -3Hn - \langle\sigma_{\text{ann}}v\rangle(n_\chi^2 - n_{\chi,\text{eq}}^2), \quad (2.6)$$

where ρ_R is the radiation energy density and $\langle E\rangle$ is the average energy of annihilating DM particles. As can be deduced from Eq. (2.6) (and even more evidently seen from a simplified solution (2.1)), the larger is $\langle\sigma_{\text{ann}}v_{\text{Mol}}\rangle$ at freeze-out the longer WIMPs χ stay in thermal equilibrium and therefore the lower relic abundance $\Omega_\chi h^2$ one obtains.

One should mention here the related thermal mechanism of coannihilation [75]. If there is some other particle χ' in thermal equilibrium, nearly degenerate in mass with the DM WIMP χ , and such that it annihilates with χ more efficiently than χ with itself, then it is the mechanism of coannihilation that primarily determines the relic density of dark matter. A more detailed discussion of coannihilation is postponed to Subsec. 4.2.1, where we apply it to the case of the neutralino of supersymmetry. It is worth mentioning, though, that the mass degeneracy between χ and χ' can not only lead to the decrease but also to the increase of the final DM relic density. This can happen when χ' can freeze-out before decaying completely into the DM particles, with a larger yield than that of χ , and subsequently decay to χ .

⁴One assumes here Majorana DM particles. For Dirac particles there should appear an additional factor of two in the second term on the r.h.s. of Eq. (2.5). However this plays a negligible role in determining the DM relic density; see, e.g., [74]. In practice one usually neglects the second term on the r.h.s. of Eq. (2.5), which leads to $\rho_R a^4 \sim \text{const}$, where a is the scale factor. This condition, along with the Friedmann equation in the radiation dominated epoch, sets the temperature dependence on time when solving Eq. (2.6).

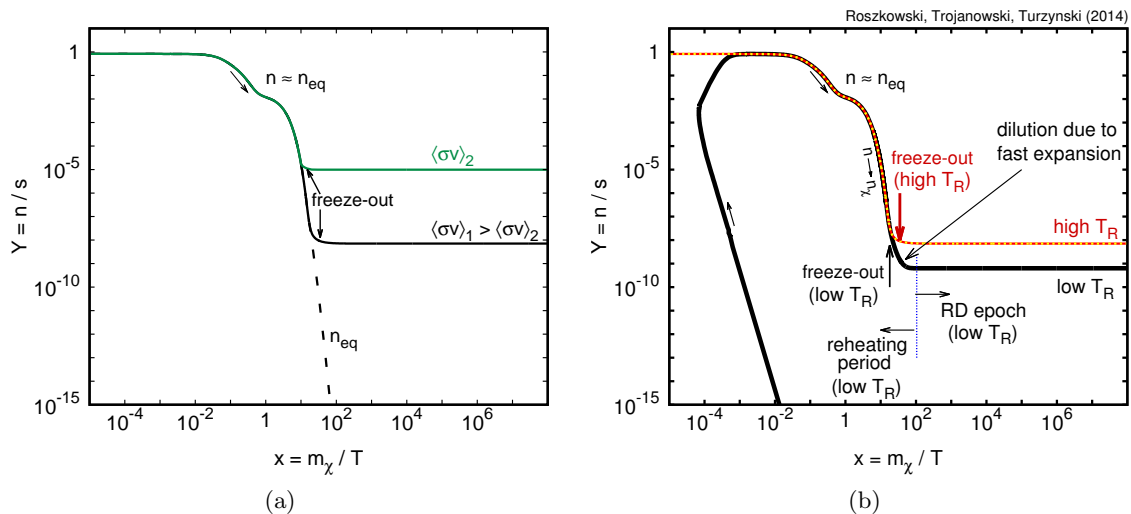


Figure 3: The DM yield, Y , as a function of $x = m_\chi/T$ for a standard freeze-out scenario. (b) Similar plot for a scenario with low reheating temperature (black solid line) compared with a standard case (high reheating temperature; indicated by dotted red-yellow line). The beginning of the RD epoch for the low T_R scenario is denoted by vertical dotted blue line. Taken from Ref. [77].

2.2.2 Other WIMP production mechanisms

Even though the freeze-out mechanism always contributes to the WIMP DM abundance, in order to be the dominant process a fairly specific range of $\langle\sigma_{\text{ann}}v_{\text{Mø}}\rangle$ at freeze-out is required. However, several other modes of WIMP production exist which can still lead to the correct $\Omega_\chi h^2$ even when this condition is not satisfied. Here we will merely mention some such mechanisms and their specific implementations. A more general and exhaustive discussion can be found in Sections IV and V or Ref. [10].

First, however, let us mention the situation when $\langle\sigma_{\text{ann}}v_{\text{Mø}}\rangle_f$ is too low in which case freeze-out occurs too early and the final relic density of DM may become too large. In such a case the DM relic density must be reduced. This can be achieved by an additional entropy production from out-of-equilibrium decays of some heavy species that occur between the time of the DM freeze-out and BBN which marks the epoch of standard cosmological expansion. In particular such heavy particles could dominate the energy density of the Universe during the period of reheating, i.e., before the radiation dominated (RD) epoch (for a discussion see [1, 76]). If the reheating temperature T_R , i.e., the temperature at which the RD epoch begins, is lower than the DM freeze-out temperature, T_f , the additional entropy production due to, e.g., decays of an inflaton or moduli fields, can effectively dilute away thermally overproduced DM particles. See Fig. 3(b) and Section 4.5.2 for a discussion about neutralino DM.

If $\langle\sigma_{\text{ann}}v_{\text{Mø}}\rangle$ is so low that χ particles never reach thermal equilibrium after reheating then they actually never freeze out. In this category of EWIMPs,⁵ DM relics can be

⁵They are also called super-WIMPs [279] or FIMPs [78] (feebly interacting massive particles, although the name of frozen-in massive particles would perhaps be more appropriate [10]) in this case. See also a

produced through at least one of two, distinct but not mutually exclusive, mechanisms. Firstly, some heavier particle can first freeze out and then decay into EWIMPs. Note that in this case the resulting number density of DM is still determined at freeze-out. Alternatively, EWIMPs can be produced in scatterings or decays of some heavier particles in the thermal plasma. The production of EWIMPs from decays is most efficient at lower temperatures, $T \sim m$, just before the Boltzmann suppression kicks in. The production through scatterings is not accompanied by a reverse process which is too inefficient due to low cross sections. In the case of non-renormalizable interactions – typical for gravitinos and axinos – the process is typically more efficient at high temperatures, near the reheating temperature T_R . When interactions are renormalizable, scatterings continuously contribute to the DM relic density until the temperature drops down below a certain value. This has recently been advocated under the name of so-called freeze-in mechanism [78], as the final yield increases with $\langle\sigma_{\text{ann}}v_{\text{Møl}}\rangle$. Note, however, that, strictly speaking, freeze-in is not a new mechanism of DM production but simply refers to a certain type of particle physics interactions that is responsible for generating DM.

Both mechanisms are different from the standard picture based on freeze-out, and both can be efficient, depending on some other quantities (e.g., the DM particle mass or the reheating temperature T_R). This greatly relaxes the standard thermal WIMP paradigm, as has been shown in the case of axinos [64, 65, 80] (for a recent review see [81]) and gravitinos [59, 62, 63] both of which belong to the class of EWIMPs.

In contrast, if $\langle\sigma_{\text{ann}}v_{\text{Møl}}\rangle_f$ is larger than the canonical value from Eq. (2.3), then the thermal yield of WIMPs is too low to produce the DM relic abundance. The DM particles can be additionally produced in late-time decays (after DM freeze-out) of some heavier species. Examples include moduli field (see [82, 83] and references therein), Q-balls (see, e.g., [84]), the inflaton field (see, e.g., [85]) or cosmic strings [86]. Such a non-thermal production of DM is often associated with the aforementioned additional entropy production that also partially reduces the increase of $\Omega_\chi h^2$. As mentioned above, late-time decays can also occur for another species χ' , almost mass degenerate with the DM particles. In principle, coannihilations reduce both Y_χ and $Y_{\chi'}$. However, it is possible that the yield of χ' after freeze-out is larger even than the yield of χ calculated in absence of any mass degeneracy. In this case the final DM relic density can be increased with respect to the non-degenerate scenario.

In the (partially) asymmetric DM (ADM) scenario [87, 88] one can accommodate an otherwise too low $\Omega_\chi h^2$ by assuming that one component of the DM relic density from freeze-out is accompanied by one which is set by an initial asymmetry between DM and their antiparticles, in a way analogous to the mechanism of baryogenesis. It is worth noting that, since in the ADM scenario the DM is not its own antiparticle and the abundance of χ and $\bar{\chi}$ particles can be highly asymmetric nowadays, the expected indirect detection rates from $\chi\bar{\chi}$ annihilations are typically suppressed with respect to, e.g., Majorana DM. A more detailed discussion can be found in, e.g., Ref. [89].

Among various other possible ways to deal with too large values of $\langle\sigma_{\text{ann}}v_{\text{Møl}}\rangle_f$ one

recent review [79].

should also mention an increased expansion rate of the Universe prior to, and around, the DM freeze-out due to a dynamics of the dark energy content of the Universe (see, e.g., [90] for a discussion for quintessence). This leads to an earlier decoupling of the χ particles and therefore larger $\Omega_\chi h^2$.

It is clear that the mechanism of freeze-out, while remaining attractive and robust, provides only one of several possible ways of generating WIMP relics in the early Universe. As we shall see later, this will have implications for prospects for DM searches.

2.3 Examples of WIMP candidates

To give a taste of the particle physics context of DM candidates, in this subsection we give examples of some specific WIMPs that either have withstood the test of time, or where there has been some fairly recent activity.

First, to give a wider context, we start with a broad brush picture of different classes of DM candidates that have emerged from particle physics. In Fig. 4, adapted from [10] (and originally from [91]), we show where different DM candidates lie in terms of their masses and typical detection cross section.⁶ The red, pink and blue colors represent HDM, WDM and CDM, respectively. Both axes span several orders of magnitude making clear that a large range of interaction strengths and masses become allowed by going beyond the thermal WIMP paradigm. Otherwise one would remain confined basically only to the light blue rectangle labeled “WIMP”. Such “proper”, or thermal, WIMPs have a larger interaction cross section than axions, axinos, gravitinos and sterile neutrinos making them a promising target for experiments. In contrast, neutrinos have a much larger cross section but would only constitute HDM which is disfavored, as discussed earlier.

Within this class of WIMPs from thermal freeze-out a large number of particle candidates for DM have been proposed in the literature, and new ones (sometimes in a reincarnated form) appear on a frequent basis. For one, this means that it is actually fairly easy to invent DM-like WIMPs. On the other hand, it is fair to say that, from the perspective of today’s (or foreseeable) experimental sensitivity, it would be very difficult to distinguish many (perhaps most?) of them from each other or from well established and popular candidates, like the lightest neutralino of SUSY. Furthermore, one should not forget that the underlying frameworks that predict many, if not most, of them, while interesting, very often lack a deeper or more complete theoretical basis and instead invoke some sort of “dark portal”. For instance, many such approaches lack a UV completion, do not address other serious questions in particle physics or cosmology, etc.

The lightest neutralino of low energy supersymmetric models has long been recognized as an attractive WIMP candidate for DM [93, 94]. It is the lightest mass state of a combination of the superpartners of the neutral gauge bosons and Higgs particles. The neutralino is characterized by a mass range from about 2 GeV to 10^4 GeV and can span a large range of the interaction cross section depending on its composition. The relic density and detection prospects of the lightest neutralino have been extensively studied in a large number of papers giving rise to several distinct scenarios. Since the neutralino remains by

⁶For another broad-range of DM candidates see Fig. 1 or Ref. [92].

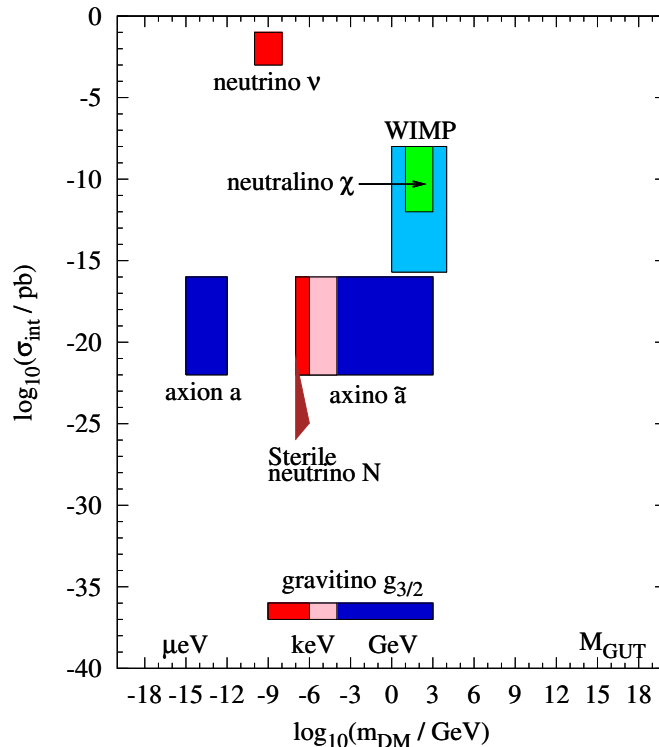


Figure 4: Typical ranges of the cross section of DM interactions with ordinary matter as a function of DM mass is shown for some of DM candidates that are strongly motivated by particle physics. The red, pink and blue colors represent HDM, WDM and CDM, respectively. Adapted from Ref. [10, 91].

far the most popular WIMP and detection cross section of many other candidates often fall into the ballpark of the case of the neutralino, we will devote to this case a detailed discussion, which we postpone to Section 4.

Two Higgs Doublet Models (2HDM) extend the Higgs sector by the addition of another doublet giving rise to additional charged and neutral Higgs bosons [95], see [96] for a review of 2HDM phenomenology. In the simplest extension, the inert doublet model (IDM) [97–99], a \mathbf{Z}_2 symmetry is imposed under which all the SM fields are even while the additional Higgs doublet is odd. The neutral additional Higgs boson states, H^0 or A^0 can then play the role of DM if one of them is the lightest odd particle. The DM couples to the SM via the Higgs boson leading to possible signals from spin-independent scattering in direct detection experiments. Alternatively the DM can be provided by an additional field coupled to the extended Higgs sector and stabilized by the \mathbf{Z}_2 see for example [100–102].

Little Higgs models represent a class of possible solutions to the naturalness problem [103–109] (see [110] for a comprehensive review). In little Higgs models the Higgs fields are the Goldstone bosons of global symmetry broken at the cut off scale. The Higgs becomes massive due to symmetry breaking at the electroweak scale, however, the mass is protected by the approximate global symmetry and is free from 1-loop corrections from the cutoff scale. This allows little Higgs models to remain natural with a cutoff scale of up

to 10 TeV. In little Higgs models new heavy states are introduced to act as partners of the top quark and gauge bosons, such that the divergences are cancelled at the 1-loop level. To have a DM candidate in little Higgs models there must be a remaining \mathbf{Z}_2 symmetry often called T-parity [111–113]. The new heavy partner fields are odd under the symmetry while the SM particles are even, this results in lightest partner field being stable. The DM candidate can come in the form of additional scalars which can be charged under $SU(2)$ or a singlet [114, 115]. Alternatively, little Higgs models can have extended gauge sectors with a heavy partner to the photon which can act as a WIMP giving an example of vector DM [112, 116, 117].

The *twin Higgs* mechanism [118–121] was introduced to solve the naturalness problem by positing a twin sector, which is a copy (or partial copy) of the SM related via a \mathbf{Z}_2 symmetry. The combined Higgs sector possesses an approximate $U(4)$ symmetry, and the lightest Higgs then comprises the pseudo-Goldstone boson of the broken $U(4)$. A WIMP DM candidate can arise in twin Higgs models as a member of the twin sector [122] see also [123, 124]. Alternatively the DM can form part of the scalar sector [125] with similar properties to the IDM. The twin DM couples to the Standard Model via the Higgs leading to a spin-independent scattering cross section that can be searched for with direct detection experiments [122–124]. Annihilation of twin DM can also produce indirect detection signals if it has a sizable annihilation fraction to SM states.

Sneutrinos are an example of a non-thermal WIMP. Sneutrinos are the scalar partners of the neutrinos in SUSY models. For the sneutrinos that were originally proposed as a DM candidate [126, 127] as partners of the SM left handed neutrinos, the spin-independent scattering cross section is generically of weak interaction strength and already firmly ruled out by direct detection experiments unless the sneutrino makes up only a subdominant component of the DM [128–130].

For sneutrino DM to be viable there must be either mixing between the sneutrinos partners of left handed neutrinos and those of the right handed neutrinos [130–134], or lepton violating mass terms that split the sneutrino eigenstates such that elastic scattering via the Z -boson is not possible [129, 135, 136]. Typically purely right-handed sneutrinos have too small coupling to the SM to be a WIMP candidate but may be a viable non-WIMP candidate; see for example [137]. The mixed left-right handed sneutrino DM has recently been reanalyzed in the context of constrained SUSY with updated LHC results in [138].

Models with compactified *universal extra dimensions* (UED) possess a DM candidate from the tower of Kaluza-Klein (KK) states. In these models SM particles can propagate in the new compactified dimension [139] and particles with quantized momenta in the new spatial dimension appear as heavier copies of the standard model particles and the lightest KK state is stable. The lightest KK state is often a heavy copy of the hypercharge gauge boson and can have the properties of a WIMP [140–143]. Run 1 of the LHC ruled out many of the minimal UED models; see [144, 145] for the status of minimal UED theories post LHC Run 1.

A plethora of other DM candidates exist in the literature and it is clear that it will be up to experiment to identify which of them (if any) is the choice made by Nature. It is also possible to study WIMP DM properties within a framework of generic portals between the

dark sector and the SM without specifying other contents of models that are not directly related to DM interactions (see [9] and references therein). Many such possibilities has been explored in the literature including scalar, fermion or vector DM (see, e.g., [146, 147]) with various kinds of mediators that can either belong to the SM, i.e., the Higgs or Z bosons, or can themselves belong to the hidden sector. Such an approach might have less predicting power than well-defined models described above. However, the advantage is that within this framework one can study DM-specific features of many definite models at a time and therefore derive more general conclusions. In particular, it can be checked that Z boson-portal models are already excluded by the current limits with the exception of the case of Majorana DM particles, while for the Higgs boson-portal the only allowed regions for $m_\chi \lesssim 1$ TeV can be obtained for the resonance scenario in which $m_\chi \approx m_h/2$ (see a discussion in [9]).

3 Experimental situation

For nearly three decades now the experimental search for DM has continued its intense activity and generally impressive progress that has led to several strongly improved bounds on WIMP interactions. At the same time, with improving sensitivity in some cases new effects have been identified which could be interpreted as caused by DM. We will pay attention to a possible WIMP (or WIMP-like) interpretation of these effects when in this section we make an updated survey of the current situation in several modes of DM searches.

3.1 Direct detection: limits and anomalies

One of the most important strategies to search for WIMP DM is its possible direct detection (DD) through elastic scatterings of DM particles off nuclei [148] (for reviews see, e.g., [149–152]). For WIMPs that interact efficiently enough with baryons this process can lead to a clear signature in low-background underground detectors. In order to distinguish a DM recoil signal from background, today’s detectors typically employ some methods of discrimination (see below). In some cases one looks for the annual modulation of the signal due to the Earth’s movement with respect to the DM halo [153] (for review see [154]). In addition, in the current and the next generation of the DD experiments effort is made to see further DM-specific features in the nuclear recoil energy distribution due to a possible directional detection [155] (for review see [156]).

Formalism An evaluation of a DM event rate in DD experiments necessarily involves factors from particle physics and nuclear physics, as well as from astrophysics. This can be seen from the formula for the differential recoil event rate⁷ as a function of the recoil energy E_r

$$\frac{dR}{dE_r}(E_r) = \left(\frac{\sigma_0}{2\mu^2 m_\chi} \right) \times F^2(E_r) \times \left(\rho_\chi \int_{v \geq v_{\min}}^{v \leq v_{\text{esc}}} d^3v \frac{f(\mathbf{v}, t)}{v} \right), \quad (3.1)$$

⁷Note that for directional detection one needs to consider a double differential rate that takes into account the dependence on the recoil angle (see [156]). Higher order corrections to the differential event rate can be found in [157].

where σ_0 is the DM-nucleus scattering cross section in the zero momentum transfer limit, m_χ is the DM mass, $\mu \equiv m_\chi M / (m_\chi + M)$ is the reduced mass of the WIMP-nucleus system for nucleus of mass M , $F(E_r)$ is the nuclear form factor of the target nucleus, ρ_χ is the local DM density and v is the relative velocity of DM particle with respect to the nucleus, while $f(\mathbf{v}, t)$ denotes the distribution of the WIMP velocity with cut-off at the galaxy escape velocity v_{esc} . The minimum velocity that can result in an event with the recoil energy E_r is given by $v_{\text{min}} = (\delta + ME_r/\mu) / \sqrt{2M E_r}$, where $\delta = 0$ for elastic scatterings.

Since DM WIMPs are characterized by non-relativistic velocities, one typically applies the limit $v \rightarrow 0$ when calculating the cross section. In this case the corresponding cross section can be decomposed into two contributions: the spin-independent (SI) and the spin-dependent (SD), $\sigma^0 F^2(E_r) \simeq \sigma^{\text{SI}} F_{\text{SI}}^2(E_r) + \sigma^{\text{SD}} F_{\text{SD}}^2(E_r)$, where σ^{SI} and σ^{SD} are given at zero momentum transfer, q , while the dependence on q is encoded in the form factors.⁸ In the absence of isospin violating interactions between DM and nucleons one obtains $\sigma^{\text{SI}} = \sigma_p^{\text{SI}} (\mu^2 / \mu_p^2) A^2$ where $\sigma_p^{\text{SI}} = (4\mu_p^2 / \pi) f_p^2$ and μ_p is the reduced mass of the WIMP-proton system; for a discussion in presence of isospin violation see, e.g., [162]. The limits for the SI cross section are typically presented in the $(m_\chi, \sigma_p^{\text{SI}})$ plane. Note the characteristic $\sim A^2$ dependence (coherent enhancement) that results in an increased differential recoil event rate for heavier target nuclei. The lack of coherent enhancement in SD cross section results in typically lower differential recoil event rates than in the SI case and therefore weaker exclusion limits for σ_p^{SD} than for σ_p^{SI} . In addition, it is important to note that spin-zero isotopes do not give any signal in DM searches based on SD.

Experiments: limits and anomalies Scatterings of DM particles off nuclei can be detected via subsequently produced light (scintillation photons from excitation and later de-excitation of nuclei), charge (ionization of atoms in a target material) or heat (phonons in crystal detectors). Using one or a combination of two such discrimination techniques is now often employed to disentangle a potential WIMP signal from nuclear recoils and background electron recoils. This is possible due to different quenching factors that describe the difference between the recorded signal and the actually measured recoil energy. The electron recoils constitute the background of the experiment and can come from, e.g., γ -radiation from natural radioactivity or β -decays that take place in the detector surrounding materials, on its surface or even inside the detector. Other sources of background, e.g., neutrons or α -decays, can be associated with nuclear recoils that can mimic the WIMP signal. Therefore they need to be either screened out or rejected at the level of signal analysis. A particularly challenging type of such a background that will be very important for future detectors, especially for DM mass below 10 GeV, comes from coherent elastic neutrino-nucleus scatterings [163] and cause the existence of the so-called coherent solar neutrino background [164, 165].

Depending on the choice of signal detection technique a variety of target materials can be employed in DD searches. Light signal from DM-nucleus scattering can be collected,

⁸Recently, increased attention has been paid to studies of more general scenarios for scatterings of the DM particles on nuclei in which this interaction is described in terms of extended set of effective operators that go beyond pure SI and SD cases (see, e.g., [158, 159]). See also [160, 161] for related discussion.

e.g., by using scintillating crystals.⁹ A well-known example of such a detector is that of the DAMA/LIBRA experiment [167] operating at the LNGS laboratory in Italy, which for two decades have been reporting to see an annually modulated DM-like signal, currently with the significance at the level of 9.3σ [168]. The estimated mass of the DM particles from this measurement would range between 10 to 15 GeV or between 60 to 100 GeV depending on the actual nucleus involved in the scattering process (sodium or iodine, respectively). However, the DM interpretation of these results is in strong tension with null results published by some other collaborations: the first XENON1T limits [169, 170], the final LUX [171] and the PandaX-II [172] limits, as well as, in the low mass region, with the limits from CDMSlite [173] and XMASS [174], which excluded the annual modulation of DM interpretation of the effect claimed by DAMA/LIBRA. Non-DM explanations were also considered, including an unknown source of background, as well as possible errors in data collection and processing (for a review see [175]). In addition, other experiments employing similar detection strategy have been proposed to verify the DAMA/LIBRA results. In particular, the results of the KIMS-CsI experiment [176] disfavor interpretation of DAMA/LIBRA signal in which the DM particles scatter off iodine nuclei. This could be circumvented in specific scenarios, e.g., for Magnetic Inelastic DM (see, however, recent XENON1T limits [177]), in models with dominant WIMP inelastic spin-dependent coupling to protons if different quenching factors are assumed in both experiments [178, 179] (for an extensive discussion see also [92]; for recent limits see [180]) or leptonically interacting DM particles that induce electron recoils [181] (see, however, Ref. [182] and references therein).

Charge (ionization) signal from DM-nuclei scatterings can be efficiently measured by low-temperature ultra-low background germanium detectors [183].¹⁰ This technique has been employed by the CoGeNT Collaboration leading to the claim of an observation of an annually modulated signal in their data [184]. The signal could be consistent with WIMP DM-hypothesis with mass about 7 – 10 GeV, although it only had 2.8σ significance and it was not confirmed in later searches in the similar mass range. On the other hand, the observed excess of events may be fully explained when an improved background treatment is applied, as pointed out in [185, 186]. The DM interpretation of the CoGeNT data has also been disfavored by other germanium detectors, e.g., CDEX [187] and MALBEK [188]. A halo-independent analysis performed in [189] for light ($\lesssim 10$ GeV) WIMPs showed a strong tension between the DM interpretation of the annual modulation of DAMA/LIBRA and CoGeNT events when compared with the CDMS-II silicon data.

Phonon signal coming from DM-nuclei scatterings in crystals can provide another important experimental signature in DM DD searches. This technique is particularly useful when looking for low mass DM due to a very good energy threshold. Moreover, one typically further improves the treatment of the background in such experiments by using cryogenic bolometers with additional charge or scintillation light readouts. In 2013 CDMS-Si detector results were published [190] reporting observation of 3 WIMP-candidate events with only

⁹Signal in single-phase liquid noble gas detectors also comes entirely from scintillation light emitted by ionized or excited dimers (for a review see [166]).

¹⁰Another important example of detection technique that focuses on ionization signal from DM-nuclei scatterings is used in gaseous detectors employed in directional dark matter searches (for review see [156]).

0.19% probability for the background-only hypothesis. The highest likelihood occurred for WIMP-DM with 8.6 GeV mass. However, these results were not confirmed by the germanium CDMS-II [191] and SuperCDMS [192] detectors and there is no plausible DM halo function for which this tension could be alleviated unless one assumes, e.g., exothermic DM with Ge-phobic interactions as discussed in [193].

DM-nuclei scatterings also can be detected via heat signal in experiments based on superheated fluids used as a target material. DM particle passing through a detector can then be visualized thanks to initiated process of bubble creation.

Another DM-like signal was found in the data obtained by the CRESST-II Collaboration [194] in 2011. An excess in the expected number of events was observed in two mass ranges around 10 GeV and 25 GeV with the significance at the level of 4.2σ and 4.7σ , respectively. However, as it was pointed out in [195] and confirmed in a later study by the collaboration [196], the excess was mainly due to a missing contribution to the background (see also [92] and [175] for an updated discussion).

The most stringent current limit on σ_p^{SI} for large DM mass comes from null results of DM searches in dual phase (liquid-gas) xenon detectors: XENON1T [169, 170] – the most recent (and currently the strongest) – the final LUX result [171] and that of PandaX-II [172], both of which improved the previous limits of XENON100 collaboration [197]; see Fig. 5. The strongest up-to-date exclusion lines for spin-dependent cross section, σ_p^{SD} , from DD experiments were published by the PICO collaboration [198, 199] (see also LUX [200] and XENON100 [197] results). However, σ_p^{SD} can also be effectively constrained by neutrino telescopes as will be discussed in Section 3.5.

A further significant improvement is expected from the currently running XENON1T, later from XENONnT [201], LZ [202], and eventually from planned xenon detectors, e.g., DARWIN [203], and for argon as a target material: DEAP3600 [204], ArDM [205] and DarkSide G2 [206]. In the low mass regime large part of the $(m_\chi, \sigma_p^{\text{SI}})$ parameter space will be probed by the future germanium and silicon detectors in the SuperCDMS experiment operating at SNOLAB [207].

A summary of the above discussion about experimental results is presented in Fig. 5 where we show current and expected future limits on σ_p^{SI} as a function of the DM mass. Anomalies reported in the past by some of the experimental collaborations were not confirmed and are probably due to some non-DM effects that occur either inside or outside the detectors. However, the upcoming years should deliver new data covering regions in the $(m_\chi, \sigma_p^{\text{SI}})$ plane well below the current limits and, hopefully, eventually producing a genuine DM signal.

It is important to note that the limits presented in the $(m_\chi, \sigma_p^{\text{SI}})$ plane can vary depending on the underlying assumptions about relevant astrophysical quantities, e.g., the local DM density and the DM velocity distribution (see, e.g., [211] and references therein). The dependence on the velocity distribution is typically weak [212], but can become more important, e.g., if the detector is sensitive only to the tail of the distribution [213]. Alternatively, the limits can be shown in a DM halo-independent way [214] (see also [215] and references therein) if a positive signal is measured by at least two different targets.

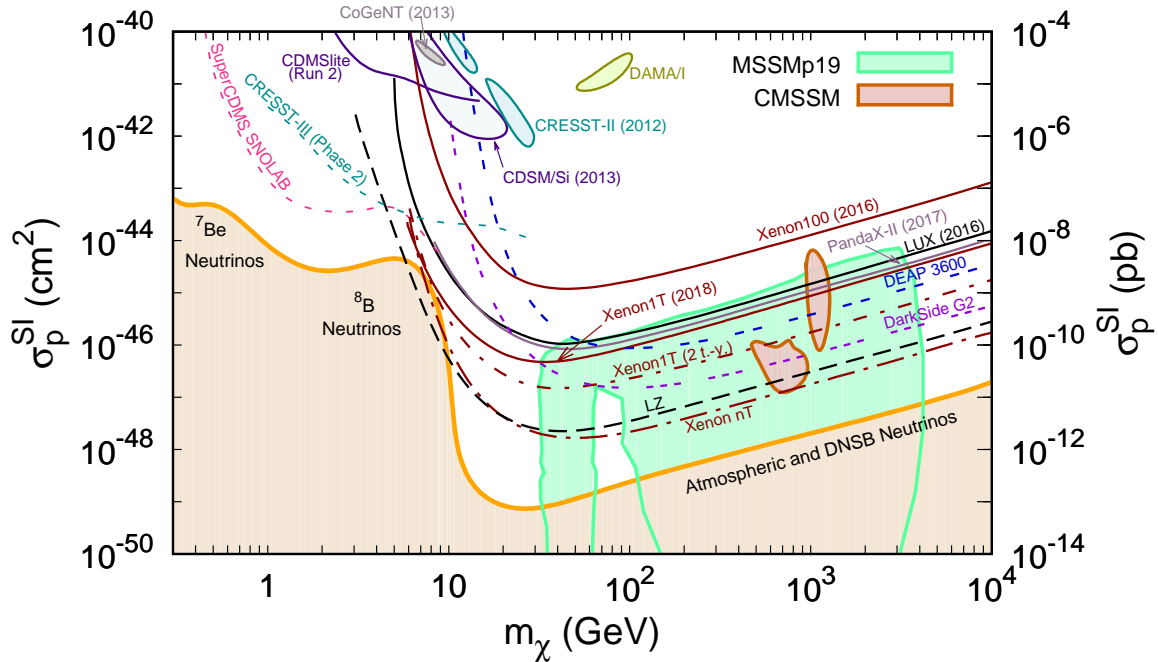


Figure 5: Current and future limits on DM direct detection spin-independent cross section, σ_p^{SI} , as a function of DM mass, m_χ . The current limits are shown with solid black (LUX [171]), gray (PandaX-II [172]), brown (XENON100 [197] and XENON1T [170]) and violet (CDMSlite-II [173]) lines. Future projections correspond to CRESST-III (Phase 2) [208] (light blue), DarkSide G2 [206] (violet triple-dashed line), DEAP3600 [204] (blue double-dashed line), LZ [202] (black long-dashed line), SuperCDMS at SNO-LAB [207] (pink short-dashed line) as well as XENON1T/nT [201] (brown dash-dotted lines). We also show the 95% C.L. region for the 19-parameter version of the MSSM (green shaded area) [209] and posterior plot for the allowed parameter space of the CMSSM (brown area enclosed with the solid brown line) [210]. The shaded areas on top of the plot correspond to the favored regions for DM interpretations of anomalies reported in the literature by the CDMS-Si [190] (blue), CoGeNT [184] (gray) CRESST-II [194] (light blue) and DAMA/LIBRA [167] (light green) collaborations. The shaded area below the solid orange line on the bottom of the plot corresponds to the irreducible neutrino background [165].

Implications for WIMP models Direct detection searches play a vital role in constraining various models of WIMP as DM. For instance, early negative results from the Heidelberg-Moscow experiment [216] led to an exclusion of the scenario in which the majority of DM was composed of left-handed sneutrinos in the MSSM [128], as discussed in Section 2.3. Since then many other theoretical candidates have been constrained by null results of searches for the DM particles in DD experiments.

Limits from DD have also been derived on effective contact operators describing possible interactions between DM and the SM particles (for studies related to DD see, e.g., [158, 159]). One can then translate the usual DD limits shown in the $(m_\chi, \sigma_p^{\text{SI}})$ plane into the actual limits on the coefficients of the operators that contribute to σ_p^{SI} , while the other coefficients remain free and can, e.g., help to achieve the proper value of the DM relic density. Stronger constraints can be obtained when both DD and ID searches are taken into account (see, e.g., [217]).

Another phenomenological approach consist in “expanding” the contact operator ap-

proach by introducing specific mediators (“portals”) between the DM sector and the SM particles in a framework of so-called simplified models. For studies related to DM DD see, e.g., [218–222]. It has been pointed out that gauge invariance and perturbative unitarity need to be carefully taken into account when constructing simplified models of DM interactions [223, 224]. For further discussion about the effective theory approach (EFT) and simplified models see, e.g., [225] and references therein.

3.2 Gamma rays: limits and Galactic Center excess

Gamma-rays represent a promising channel in which to search for dark matter (for reviews see, e.g., [11, 12, 226]). WIMPs are expected to annihilate at present leading to the possibility of detecting annihilation products, in particular a spectrum of gamma-rays. Since gamma-rays are not deflected in their journey from the emission point to detection on Earth, the direction of the source can be determined, thus allowing specific targets or regions of DM annihilation to be identified. This can be compared to the situation with charged cosmic rays which are deflected by the magnetic field of the Galaxy. It is therefore possible to use the expected morphology of the DM signal to discriminate it from background [227].

Gamma rays from DM The spectrum of gamma rays expected from a DM annihilation depends on particles produced in the final state. Typically one assumes that the DM annihilates to Standard Model particles, which must account for at least some fraction of the annihilations for a WIMP produced through thermal freeze-out. Gamma-ray emission from DM annihilations can be of two types: a continuous spectrum generated by the decay, hadronization and final state radiation of the SM particles produced, and spectral features in the form of gamma ray lines and internal bremsstrahlung.

The continuous spectrum of gamma rays for a specific SM final state can be estimated via Monte Carlo simulation using standard event generators [228–230] that include parton showering and hadronization. There is therefore some uncertainty associated with the choice of event generator. Additionally it can also be important to include polarization and electroweak corrections, see [231] for a full discussion. Gamma-ray lines appear from the processes $\chi\chi \rightarrow \gamma\gamma$ and $\chi\chi \rightarrow Z\gamma$, since the DM must be electrically neutral these must arise at the loop level but are nearly impossible to mimic by astrophysical background [232]. Internal bremsstrahlung can also lead to sharp spectral feature as well as lifting chiral suppression in some models [233]. In addition, γ -rays can also be produced as secondary products of DM annihilations into other particles once the latter interact in interstellar medium, e.g., thanks to inverse Compton scattering (ICS), bremsstrahlung off of galactic gas, neutral pion decays originating from interactions of hadronic cosmic rays with interstellar gas or synchrotron emission induced by propagation in magnetic fields.

Targets for gamma-ray searches The morphology of the DM signal can be used to discriminate DM annihilations from the background by focusing searches in regions with a high density of DM. The Galactic center (GC) is expected to be the brightest source of gamma rays from annihilating DM and has attracted considerable attention as a target for indirect detection experiments [234]. The main argument for a high density of DM in

the inner regions of galaxies comes from N-body simulations that determine the expected halo distribution (see, e.g., [235] and references therein). Dynamical and microlensing observations act to constrain the halo profile [236] but there remains significant uncertainty particularly in the GC, see [237, 238] for some recent determinations. These uncertainties are further compounded by the complex background of conventional astrophysical sources of gamma rays present in the GC [239].

Dwarf spheroidal galaxies (dSphs) in the Local Group do not suffer from the same problems as the GC of the Milky Way. The dSphs are expected to be DM dominated [240, 241] and are free from the astrophysical backgrounds plaguing the GC. In addition the distribution of DM can be estimated from the dynamics of stars inside the dSphs [242–244]. This makes limits obtained from dSphs more robust, however the expected signal is much lower for a single dSphs than for the GC therefore a stacking analysis is required to obtain competitive limits.

Galaxy clusters are another promising target for gamma-ray searches [245, 246]. The main drawback compared to dSphs is that they suffer from large and poorly understood astrophysical backgrounds, and the expected sensitivity depends strongly on the DM substructure which is unknown.

Finally the full sky can be observed to place limits on annihilations summed over all halos [247]. Since the cosmological DM halos are in general unresolved they contribute to an approximately isotropic background. The isotropic gamma-ray background can be searched for spectral features that would indicate DM annihilations. However, large uncertainties in the backgrounds and expected rate make setting robust limits difficult. A related idea is to measure the angular correlations or cross-correlations to search for a DM signal above the expected isotropic background. Angular correlations can be used to search for extragalactic halos or subhalos as well as other sources such as annihilation of DM around intermediate mass black holes [248]. Cross correlations can also be searched for between the diffuse extragalactic gamma-ray signal and the cosmological DM distribution inferred in other channels such as the CMB and structure surveys (see [249] and references therein).

Figure 6, taken from [250], summarizes the discussion of different targets of gamma-ray observations in terms of the expected signal strength and uncertainty associated with an observed signal or limit. While the strongest case for the observation of DM would be made by complementary observations in several of those channels, two particular targets stand out as currently being most relevant. These are the GC, which has the largest expected signal strength and is therefore the most likely target for a signal to show up first, and combined data from dwarf galaxies of the Local Group, which currently produce the strongest and most robust limits.

Gamma-ray telescopes There are two main strategies to observe gamma rays. Since gamma rays interact with the atmosphere direct observation can only be made by space telescopes. On the other hand the ground based telescopes are able to detect gamma rays indirectly by observing the Cherenkov light produced by the showers of charged particles produced by the gamma ray as it hits the atmosphere. Direct observation of gamma rays using space telescopes has been performed by EGRET [251] and the currently running

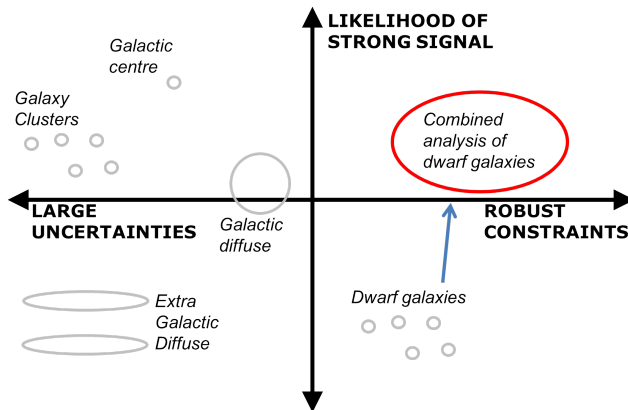


Figure 6: A cartoon, taken from [250], of the relative merits of different gamma-ray observation regions, projected into the expected strength of a signal and relative uncertainties that are associated with the backgrounds and signal strength.

Fermi-LAT [252]. Fermi-LAT uses pair conversion inside a tracking detector, and an electromagnetic calorimeter to determine the energy and incident direction of the gamma-ray. Charged cosmic rays are rejected using an anti-coincidence shield. Fermi-LAT is able to observe gamma rays in the range 20 MeV to 300 GeV and has an effective area of $\sim 1\text{m}^2$. It typically scans the full sky continuously taking advantage of its large field of view. This means that Fermi-LAT is able to make observations of all of the promising targets for DM annihilation.

The most promising ground based telescopes are the Imaging Air Cherenkov Telescopes (IACTs). When a gamma ray enters the atmosphere it interacts creating a shower of secondary particles. The Cherenkov light from the shower is then captured by one or more telescopes on the ground.

One major source of background comes in the form of air showers caused by charged cosmic rays. The cosmic ray background is isotropic and greatly exceeds the gamma-ray signal. This background must be reduced by rejecting showers produced by cosmic rays. This can be done by distinguishing the patterns of Cherenkov light produced by hadronic and gamma-ray showers. Unfortunately, showers produced by electrons cannot be differentiated from gamma rays this way. Monte Carlo simulations [253] are used to model the Cherenkov light from hadronic and gamma-ray showers and to estimate the remaining background for a particular telescope configuration. IACTs have a higher energy threshold than space telescopes since lower energy gamma rays produce less Cherenkov light, however they have the advantage that the volume of atmosphere observed can be large leading to huge (energy dependent) effective area compared to space telescopes. On the other hand, the field of view of IACTs is much smaller and dedicated observations of particular target regions must be made. This means that potential time allowed for DM studies must compete with the other science goals of the IACT. Currently running IACTs include MAGIC [254], VERITAS [255] and HESS [256]. While the next generation telescope will be the currently planned CTA [257].

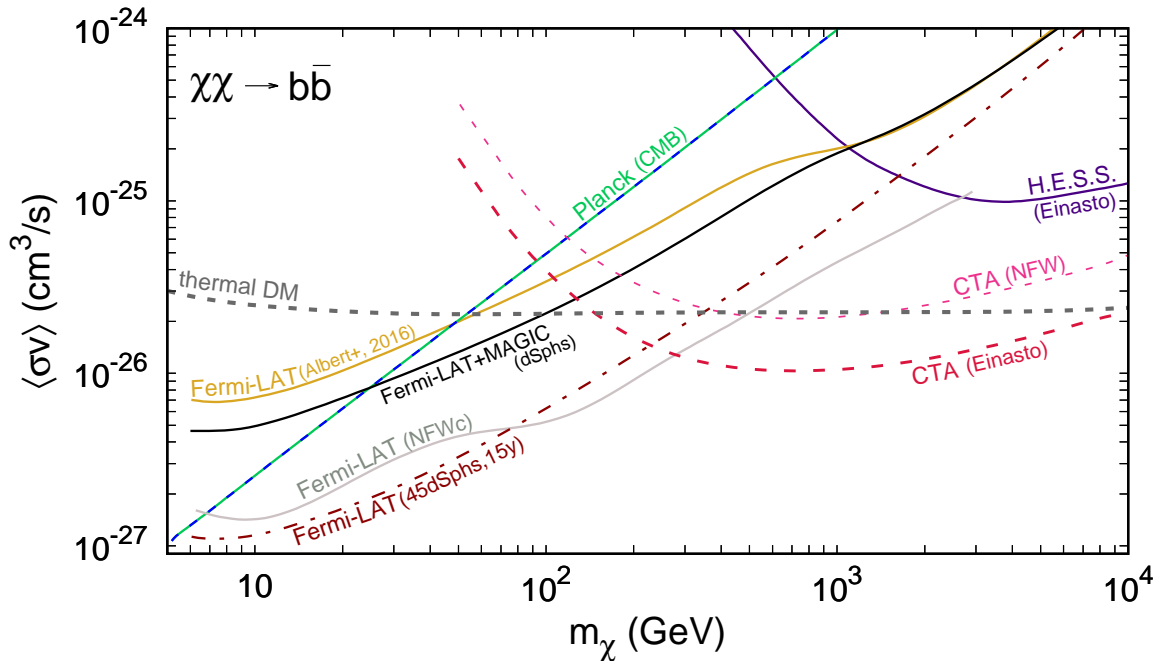


Figure 7: Limits on the annihilation cross section for the DM particles annihilating into a $b\bar{b}$ pair. Currently the strongest limits correspond to the stacked analysis of dwarf galaxies from Fermi-LAT [258] (solid golden line), combined analysis of both Fermi-LAT and MAGIC [259] (solid black line) collaborations, H.E.S.S. observations of the GC [260] (solid violet line) that we show for the assumed Einasto profile of the DM in the Galactic halo and the Fermi-LAT observations of the Inner Galaxy [261] (solid gray line) if the DM distribution is assumed to be consistent with the compressed NFW profile (NFWc). In the low DM mass regime the important limits come from the CMB analysis released by the Planck collaboration [28] which constraints σv around the time of recombination (dashed blue-green line). The future projections are shown for the stacked analysis of 45 dwarf galaxies and 15 years of data taking [262] (dash-dotted brown line), as well as for the CTA collaboration [263] based on the assumed NFW (dashed pink line) and Einasto profiles (dashed red line). The value of the annihilation cross section that corresponds to the thermal production of WIMP DM [72] is denoted with dotted gray line.

Current limits and future prospects We summarize some of the recent limits from Fermi-LAT and the IACTs, as well as future projections in Fig. 7. On the direct observation side the strongest limits come the stacked analysis of dwarf galaxies [258, 259]. The canonical thermal annihilation rate [72] is shown as a gray dotted line and the current limits from Fermi-LAT exclude WIMPs annihilating to $b\bar{b}$ with this cross section below ~ 100 GeV. The limits from the GC [261, 264] are competitive but are weaker due to the uncertainty in the halo profile. Observations of the Galactic halo [239], galaxy clusters [265] and the Fermi analysis of the intensity [266] and angular power spectrum [267] of IGRB are weaker by about an order of magnitude.

Turning to the current generation of IACTs, Fig. 7, we first note that the Cherenkov telescopes are sensitive to larger DM masses, whereas Fermi-LAT loses sensitivity as the DM mass increases. The strongest limits come from H.E.S.S. observations of the Galactic center [260] which at ~ 1 TeV become stronger than the Fermi-LAT limit. The limits from MAGIC’s observation of the dwarf galaxy Segue 1 [268] and the H.E.S.S. combination

analysis of dwarf galaxies [269] are comparable with H.E.S.S. extending the analysis to higher masses. The VERITAS analysis of the Fornax galaxy cluster [270] is the least sensitive and has large uncertainties from the modeling of the substructure and backgrounds (see also recent VERITAS limits from joint analysis of four dSphs [271]). In the search for spectral features the most relevant limits come from Fermi-LAT and H.E.S.S. searches for gamma-ray lines in the GC [272, 273] and galaxy clusters [274].

In the short term, Fermi-LAT, H.E.S.S. and VERITAS are currently taking data, which will continue to place limits on DM annihilation to gamma rays. In particular the best prospects for Fermi-LAT consist of observations of dSphs with more dSphs expected to be discovered in the future (see, e.g., [262]).

Other stringent limits come from possible deviations from a standard recombination history caused by DM-induced cascades of highly energetic particles around this period in the evolution of the Universe [275]. Depending on the actual dominant annihilation final state and on the associated efficiency parameters that describe the fraction of the rest mass energy contributing to CMB distortions, the current limits sometimes reach up to the values of the thermal annihilation cross section for low DM mass [28]. It is important to remember that limits derived this way constrain the value of the annihilation cross section around the time of recombination and therefore they are not necessarily directly comparable with the DM ID lines discussed above unless DM annihilation is predominantly of *s*-wave type.

Looking a few years ahead, the CTA experiment [257] is expected to improve on the current limits from H.E.S.S. CTA will be the next very large IACT consisting of arrays in the northern and southern hemisphere, with small, medium and large telescopes giving CTA improved sensitivity over a large energy range from ~ 100 GeV to tens of TeV [276]. This results in strong expected sensitivity of the CTA to DM annihilations based on observations of the GC [263].

Future gamma-ray space telescopes are planned, e.g., CALET [277], GAMMA-400 [278] and HERD [279]. CALET, recently launched in 2015, has excellent energy resolution above 100 GeV and is likely to place strong limits on gamma-ray lines [277] although will not be competitive with Fermi-LAT for limits on the continuous spectrum of gamma-rays. The Russian-led GAMMA-400 is in preparation and will also mostly contribute to searches for spectral features due to its improved energy resolution compared to Fermi-LAT. The HERD telescope, to be launched in 2020, on the other hand will represent an increase in the effective area and thus should improve on the limits set by Fermi-LAT [279], although detailed studies have not yet been performed.

Galactic Center Excess One of the most intriguing hints of DM detection that has emerged in the last few years is a consistent excess above the expected background observed in the diffuse gamma-rays coming from the GC in the Fermi-LAT data [280, 281]. This signal, known as the Galactic Center Excess (GCE), appears to be peaked around photon energy of a few GeV and was consistently confirmed by many independent analyses (see, e.g., [282–288] and references therein). The Fermi-LAT Collaboration released their own analysis [289] in which GCE is studied employing multiple specialized interstellar emission

models (IEMs) that enabled to separate the signal coming from the region surrounding the GC (within ~ 1 kpc) from the rest of the Galaxy (see also [290, 291] for related discussion). The excess of gamma rays remained, however its origin is still unclear since the spectral properties of the signal strongly depend on the assumed IEM. In particular, it was pointed out that the photon clustering in the observed excess could be inconsistent with the signal expected from smooth DM distribution [292–294]. Such a possibility has been recently confirmed by the Fermi-LAT collaboration [295]. However, it is also possible that what seems to be a point-like nature of the excess is in fact a result of uncertainties in the background modeling [296]. On the other hand, recent Fermi-LAT analysis of the GCE [297] confirmed the existence of the excess and studied in detail its morphology. In particular, it was shown that the excess is likely to have at least partial astrophysical origin, but the DM interpretation is not excluded. In addition, the excess in the γ -ray signal with a possible DM origin, which is consistent with the GCE, was found in the recent Fermi-LAT study of the center of M31 [298].

The most popular astrophysical explanation is a population of unresolved millisecond pulsars (MSPs) in the GC. The gamma-ray spectrum produced MSPs is known to be compatible with a power law exhibiting an exponential cutoff around $2 - 3$ GeV [299]. It was shown that the GCE can be partly or completely explained by a population of MSPs in the GC [283, 300]. However there is some disagreement as to whether MSPs are really a viable explanation for the GCE based on, e.g., the expected distribution of X-ray binaries [301, 302] (see also [283] for early study in this direction), detailed analysis of the spectra shape of the GCE [303] or distribution of globular clusters [304]. Non-equilibrium processes were also proposed as an explanation for the GCE. In particular, a large injection of CRs into the GC at some point in the past could produce the observed GCE [305–307]. The observed excess can also be associated with X-shaped stellar over-density in the Galactic bulge [308].

As discussed above, it is still possible that DM-induced γ -rays contribute to the GCE. If the GCE is indeed originated from DM annihilations it should then be possible to find their trace in other observation targets or channels. In particular a similar excess can be searched for in the dwarf spheroidal galaxies. Recently the Dark Energy Survey discovered several new dwarf galaxy candidates [309]. In particular, some tentative evidence was proposed for a gamma-ray excess in the direction of nearby Reticulum II [310, 311] and for a faint excess that can come from Tucana III [312], both can be compatible with the GCE. The Fermi Collaboration also performed an analysis in which no evidence of an excess was found [313]. Another hint of possible DM discovery was reported in [314] based on the analysis of Fermi-LAT data obtained for nearby galaxy clusters. The observed excess, if interpreted in terms of DM annihilation, can point towards similar mass range for the DM particles as the GCE. However, this requires assuming relatively large boost factors.

Alternatively, one can consider looking for a corresponding excess in the anti-proton spectrum. Comparisons of the GCE and limits from anti-protons were made in [315, 316]. However, the situation is currently unclear with different analyses claiming that the GCE can be ruled out or is allowed depending on the modeling of the anti-proton propagation (for a recent discussion see, e.g., [317]).

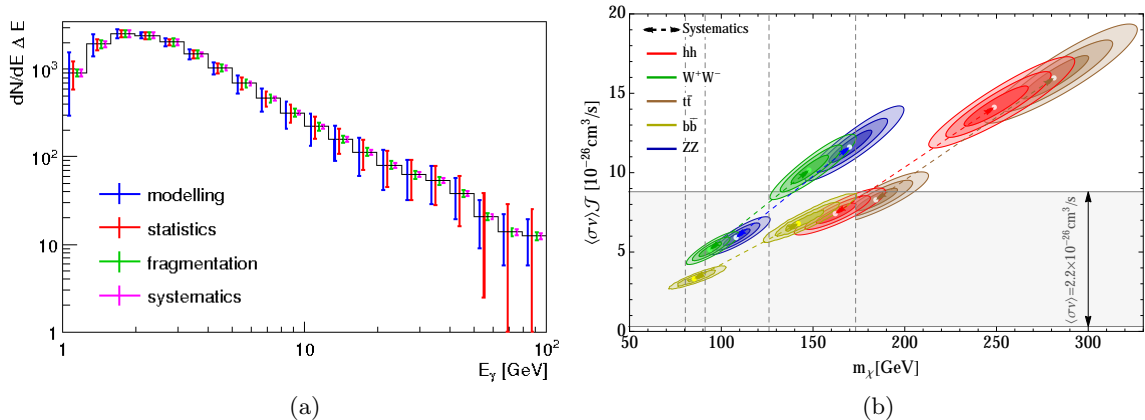


Figure 8: (a) Residual spectra of the GCE with various astrophysical and instrumental uncertainties as discussed in [318]. Taken from Ref. [318]. (b) Regions of parameter space that fit two of the Fermi best fit spectra for different final states. Parameter space between the contours indicated by dashed line is likely allowed by variation of the background model [319]. Taken from Ref. [319].

The GCE attracted a great deal of attention also in terms of model building including neutralino DM (see, e.g., [318–325]). Some notable non-SUSY attempts include: multi-step cascade annihilations where the dark matter annihilates to some intermediate states that decay to Standard Model particles [326–328], approaches based on effective field theory and simplified models of DM [288, 329, 330], Higgs portal models [319, 331, 332], two Higgs doublet models [333, 334], models with a Z' [335] and vector dark matter models [336].

We summarize our discussion of the GCE in Fig. 8 taken from [318, 319]. Fig. 8(a) shows the residual spectrum for the GCE, as well as various instrumental and astrophysical uncertainties, as discussed in [318]. Initially, fits to the excess favored DM annihilating to $b\bar{b}$ and $\tau^+\tau^-$ with $m_\chi \approx 40$ GeV and $m_\chi \approx 10$ GeV, respectively. The annihilation cross section was reported as $2-3 \times 10^{-26} \text{ cm}^3/\text{s}$ [286] for $b\bar{b}$ and $7-9 \times 10^{-27} \text{ cm}^3/\text{s}$ for $\tau^+\tau^-$ [281] final states which are remarkably similar to the annihilation cross section required for a thermal relic. However, these are not the only possible annihilation final states that can fit the GCE signal. Fig. 8(b), taken from [319], shows the allowed parameter space for a WIMP annihilating to hh , W^+W^- , ZZ , $t\bar{t}$ and $b\bar{b}$ for two different Fermi background models. These models favor the lightest and heaviest DM masses. The parameter space between the two fits, indicated by a dashed line, is likely allowed by variation of the background model [319]. Annihilation to leptonic final states also still provides a good fit to the GCE where the effect of secondary gamma-rays is important [337].

Other anomalies Another excess in the Fermi-LAT data from the GC was reported in 2012 by [338, 339]. At that time it was found to be consistent with the γ -ray line around 130 GeV with possible origin from DM annihilations or decays. However, it was soon pointed out that the line was not associated with enough signal in the continuum spectrum which caused some tension with popular DM candidates trying to fit the observed excess, including the lightest neutralino [340, 341]. It has been later shown that the existence

of the excess was a statistical fluctuation as its significance has diminished in subsequent improved analyses performed by the Fermi-LAT Collaboration [272].

Interesting features were identified in the spectrum of γ -rays originating from regions around the GC in the WMAP data [342] (so-called WMAP haze), Fermi-LAT data [343, 344] (Fermi bubbles) and Planck data [345] (Planck haze), with a possible common origin. The hard edge-like structures observed for Fermi bubbles disfavor its DM-induced origin. However, it is still possible that some part of the WMAP/Planck haze are not due to the Fermi bubbles and can be better fitted with DM annihilations associated with subsequent microwave synchrotron emission (see, e.g., [346]).

A possible hint of light DM was provided by the excess of γ -rays observed by the INTEGRAL collaboration [347, 348]. It corresponds to 511 keV γ -ray line that has no widely accepted astrophysical explanation. The signal could be compatible with MeV DM annihilating into e^+e^- pairs [349]. Similar signal was found in the direction of Reticulum II, however astrophysical explanations of the excess observed there are favored (for further details see, e.g., [350] and references therein).

The excess in extragalactic radio background found in the ARCADE 2 data [351, 352] could be explained by leptophilic DM with mass typically of order 5–50 GeV [353, 354] that annihilate mostly into electrons and/or muons inducing γ -ray production via subsequent ICS processes. This scenario, however, can already be excluded by the AMS positron data [355]. On the other hand various astrophysical explanations of the observed excess were proposed which, however, also often struggle to accommodate for the whole excess unless numerous faint sources are considered [356] (see, however, [357] for an updated discussion).

3.3 Interlude: WIMP reconstruction from direct detection and gamma rays

Before we proceed with other modes of DM searches, we digress here to consider what information about WIMP properties one could realistically derive in case a real DM signal is actually recorded in either direct detection or in gamma ray experiments, or – even better – in both.

Reconstruction Once one day a genuine DM signal is observed, we will enter into a new era of reconstructing WIMP properties from experimental data. A number of theoretical studies have already been conducted to test the quality of a putative post-discovery reconstruction in DD experiments depending on the DM mass, respective cross section and target material (for a review see [151]). In particular, it has been pointed out that due to diminishing differences between recoil spectra for a larger DM mass, DD signal analysis can strongly constrain DM properties only for $m_\chi \lesssim 100$ GeV and for the values of σ_p^{SI} not far below the current limits given the realistic assumptions about achievable exposures. For larger DM mass one typically obtains a $\sigma_p^{\text{SI}}/m_\chi \simeq \text{const}$ degeneracy, as can be seen from Eq. (3.1) for $m_\chi \gg M$.

However, this can be partially overcome by a possible complementarity between DD and ID searches [358–361], provided of course that a DM-induced signal is found in both types of experiments. We illustrate this in Fig. 9(a) where we show an interplay between

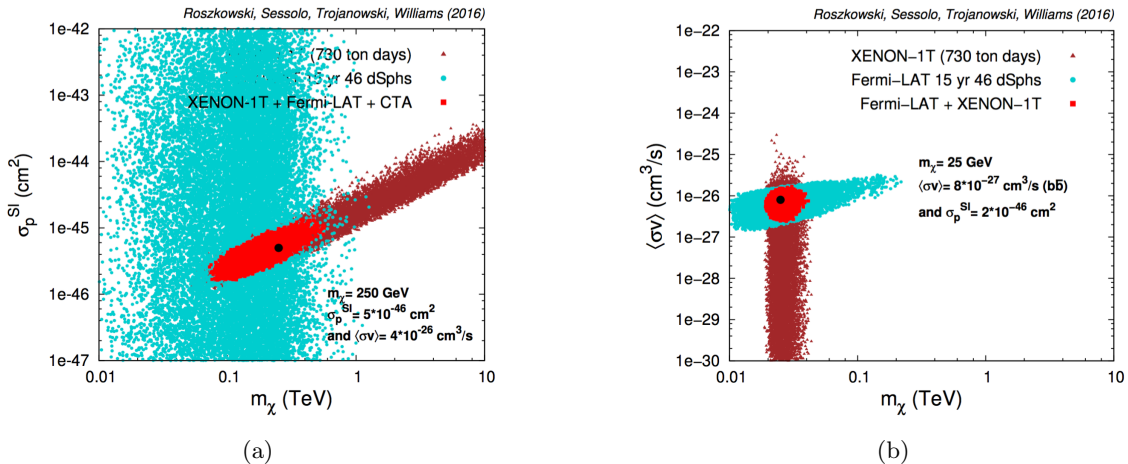


Figure 9: (a) Comparison of DD (XENON1T) and ID (CTA and Fermi-LAT) experiments in reconstructing the DM properties for the benchmark point with $m_\chi = 250$ GeV and $\sigma_p^{\text{SI}} = 5 \times 10^{-46}$ cm², while the annihilation cross section is equal to $\sigma v = 4 \times 10^{-26}$ cm³/s for a pure $b\bar{b}$ final state. The brown region corresponds to 2σ reconstructed region for only XENON1T simulated data, the light blue one for Fermi-LAT data (assuming 15 years of exposure and 46 dSphs in the stacked analysis), while the red region was obtained for XENON1T+CTA+Fermi-LAT joint analysis. (b) Similar to (a), but for the benchmark point defined by $m_\chi = 25$ GeV, $\sigma_p^{\text{SI}} = 2 \times 10^{-46}$ cm², $\sigma v = 8 \times 10^{-27}$ cm³/s and pure $b\bar{b}$ annihilation final state. Light blue region corresponds to the the Fermi-LAT reconstruction, while brown one to XENON1T. Combined analysis leads to improved reconstruction of σv as indicated by the red region. Both figures are taken from [361].

putative signals from XENON1T and from two ID experiments: CTA [257] and Fermi-LAT [252] (for which we assume 15 years of exposure and 46 dSphs). We consider a benchmark point with $m_\chi = 250$ GeV and $\sigma_p^{\text{SI}} = 5 \times 10^{-46}$ cm², as well as the annihilation cross section lying just below the current exclusion bound [259], $\sigma v = 4 \times 10^{-26}$ cm³/s assuming a pure $b\bar{b}$ final state. As can be seen, an improved mass reconstruction in the ID experiments allows one to strongly constrain σ_p^{SI} which remains unconstrained from above using the XENON1T (and in fact, any DD) data alone.

For a low DM mass a good reconstruction of m_χ in DD can help interpret the results of ID searches. This is because it is difficult to distinguish among different DM scenarios based on results from ID only, due to an a priori unknown nature of the annihilation final state and the lack of characteristic spectral features for typical final states channels, e.g., $b\bar{b}$ or $\tau^+\tau^-$. However, different annihilation final states that provide a good fit to the same signal observed in ID are often associated with different m_χ and σv . This is, e.g., the case of a well-known Galactic Center excess discussed in Section 3.2. Hence, improved DM mass reconstruction in DD experiments could help in better discriminating among various annihilation final states and, eventually, constrain the annihilation cross section. We illustrate this in Fig. 9(b) for the benchmark point characterized by $m_\chi = 25$ GeV, $\sigma_p^{\text{SI}} = 2 \times 10^{-46}$ cm², $\sigma v = 8 \times 10^{-27}$ cm³/s and pure $b\bar{b}$ annihilation final state. As can be seen the DM mass reconstruction in Fermi-LAT is limited and it is a consequence

of the aforementioned degeneracy in annihilation spectra.¹¹ On the other hand, a DD measurement of a WIMP signal, which is obviously not sensitive to σv , helps to reconstruct m_χ . As a result also the annihilation cross section that fits to the assumed ID signal from the benchmark point is constrained better (for a more detailed discussion see [361]). The reconstructed value of the annihilation cross section could then be mapped into the values of the DM relic density upon additional general assumptions about the WIMP interactions or within the framework of specific models [362].

3.4 Cosmic rays: limits and AMS02/Pamela

Charged cosmic rays (CRs) as a tool for DM searches [363] play an important and complementary role to γ -rays as both are typically produced jointly when the DM particles annihilate or decay (for recent review see, e.g., [12]). The most common types of charged cosmic rays are evidently electrons, e^- , and protons, p , that can originate from many astrophysical sources [364]. On the other hand, in the case of the annihilations or decays of neutral DM particles, one expects to produce an equal number of both matter and antimatter particles. The latter, including energetic positrons, e^+ , antiprotons, \bar{p} , antideuterons, \bar{d} (see, e.g., [365]), as well as heavier nuclei, e.g., anti-helium [366, 367] are particularly promising tools for DM ID due to relatively low astrophysical background.

Production and propagation Charged cosmic rays, similarly to photons, can be produced both directly in the annihilation and decay processes as well as in the DM-induced cascades of particles. As a result one obtains a diffuse spectrum of cosmic rays with a cut-off at energies close to m_χ or $m_\chi/2$ for DM annihilations or decays, respectively. A sharp cut-off can be a “smoking-gun” for DM detection since astrophysical sources are expected to result in a more gradual fall. However, both scenarios can be distinguished only if sufficient amount of data is collected.

Prompt spectra of DM-induced cosmic rays are subsequently modified due to diffusion in the Galactic magnetic field during their propagation to the Earth (for a detailed discussion see, e.g., [226] and references therein). In the case of electrons and positrons one also needs to take into account various mechanisms of energy-loss, including synchrotron radiation and the inverse Compton scattering on CMB photons or galactic starlight (for a more detailed discussion see [368]). These mechanisms typically play a less important role for antiprotons and antideuterons, since the corresponding terms in the diffusion loss equation are suppressed by the proton or deuteron mass, respectively. However, the spectrum of \bar{p} and \bar{d} is affected by their possible interactions with protons in the interstellar medium, as well as by convective Galactic winds that push antiparticles away from the Galactic plane, by diffusive reacceleration and by the solar modulation (see, e.g., [369–371]).

Experiments and anomalies Searches for charged cosmic rays employ several detection techniques including balloon-type (e.g., HEAT [372], ATIC [373]) and ground-based tele-

¹¹Specifically, in reconstruction we take into account $b\bar{b}$, $\tau^+\tau^-$, hh and W^+W^- final states.

scopes (e.g., Pierre Auger Observatory [374], the Telescope Array [375]), as well as satellite-based experiments including, e.g., PAMELA [376], AMS-02 [377], Fermi-LAT [252].¹²

In particular, in 2009 the PAMELA Collaboration reported an excess in the positron spectrum [378] which was subsequently confirmed by the Fermi-LAT [379] and the AMS-02 [377] experiments. The excess was observed for the energies between ~ 20 GeV and ~ 200 GeV [380]. The distribution of the high-energy positrons detected by the PAMELA experiment was found to be isotropic [381]. This could be consistent with their DM origin, but can also be explained by astrophysical sources, especially given the uncertain impact of magnetic field configurations on the positron trajectories. Indeed, a DM-related interpretation of the signal was extensively studied both at the level of general WIMPs [382] and within the framework of particular models (see, e.g., [383–387]). As the DM interpretation of the excess typically requires large annihilation cross section and/or boost factors, it was constrained to leptophilic DM models [388, 389] by null results of searches for DM-induced antiprotons of similar strength [390]. However, the leptophilic models themselves seem to be in tension with limits from gamma-ray and X-ray backgrounds [391, 392], the optical depth of the Universe [393, 394], as well as from radio data [395] and the observations of the CMB radiation [28]. The tension is even more pronounced in light of recent limits on γ -rays discussed in Section 3.2. On the other hand, one needs to note that viable astrophysical scenarios were proposed to accommodate for the observed excess (see, e.g., [396]).

Recently an excess in antiproton flux has been confirmed in the AMS-02 data [397] (see, however, [398]). It can be explained by the annihilation of the DM particles with the cross section into hadronic final states of order $3 \times 10^{-26} \text{ cm}^3/\text{s}$ and the mass that can be compatible with the γ -ray GCE [399, 400]. On the other hand, it was shown [399] that these AMS-02 results interpreted in terms of upper limits lead to an improvement with respect to the limits from γ -rays coming from dSphs discussed in Section 3.2.

All the observed anomalies, as well as other searches for DM-induced charged cosmic rays will be subject to further studies in currently operating or future experiments, e.g., CALET [401], DAMPE [402], GAPS [403], in addition to AMS-02.

3.5 Neutrinos: limits and anomalies

Attempting to discover one elusive particle by capturing another very weakly interacting particle is definitely a very challenging task. However, neutrino detectors proved their unquestionable usefulness as a tool for DM searches thanks to an enormous experimental progress. In particular, current best limits on DM-nuclei spin-dependent cross section σ_p^{SD} are based on the results obtained by several neutrino detectors, including ANTARES [404], IceCube [405] and Super-Kamiokande [406].

Neutrinos from DM annihilations Depending on a particular DM model, neutrinos can be produced mainly in cascades of particles originating from DM annihilations or decays, or even directly in these processes. However, since annihilation or decay rates are typically very small, in order to be able to detect DM-induced neutrinos, one needs to focus

¹²Note that γ -rays and electron/positron signals cannot be distinguished based on the recorded air shower, but ground-based telescopes are still capable of studying heavier charged CRs, e.g., protons.

on regions in the sky where large concentration of DM particles can be observed, e.g., the Sun, the GC, Galactic halo, nearby galaxies and galaxy clusters or even the Earth.

In particular, DM particles are expected to accumulate inside celestial bodies as their velocity can decrease below the escape velocity due to scatterings off nuclei. Neutrinos are then basically the only products of DM annihilation that can escape and reach detectors. Therefore they can provide a unique DM signature [407]. The expected flux of neutrinos passing through a detector depends on the DM annihilation rate Γ_{ann} . For heavy and dense celestial bodies Γ_{ann} is determined by the capture rate of DM Γ_{cap} due to the equilibrium condition $\Gamma_{\text{ann}} \simeq \Gamma_{\text{cap}}/2$ [408, 409].¹³

When analyzing potential signal from such neutrinos, one needs to take into account both the neutrino spectrum at production and the propagation of neutrinos from the center of the celestial body to the Earth. Both these processes in principle depend on the details of how DM-induced cascades of particles and neutrinos themselves propagate in the dense matter. Needless to mention that proper description of neutrino propagation should also include neutrino oscillations. As a result neutrino fluxes from DM annihilations in the Sun (see, e.g., [411] and references therein) differ from the ones obtained based on spectrum at production outside a dense matter object (see, e.g., [226]).

Experiments and anomalies Neutrino telescopes (for review see, e.g., [412]) can be divided into two main categories: muon counters (BAKSAN [413]) and water Cherenkov detectors (ANTARES, IceCube, SuperK).¹⁴ The latter technology will also be used in planned neutrino telescopes, e.g., BAIKAL-GVD [416], IceCube-PINGU [417], HyperK [418] and KM3Net [419]. The most important background in searches for DM-induced neutrinos originates from neutrinos produced in scatterings off cosmic rays in the Earth’s atmosphere [420]. On the other hand muons produced in the Earth’s atmosphere can be vetoed more easily in analysis focusing on upward going events. An additional source of background is associated with neutrinos produced in the Sun’s atmosphere [421], though it is expected to be a subdominant contribution [412].

Recently, some interest was raised by an observation of neutrinos with very high energies from tens of TeV up to several PeV reported by the IceCube Collaboration [422–424]. Various possible explanations were proposed including neutrino production through annihilations [425] or decays [426] of the DM particles. However, the observed signal seems to be isotropic and is consistent with the Waxman-Bahcall bound [427], which can be derived from the spectrum of high-energy cosmic rays emitted by astrophysical sources when one takes into account a fraction of energy carried away by neutrinos. This points towards a non-DM origin of the reported anomaly (for recent review see, e.g., [428] and references therein). Future generation of neutrino telescopes should allow to collect more data and therefore clarify this issue.

¹³In principle one should also take into account the evaporation process of the DM particles from the Sun, but it is negligible for $m_\chi \gtrsim 4$ GeV [410].

¹⁴Neutrino reactor experiments can also be used to constrain DM properties (see, e.g., recent studies about this in the case of JUNO [414] and KamLAND [415] detectors).

Limits As mentioned above, searches for DM-induced neutrinos can provide the strongest up-to-date limits on the spin-dependent cross section σ_p^{SD} while current limits on the spin-independent component σ_p^{SI} , as well as on the annihilation cross section σv , remain weaker than the ones derived from DD and ID experiments, respectively.

3.6 X-rays: limits and the 3.5 keV line

In 2014 a possible excess in the X-ray emission near 3.5 keV was reported after analyzing the XMM-Newton data from observations of the Andromeda galaxy and various galaxy clusters with possible connection to decays of sterile neutrino DM [429, 430] (see also e.g., [431, 432]). Subsequently, the signal was confirmed in the data obtained by the Suzaku telescope for core of the Perseus cluster [433], in the XMM-Newton data for the GC [434] and in the deep field observations by NuSTAR [435] and Chandra [436]. Interestingly, such a signal was predicted as a smoking gun for WDM in an early study [437]. In addition to sterile neutrinos, further DM interpretations of the 3.5 keV line were proposed employing, e.g., axion-like particles [438, 439], axinos [440, 441] or gravitinos [442].

The DM interpretation of the line observed in XMM-Newton data was, however, undermined by some of later studies (see, e.g., [443, 444]), as well as by results obtained for several galaxy clusters by the Suzaku telescope [433], XMM-Newton observations of the Draco dwarf galaxy [445] and the HITOMI data for the Perseus cluster [446]. Other explanations were then discussed in the literature including known emission lines from the transitions in potassium and chlorine atoms [443] (see, however, [447]) and charge exchange between bare sulfur ions and neutral hydrogen atoms [448, 449]. In addition, in [443] it was argued that a similar spectral feature is present in the data from the Tycho supernova remnant, where one does not expect to see significant amounts of DM. On the other hand, it was pointed out that the aforementioned null results of experimental searches for the 3.5 keV line are still consistent with the decaying DM interpretation discussed above while other astrophysical explanations might be insufficient to explain the observed excess [56].

At this stage both the DM interpretation, as well as astrophysical explanation of the observed 3.5 keV line cannot be fully excluded.

3.7 LHC mono-X searches

The third classical strategy for WIMP dark matter searches, after direct and indirect detection, is to directly produce a neutral stable particle in high-energy colliders. Since the typical coupling and mass range expected for the WIMP in most scenarios is around or just above EWSB, the LHC can provide in principle an optimal instrument for pursuing this experimental venue.

In fact, the vast majority of the searches for new physics at the LHC are designed to look for events that, besides the rich hadronic/leptonic activity emerging from the decay chain of the produced visible particle, are also characterized by a large amount of missing energy, as this simplifies the task of separating them from the SM backgrounds and optimize the chances for detection. In this sense, then, the discovery of one or more visible particles in a channel characterized by highly energetic jets or leptons, and large missing momentum,

would also imply the discovery of a neutral and stable (at least within the detector bounds) particle, which could be part of the dark matter or even all of it.

In many scenarios, however, one contemplates the possibility that the dark matter WIMP is the only new field around the electroweak scale, while additional visible particles, if existing, are sitting beyond the realistic reach of the detector. In this case the detection strategy must involve the identification in the scattering event of one (or a few) isolated, highly energetic, object(s) from initial state radiation (ISR), accompanied by large missing momentum. The object recoiling against the produced invisible particles can be a jet, a gauge boson, or a lepton, so that searches of this typology are commonly referred to in the literature as Mono-X and have generated a great amount of activity and excitement in recent years.

While the LHC mono-X search results have been recast in and applied to numerous models with EW dark matter interactions, and they proved particularly useful in probing compressed spectra in supersymmetry, most official comparisons with the bounds from direct and indirect detection have been presented by ATLAS and CMS in two preferential frameworks: EFT and simplified model spectra (SMS).

In the EFT framework [450–458], which was predominantly used by the LHC collaborations for their interpretations in Run 1 [459–464], one derives bounds on the strength of several contact operators, which can be then employed for a comparison with the limits on σ_p^{SI} and σ_p^{SD} from direct detection searches and neutrino detectors.

The EFT can in principle provide a good approximation as long as the interaction is mediated by particles with mass well above the collision energy. It was however pointed out in several papers [465–470] that one should use special care when comparing the Wilson coefficient bounds arising from mono-X searches with those from underground direct detection searches, as the processes involved happen at widely different scales (the EWSB scale in the former case, and the nuclear scale in the latter). The effects of renormalization group running should be properly taken into account, particularly in cases when operator mixing introduces non-negligible corrections to the expected event rates in underground detectors.

Moreover, at the center-of-mass energies typically probed in a collider environment it is often necessary to consider models defined in terms of renormalizable interactions. By making use of SMS [471–477], one introduces simple renormalizable Lagrangians, characterized by a limited number of free parameters, like the couplings of the dark matter to the visible sector, or the mass of the particles assumed to mediate the interaction between the dark matter and the partons in the nucleons.

In Fig. 10(a) we show the bounds from the CMS mono-jet search [463] in the $(m_\chi, \sigma_p^{\text{SD}})$ plane at the end of Run 1. Note that the limit is actually placed on the effective coupling, $1/\Lambda^2$, of a dimension-6 axial-vector operator (where running and operator-mixing effects are neglected). The equivalent CMS bound at the end of Run 2 [478] is shown in Fig. 10(b). It is now expressed in terms of a simplified model with Dirac dark matter, axial-vector mediator, and specific coupling strengths (see [479] for the equivalent ATLAS bound). The typical “hook” shape of the exclusion contour is due to the fact that for any specific dark matter mass the data excludes a range of mediator masses. Additional bounds on the

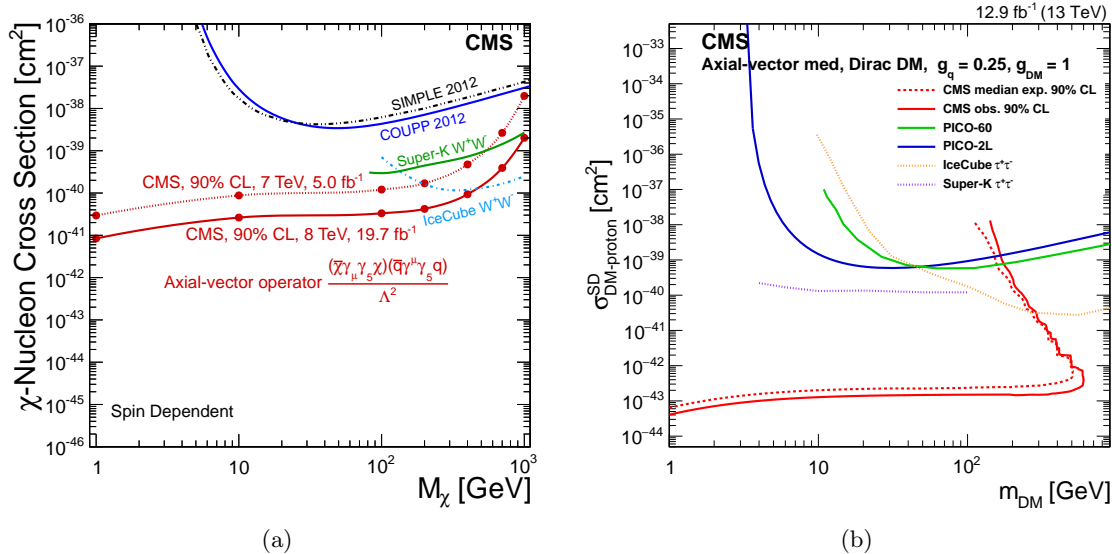


Figure 10: (a) The CMS mono-jet bound in the $(m_\chi, \sigma_p^{\text{SD}})$ plane at the end of Run 1, interpreted in the EFT framework. Plot taken from Ref. [463]. (b) The most recent CMS Run 2 mono-jet bound in the $(m_\chi, \sigma_p^{\text{SD}})$ plane, interpreted in the SMS framework. Plot taken from Ref. [478].

spin-independent cross section, σ_p^{SI} , and the annihilation cross section, σv , can be found in the experimental papers.

It is worth pointing out that the upper bounds of Fig. 10 are especially competitive in the low range of the dark matter mass spectrum, as the probability of emission of a high p_T jet drops drastically when m_χ approaches the p_T cut. Since in the remainder of this review we focus predominantly on WIMPs of mass in the hundreds of GeV to a few TeV range, we will avoid discussing mono-jet bounds in greater detail. Excellent reviews exist in the literature exploring the LHC bounds on a large range of light and not-so-light dark matter scenarios. For a very recent one see, e.g., [9] and references therein.

4 The neutralino WIMP as DM

Despite the disappointing failure to discover any superpartners at the LHC (and, in fact, any trace of “new physics”), low scale supersymmetry (SUSY) still remains arguably by far the best motivated scenario for “new physics” beyond the Standard Model. A detailed review of SUSY exceeds the purpose of this work, but numerous extensive reviews exist in the literature (see, e.g., [480–482]). We limit ourselves to recalling a few basic notions that will be relevant for the connection to DM.

4.1 Brief review of supersymmetry and the neutralino as dark matter

SUSY is a space-time symmetry relating each particle of the SM to a partner whose spin differs by $1/2$. We only consider here $\mathcal{N} = 1$ SUSY, where the space-time algebra is extended by exactly one spinorial SUSY generator, as this is the only case that admits

a phenomenology with chiral fermions, and constitutes a straightforward extension of the particle content of the SM.

Initially developed on the basis of aesthetic and “proof-of-existence” considerations, in the eighties it became arguably the most popular solution to the gauge-hierarchy problem. Roughly speaking, if a low-energy effective theory – as the SM is thought to be – includes light fundamental scalar fields, like the Higgs boson, the mass of the scalar particles is subject to strong renormalization by the fields of the UV completion. If the UV completion typical scale is close to the scale of quantum gravity, one needs a fine tuning of approximately 28 orders of magnitude to justify a scalar mass of the order of the EW scale. SUSY provides an attractive solution to this problem thanks to the non-renormalization theorem [483, 484] which precludes one-particle irreducible loop corrections to the superpotential so that, as a consequence, mass terms do not get renormalized. In other words, SUSY “protects” the Higgs mass of the SM and makes it technically natural.

Apart from solving the gauge hierarchy problem, SUSY provides a framework that naturally accommodates at the same time several theoretical expectations and a number of experimental data. Low-energy SUSY, in particular, the Minimal Supersymmetric Standard Model (MSSM), provides the right particle content for high-scale gauge coupling unification; it furnishes a rationale for the measured values of the mass of the Higgs boson and of the top quark; it provides a natural framework for models of inflation and baryo/leptogenesis; radiative electroweak symmetry breaking (EWSB) can easily be achieved in the MSSM; and, finally, but perhaps most importantly for the scope of this review, some superpartners are weakly interacting and, if stable (or very long lived) are a natural candidate for a WIMP and DM. Among them the most popular one is the lightest neutralino, which we will refer to simply as *the neutralino* and denote with a symbol χ hereafter. Countless studies, starting from [93, 94], showed it to be an excellent thermal DM candidate.

We remind the reader that the low-energy Lagrangian of the R parity-conserving MSSM consists of two parts. One comes from the superpotential, expressed in terms of superfields (marked by carets), which essentially provides a direct supersymmetrization of the Yukawa part of the SM Lagrangian:

$$W_{\text{MSSM}} = \mathbf{y}_u \hat{U}^c \hat{H}_u \hat{Q} - \mathbf{y}_d \hat{D}^c \hat{H}_d \hat{Q} - \mathbf{y}_e \hat{E}^c \hat{H}_d \hat{L} + \mu \hat{H}_u \hat{H}_d, \quad (4.1)$$

where the $\mathbf{y}_{u,d,e}$ are 3×3 Yukawa matrices and μ is the Higgs/higgsino mass parameter.

The other part is the so-called “soft” SUSY-breaking Lagrangian, which includes mass terms for the gauginos (Majorana fermion superpartners of the gauge bosons) and for the scalar superpartners of the SM fermions:

$$\begin{aligned} \mathcal{L}_{\text{soft}} = & -\frac{1}{2} \left(M_3 \tilde{g} \tilde{g} + M_2 \tilde{W} \tilde{W} + M_1 \tilde{B} \tilde{B} + \text{c.c.} \right) \\ & - \left(\mathbf{a}_u \tilde{u}^\dagger H_u \tilde{Q} + \mathbf{a}_d \tilde{d}^\dagger H_d \tilde{Q} + \mathbf{a}_e \tilde{e}^\dagger H_d \tilde{L} + \text{c.c.} \right) \\ & - \tilde{Q}^\dagger \mathbf{m}_Q^2 \tilde{Q} - \tilde{L}^\dagger \mathbf{m}_L^2 \tilde{L} - \tilde{u}^\dagger \mathbf{m}_u^2 \tilde{u} - \tilde{d}^\dagger \mathbf{m}_d^2 \tilde{d} - \tilde{e}^\dagger \mathbf{m}_e^2 \tilde{e} \\ & - m_{H_u}^2 H_u^* H_u - m_{H_d}^2 H_d^* H_d - (b H_u H_d + \text{c.c.}), \end{aligned} \quad (4.2)$$

where M_1 is the mass of the bino, M_2 of the wino, and M_3 of the gluino, which are the fermionic partners of the B , the W triplet and the gluon octet. The matrices \mathbf{m}_Q^2 , etc, \mathbf{a}_u ,

etc, and b , stand for mass squared, trilinear, and bilinear coefficients for the scalar fields, respectively.

The gauginos transform under the adjoint representation of the respective gauge groups so that, in particular, the bino transforms as a $U(1)$ phase and three wino states form a triplet of $SU(2)$. In addition, there exist two more Majorana fermions, the higgsinos of mass μ , which belong to $SU(2)$ doublets. The bino and the neutral degrees of freedom of the the winos and the higgsinos have the same quantum numbers and the neutralinos are their mass eigenstates. The masses are obtained by diagonalizing the mass matrix M_χ given by

$$\mathbf{M}_\chi = \begin{bmatrix} M_1 & 0 & -\frac{g'}{\sqrt{2}}v_d & \frac{g'}{\sqrt{2}}v_u \\ 0 & M_2 & \frac{g}{\sqrt{2}}v_d & -\frac{g}{\sqrt{2}}v_u \\ -\frac{g'}{\sqrt{2}}v_d & \frac{g}{\sqrt{2}}v_d & 0 & -\mu \\ \frac{g}{\sqrt{2}}v_u & -\frac{g}{\sqrt{2}}v_u & -\mu & 0 \end{bmatrix}, \quad (4.3)$$

where g and g' are $SU(2)$ and $U(1)$ gauge couplings, respectively, and v_u and v_d are the vevs of the neutral components of the Higgs doublets H_u and H_d .

While it is the mass eigenstates that are the physical states, they can be dominated by some gauge eigenstates which allows one to make convenient approximations. In the limit where one among M_1 , M_2 , and μ is much smaller than the other parameters, the lowest eigenvalue approximately coincides with the lightest of these masses. In other words, $m_\chi \approx M_1$ when $M_1 \ll M_2, \mu$, and so on for interchanging orders. When two or more masses are instead comparable, mixing effects come into play and can change the phenomenology. In this context, it became clear after the LHC Run 1 and beginning of Run 2 that gaugino and higgsino masses are likely to be well above the Higgs vevs, i.e., $M_1, M_2, \mu \gg v_u, v_d$.

The most popular extension of the MSSM is arguably the Next-to-Minimal Supersymmetric Standard Model (NMSSM), which can provide an elegant solution to the μ problem (see, e.g., [485] for a comprehensive review). In the NMSSM there is one additional kind of neutralino, the singlino, which is the fermionic partner of the gauge singlet Higgs field.¹⁵ Because of the presence of the singlino, the NMSSM can sometimes present complementary DM signatures with respect to the MSSM.

The neutralinos, being electric and color charge-neutral, interact with the SM with the strength of the weak interaction. The lightest among them, if it is the lightest supersymmetric particle (LSP), is stable provided an additional discrete symmetry (R -parity) is assumed. Note, incidentally, that R -parity violation is in general strongly constrained by bounds on proton decay and precision tests of the SM [70]. Below we will review the properties of the neutralino and the present status of this important candidate that has become over time the paradigm of WIMP DM.

¹⁵In the NMSSM the superpotential includes additional terms involving a gauge singlet chiral superfield \hat{S} , i.e., $W \supset \lambda \hat{S} \hat{H}_u \hat{H}_d + \kappa/3 \hat{S}^3$.

4.2 Neutralino relic abundance

We will now discuss in more detail the mechanisms that can lead to the correct value of the neutralino DM relic density. As we will see, this often requires going beyond the simplest WIMP picture that we discussed in Section 2.2.1. In particular, for the bino-like neutralino (i.e., for $m_\chi \approx M_1$), which early on [486] was the most favored scenario in SUSY models with gaugino mass unification at the GUT scale, one typically obtains too small an annihilation cross section and, therefore, exceedingly large values of the DM relic density. However, this can be improved by assuming specific mass patterns for the neutralinos and some other SUSY particles.

4.2.1 Coannihilations

One of the most important mechanisms where specific mass relations between the LSP and some other states determine the relic abundance is coannihilations (see Sec. 2.2). In phenomenologically interesting scenarios the lightest neutralino can be mass degenerate with some heavier supersymmetric species (which usually is the next-to-lightest supersymmetric particle, or NLSP) thus fulfilling some of the conditions where coannihilations can play a major role in determining the DM relic density. The mass degeneracy can lead to either a decrease or an increase of the final relic abundance, depending on whether the NLSP freeze-out occurs later or earlier than for the LSP.

The neutralino-chargino mass degeneracy plays a major role in determining $\Omega_\chi h^2$ for a wino- or higgsino-like neutralino. This is due to characteristic mass degeneracies between the higgsino-like (in which case $m_\chi \approx \mu$) or the wino-like (with $m_\chi \approx M_2$) neutralino and the lightest chargino or the second lightest neutralino that appear naturally in the MSSM – recall that higgsinos are $SU(2)$ doublets and winos are $SU(2)$ triplets.

The correct value of $\Omega_\chi h^2$ can be obtained without assuming any special mass relations. This is mainly due to the fact that the most efficient annihilation and coannihilation channels are in this case determined by the processes whose strength is set by the respective gauge couplings. As a result, the relic abundance $\Omega_\chi h^2 \sim 1/\sigma_{\text{ann}} \sim m_\chi^2/g^4$ shows a simple parabolic dependence on the neutralino mass.

The wino and, to a much lesser extent, higgsino relic density are also influenced by the Sommerfeld enhancement which is the enhancement of the annihilation cross section due to a modification of the Yukawa potential induced by the electroweak gauge bosons [487] (see also [488, 489] for a recent discussion). This effect is particularly important in the wino mass range for which one obtains $\Omega_\chi h^2 \approx 0.12$, which is then broadened to $M_2 \approx 2-3$ TeV. Although the Sommerfeld enhancement is most important for a nearly pure wino, it can also play a role for a mixed wino/higgsino state, thus modifying the relevant area of the so-called relic neutralino surface in the parameter space at which the correct value of the relic density is achieved [490]. In the case of the higgsino-like neutralino the relic density is reduced mainly thanks to a triple mass degeneracy between the two lightest neutralinos and the lightest chargino [491]. As a result, the correct $\Omega_\chi h^2$ is obtained for $m_\chi \approx 1$ TeV – we will refer to it as the ~ 1 TeV higgsino region.

In the case of bino-like lightest neutralino an important role in determining the relic density is played by stau coannihilation [492–494] when the LSP is mass-degenerate with the lightest stau, $m_\chi \approx m_{\tilde{\tau}_1} \lesssim 400 - 500 \text{ GeV}$ for $\Omega_\chi h^2 \approx 0.12$. The same effect can be obtained for other sleptons. On the other hand, coannihilations of higgsino-like or wino-like DM with sleptons lead to an increase of the relic density [495]. Interestingly, thanks to this effect one can obtain $\Omega_\chi h^2 \approx 0.12$ for higgsino mass as small as $m_\chi \approx 600 \text{ GeV}$ [209].

Coannihilations with squarks can lead to the correct value of the lightest neutralino relic density for a significantly heavier neutralino. In particular, such coannihilations can occur with the lightest stop [496], \tilde{t}_1 , or with the lightest sbottom, \tilde{b}_1 , which are often the lightest squark states [497]. A similar mechanism leads to a reduction of $\Omega_\chi h^2$ for a heavy neutralino mass-degenerate with the gluino, i.e., when $m_\chi \approx m_{\tilde{g}}$ [498]. For both the stop and gluino coannihilation it is possible to obtain $\Omega_\chi h^2 \approx 0.12$ for m_χ as large as 6–9 TeV when the Sommerfeld enhancement and gluino-gluino bound-state effects are incorporated [499, 500], although this should not be treated as a strict upper limit on phenomenologically acceptable values of m_χ .

In the framework of the NMSSM a nearly pure singlino, which can be the lightest neutralino, typically interacts very weakly. It annihilates mainly into scalar-pseudoscalar pairs, with the associated couplings proportional to κ or λ (cf. Footnote 15), which are typically small. As a result, the singlino relic density is often too large. However, this can be improved thanks to coannihilations with an higgsino, a wino, a stau/sneutrino, a stop, or a gluino (for a detailed discussion see [501]).

4.2.2 Funnel

Another important mechanism that can enhance neutralino pair annihilation and lead to the correct value of the relic density of neutralino DM in the MSSM is due to annihilations via the resonant s -channel exchange of the Z -boson, the light Higgs h [502], and/or heavy (pseudo)scalar Higgs bosons H and A , in the respective resonance (or funnel) regions of the parameter space [503] if the exchanged particle mass m is roughly twice m_χ . In a more precise treatment this condition is slightly modified by taking into account the thermal average of the relative velocity of annihilating neutralinos in the early Universe. Hence both the Z -resonance and the h -resonance regions require a light neutralino ($m_\chi < 100 \text{ GeV}$), as $m_Z = 91 \text{ GeV}$ and $m_h = 125 \text{ GeV}$. On the other hand, in the A -funnel region the lightest neutralino can be much heavier. In the NMSSM, where the Higgs spectrum is richer, accordingly more resonance channels are in principle possible.

4.2.3 Other mass patterns

In the absence of any accidental mass patterns, the bino annihilation rate is typically dominated by a t -channel slepton exchange, $\chi\chi \rightarrow ll$, and consequently $\Omega_\chi h^2 \sim m_{\tilde{l}}^4/m_\chi^2$ is also sensitive to the mass of the lightest slepton, $m_{\tilde{l}}$ [486, 503]. This can lead to the bino relic density spanning a few orders of magnitude depending on both relevant masses. In particular, one can obtain $\Omega_\chi h^2 \approx 0.12$, if $m_{\tilde{B}} < m_{\tilde{l}} \lesssim 150 \text{ GeV}$, in the so-called bulk region [75, 486, 503].

Another important option is associated with a general mixed bino-higgsino LSP. In the mass range $100 \text{ GeV} \lesssim m_\chi \lesssim 1 \text{ TeV}$ a nearly pure higgsino χ typically yields too small a value of the relic density (while for a pure bino it is typically too large). This can be circumvented for choosing an appropriate (“well-tempered”) admixture of \tilde{B} and $\tilde{H}_{u,d}$. In the context of GUT-constrained SUSY models such a scenario can be realized in the so-called hyperbolic branch/focus point region [504, 505]. The annihilation rate in this case is dominated by neutralino annihilations into gauge bosons, as well as through a t -channel exchange of a higgsino-like chargino and/or the second lightest neutralino.

Among other scenarios with mixed neutralino LSP that have been discussed in the literature one can distinguish the mixed bino-wino (see, e.g., [506–508], singlino-higgsino (in the context of the NMSSM) [501] or even bino-higgsino-wino (see, e.g., [509, 510]) states.

One loop corrections to annihilation cross sections can provide some improvement in the computation of the neutralino relic density that can introduce corrections of the order of the observational error and therefore should be taken into account when estimating the uncertainty of the determination of $\Omega_\chi h^2$ (see, e.g., [511, 512] or recent [513, 514] and references therein).

4.3 Simplest models defined at the GUT scale: the CMSSM and the NUHM

As was mentioned above, the MSSM can feature many non-trivial phenomenological signatures and it is important to understand that predictions in different sectors of the theory can be intertwined.

In this subsection, we show how these relations affect the DM predictions in two popular SUSY models with simple unified, or constrained, boundary conditions set at the GUT scale, the constrained MSSM (CMSSM) [515] and the Non-Universal Higgs Model (NUHM) [516]. The CMSSM, inspired by supergravity constructions, is characterized by a set of four parameters defined at the GUT scale: the unified scalar and gaugino masses, m_0 and $m_{1/2}$, respectively; the unified trilinear coupling A_0 ; ratio of the Higgs vevs $\tan \beta$, and the sign of the μ parameter. In the NUHM, one instead does not assume the soft Higgs masses $m_{H_u}^2$ and $m_{H_d}^2$ to be unified with the other scalar masses at the GUT scale, thus introducing two additional free parameters. For many years these models remained an important playground for SUSY phenomenology in the context of unification. In particular, we focus on the implications of the recently discovered the Higgs boson with mass close to 125 GeV and the nature and associated discovery prospects of the DM.

In Sec. 4.4, we extend the analysis to a more general case of the phenomenological MSSM (pMSSM), which roughly encompasses the remainder of signatures and possibilities for the discovery of neutralino DM in the general MSSM.

First, however, we discuss important implications of the properties of the Higgs boson discovered at the LHC on the expected mass range of superpartners. As we will see, in the framework of unified SUSY models this will have important ensuing implications for the nature and discovery prospects of WIMP DM in this class of models.

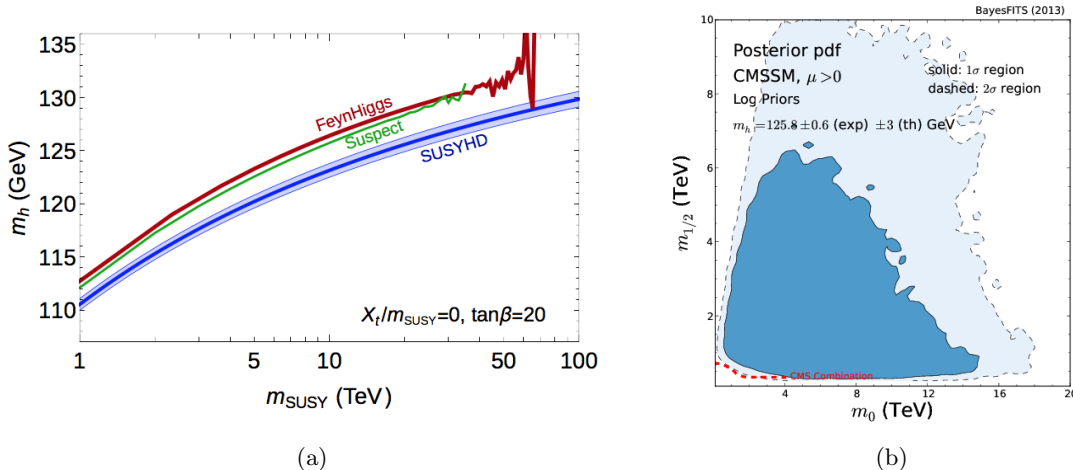


Figure 11: (a) A calculation of the Higgs mass obtained with different numerical programs. Taken from Ref. [518]. (b) The 1σ and 2σ regions of marginalized 2-dimensional posterior probability density function in the CMSSM that are consistent with the Higgs mass. Taken from Ref. [519].

4.3.1 Implications of the Higgs boson for SUSY breaking scale

In the MSSM the mass of the Higgs boson is not a free parameter of the theory, in contrast to the SM. Its value is calculated in terms of the parameters of the model. Since the quartic couplings of the Higgs fields are roughly given by the EW gauge couplings, the tree-level value of the Higgs mass presents an upper bound determined by the mass of the Z boson, M_Z . As a consequence, the observed value of the Higgs mass, $m_h = 125$ GeV, implies the presence of significant radiative corrections, which increase logarithmically as the SUSY scale increases.

It is convenient to express the dominant 1-loop contribution to the radiative corrections of the Higgs mass in terms on the stop mass and stop mixing (see, e.g., [517]),

$$\delta m_h^2 \approx \frac{3y_t^4}{16\pi^2} v^2 \left[\ln \left(\frac{M_{\text{SUSY}}^2}{m_t^2} \right) + \frac{X_t^2}{M_{\text{SUSY}}^2} \left(1 - \frac{X_t^2}{12M_{\text{SUSY}}^2} \right) \right], \quad (4.4)$$

where y_t and m_t are the top Yukawa coupling and the top quark mass computed in the \overline{MS} scheme, respectively, $v = \sqrt{v_u^2 + v_d^2} \simeq 246$ GeV is the EW vev, the SUSY scale is set at the geometrical average of the stop masses, $M_{\text{SUSY}} = \sqrt{m_{\tilde{t}_1} m_{\tilde{t}_2}}$, and $X_t = A_t - \mu \cot \beta$ gives the main stop mass matrix off-diagonal term.

Equation (4.4) is sufficient to describe the qualitative behavior of the Higgs boson mass but higher-order corrections are necessary to obtain a more precise quantitative estimate of the favored value of M_{SUSY} after the Higgs discovery. Several numerical codes are available to calculate the Higgs mass in terms of the MSSM parameters. The results are subject to significant uncertainty, which is due to missing higher-order loop corrections, the choice of renormalization scheme, etc. Figure 11(a), taken from Ref. [518], presents a comparison of the Higgs mass obtained by different codes. The dependence on the geometrical average of the stop masses, M_{SUSY} , is presented in the MSSM. Fig. 11(b),

taken from Ref. [519], shows in the plane $(m_0, m_{1/2})$ of the CMSSM the 1σ and 2σ regions of marginalized 2-dimensional posterior probability density function (pdf) consistent with the Higgs mass, taking into account errors, both experimental (which have since decreased considerably) and theoretical (which are estimated at the level of $2 - 3$ GeV). One can see that the measured Higgs mass value alone suggests typical superpartner masses to be in the multi-TeV range. Strictly speaking, in phenomenological models like the phenomenological MSSM (pMSSM) this conclusion applies to the masses of the stops, but in unified models this sets the overall scale of SUSY breaking, since in those models superpartner masses are related by boundary conditions in the UV. Note, that no additional conditions, in particular of satisfying the relic density constraint, have been imposed here.

We stress that the above conclusion applies not only to the CMSSM, but to a much wider class of models, some equally well inspired by supergravity, like the NUHM and non-universal gaugino mass models, and other ones for which SUSY breaking is transmitted to the visible sector via other high-scale messengers, like in the case of gauge mediation. On the other hand, multi-TeV expectations for the scale of superpartner masses are independently supported by increasingly stringent lower limits from the LHC and by the lack of any convincing departure from Standard Model values of rare processes involving flavor, e.g., $b \rightarrow s\gamma$, $B_s \rightarrow \mu^+\mu^-$, etc.

4.3.2 Neutralino DM in unified models in light of LHC and other recent data

The requirement that the neutralino relic density is close to the observed value places an additional strong constraint on unified SUSY models. (In contrast, the impact of limits from direct searches for DM has not been as strong as that from collider searches [520].) In these models this additionally implies specific properties for the neutralino LSP and, therefore, for DM searches.

A large number of global studies (see, e.g., [210, 519, 521–537]) has been performed over the recent years in which the parameter space of the CMSSM was confronted with a broad set of experimental constraints on several observables: the Higgs mass and the Higgs decay rates in different channels at the LHC; the value of the relic density as measured by PLANCK (and previously WMAP); the lower bounds on SUSY masses as directly measured by CMS and ATLAS; the measured values of several b -physics rare decays like, e.g., $\text{BR}(\bar{B} \rightarrow X_s\gamma)$, $\text{BR}(B_s \rightarrow \mu^+\mu^-)$, or $\text{BR}(B_u \rightarrow \tau\nu)$; the measurement of the anomalous magnetic moment of the muon, $\delta(g-2)_\mu$, which shows a $\sim 3\sigma$ discrepancy with the SM value. In the modern, state-of-the-art approach, these constraints are generally implemented via a global likelihood function, constructed to compare the measured value of the observables with their calculated values in the SUSY parameter space. Observables are usually calculated with sophisticated numerical codes, and the likelihood function is used to determine statistically preferred likelihood (if one performs a frequentist analysis based on the profile likelihood) or, alternatively, credibility (if one performs instead a Bayesian analysis based on the posterior probability) regions of the parameter space.

In Fig. 12(a) we present the 1σ and 2σ Bayesian credibility regions of the marginalized posterior probability in the $(m_0, m_{1/2})$ plane of the CMSSM. The figure presents an updated version of plots previously shown in Refs. [519] and [210], obtained now by incorporating in

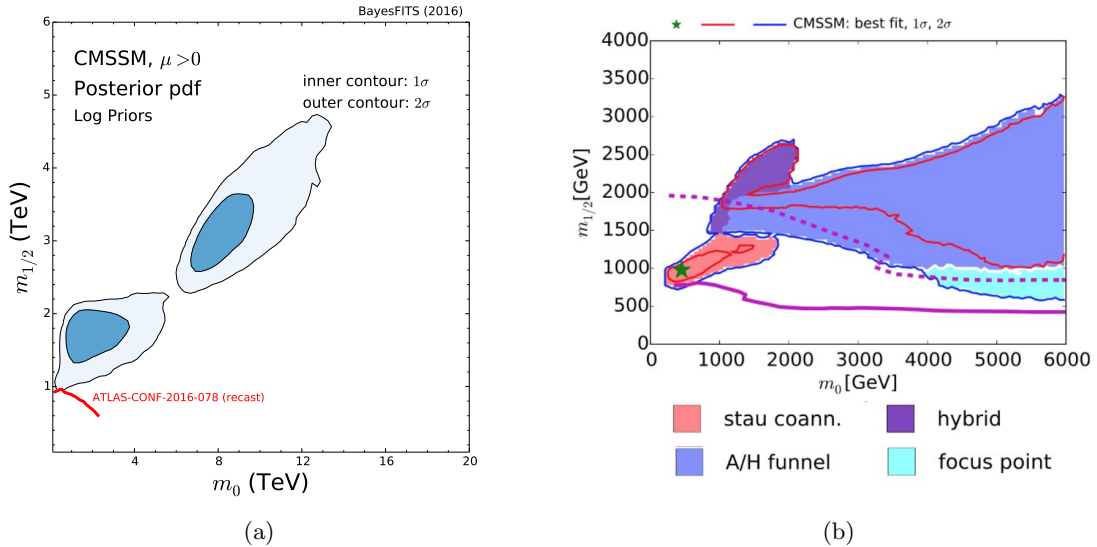


Figure 12: (a) The updated 1σ and 2σ Bayesian marginalized credibility regions of the $(m_0, m_{1/2})$ plane according to the BayesFITS group. [210, 519]. The most recent constraint from SUSY searches at the LHC [538], recast using the code of [539], is shown as a solid red line for comparison. (b) The 1σ and 2σ profile-likelihood regions in the $(m_0, m_{1/2})$ plane of the CMSSM according to the MasterCode group [540]. The color code describes the mechanism for the neutralino relic abundance in each region.

the likelihood function the most recent constraints from direct squark and gluino searches at the LHC [538] (we use the code of Ref. [539] to recast the experimental data) and the recent constraints from direct searches of DM in LUX [171]. In Fig. 12(b) we show the 1σ and 2σ likelihood regions in the $(m_0, m_{1/2})$ plane of the CMSSM, following from a frequentist analysis of Ref. [540]. The color code is used to indicate the different mechanisms by which the correct relic density of the neutralino is obtained in the early Universe, see Sec. 4.2.

Note that credibility and likelihood regions are not extremely dissimilar from one another (within the overlapping ranges of m_0 and $m_{1/2}$) despite the very different concepts of statistics applied in both panels. In the bottom left corner of Fig. 12(a) one can see a Bayesian credibility “island”, representing the bulk of the A -funnel region and a faint appearance of the stau-coannihilation region surviving the most recent LHC bound, in agreement with Fig. 12(b). This is the region of the parameter space where the neutralino is predominantly bino-like.

In Fig. 12(a) the parameter space is scanned to larger values of m_0 and $m_{1/2}$, well into the TeV-scale region that most easily allows one to accommodate the correct value of the Higgs mass. This region features the existence of a second, and actually larger, “island” in the parameter space, characterized by an almost pure higgsino-like neutralino that, as was explained in Sec. 4.2, is characterized by the LSP higgsino-like mass around 1 TeV in order to give the correct relic density. Frequentist analysis also shows the emergence of this region, despite the smaller region of m_0 and $m_{1/2}$ covered in Fig. 12(b).

Taking the view that the Higgs mass implies a multi-TeV scale of superpartners, having the LSP at 1 TeV without having to adhere to any special mechanism for obtaining

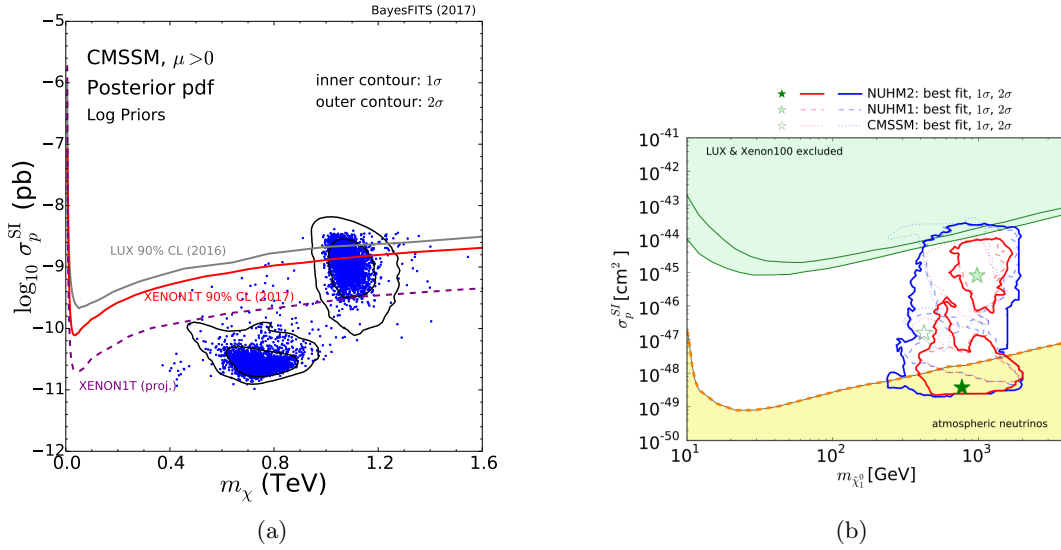


Figure 13: (a) Solid contours show the Bayesian 1σ and 2σ credible regions of the CMSSM in the $(m_\chi, \sigma_p^{\text{SI}})$ plane, with LHC and DD constraints updated with respect to [210, 519]. The scattered blue points, sampled from the posterior probability distribution, belong to the 2σ region of the global profile likelihood. For comparison, the solid gray line marks the final published 90% C.L. LUX bound [171], which is included in the likelihood function. The solid red line shows the recent first limit from XENON1T [169], whereas the dashed purple line gives the projected reach of XENON1T. (b) The 1σ (red solid) and 2σ (blue solid) profile likelihood region in the $(m_\chi, \sigma_p^{\text{SI}})$ plane of the NUHM according to the MasterCode group [541].

the right $\Omega_\chi h^2$ appears to be a rather intriguing and well motivated solution [520], with promising prospects for DM searches, as discussed below.

4.3.3 Prospects for WIMP searches in GUT-constrained models

Contours of the 68% and 95% Bayesian credible region of the CMSSM in the $(m_\chi, \sigma_p^{\text{SI}})$ plane are shown in Fig. 13(a), which updates the equivalent plots presented in Refs. [519] and [210]. As stated above, the likelihood function includes the recently published LUX data [171], which we have incorporated here following a procedure similar to Ref. [361]. Note that in recent years several numerical codes have been devised to appropriately account for DD data in the form of a likelihood function, see Refs. [542–545]. To facilitate comparison, we mark as a solid gray line in Fig. 13(a) the 90% C.L. upper bound as given by the LUX collaboration. The newest first results from XENON1T [169] are shown instead as a solid red line.

Note how parts of the 95% credible posterior regions extend somewhat above the 90% C.L. limit given by the experimental collaboration. This is due, on the one hand, to the non-negligible difference that exists between the 90% and 95% confidence bound (which Ref. [546] did not take into account) when the likelihood function is not very steep over the parameter space. On the other hand, as the likelihood function’s slope is quite gentle, the probability density shows some sensitivity to the choice of Bayesian priors, which in this case pull towards larger values of σ_p^{SI} by favoring lighter gauginos. If, for instance, a

linear (flat) prior was chosen instead, then the ~ 1 TeV higgsino would become even more pronounced. However, the corresponding ranges of σ_p^{SI} are not as much prior-dependent. For completeness, we superimpose to the plot a set of viable scan points (in blue) that, while drawn from the posterior probability density, delimit the extension of the 95% C.L. profile-likelihood region. It is important to note that in the models with unified gaugino masses at the GUT scale, e.g., the CMSSM, one typically does not obtain nearly pure higgsino DM, for which σ_p^{SI} could be arbitrarily low, as it is seen in the low-energy MSSM. Once gaugino masses are allowed to grow large to minimize their mixing with the higgsino component, also the SM-like Higgs boson mass increases due to the impact of gaugino mass parameters on the RGE running of the stop and soft Higgs masses. Precise determination of the lower limit on σ_p^{SI} is sensitive to the accuracy of the calculation of m_h . The results presented in Fig. 13(a) correspond to m_h obtained with `FeynHiggs 2.10.0` [547, 548].

Figure 13(a) shows the same two regions featured in Fig. 12(a): the A -funnel on the left, and the ~ 1 TeV higgsino on the right. The latter clearly presents the better prospects for DM searches, as the bulk of the parameter space falls within the reach of tonne-scale underground detectors, which we summarize here schematically with the dashed purple line giving, technically, the projected 2-year sensitivity of XENON1T from Ref. [201].

It is worth emphasizing that the ~ 1 TeV higgsino region emerges as a robust solution in a much wider class of constrained SUSY models – in fact it appears without having to employ any special mass relations to obtain the correct relic density – as soon as the gauginos become heavier than 1 TeV, consistent with the SUSY breaking scale in the multi-TeV regime, as suggested by the Higgs boson mass value and LHC direct limits on superpartners. As an example, in Fig. 13(b) we show the 1σ (red solid) and 2σ (blue solid) profile likelihood region in the $(m_\chi, \sigma_p^{\text{SI}})$ plane of the NUHM according to the MasterCode group [541]. The figure shows the presence of the ~ 1 TeV higgsino on the right.

In contrast, the existence or not and the relative sizes of the stau-coannihilation and A -funnel regions depend to some extent on the initial boundary conditions assumed for the parameters of the model at hand – as they both require in some form the overlapping of certain mass values that could originate from different sectors of the theory.

4.4 The pMSSM

As we have seen in Sec. 4.3, the ~ 1 TeV higgsino seems to be an attractive candidate for WIMP DM in SUSY models with boundary conditions defined at the GUT scale, and it features very good potential for a timely detection in one-tonne detectors.

Low energy SUSY is a very broad framework, able to accommodate several possibilities for the spectrum of superpartners. As SUSY must be broken in a hidden sector, little is known about the most likely mass pattern for the supersymmetric particles, and one must rely on reasonable assumptions driven by theory considerations. Thus, in order to analyze DM signatures in a general and model-independent SUSY scenario we analyze here the DM issue in the phenomenological MSSM (pMSSM).

The pMSSM [549] is the most general parametrization of the MSSM, based only on assumptions of Minimal Flavor Violation, R -parity conservation, and a level of CP violation not exceeding that of the SM. These assumptions reduce the over hundred free parameters

potentially present in Eq. (4.2) of the MSSM down to 19, all defined at the SUSY scale. It is easy to see that all the scenarios discussed in Sec. 4.3 can be described in this framework by choosing appropriate boundary conditions. The same is true for other popular scenarios for SUSY breaking like, e.g., anomaly mediation [550, 551].

Since the number of free parameters in the pMSSM remains quite large, there is no real issue in fitting all the constraints belonging to the standard set described above. In particular, $\Omega_\chi h^2 \approx 0.12$ – in addition to all relevant collider constraints – can be fairly easily satisfied in different parts of the parameter space for different neutralino WIMP compositions.

We show in Fig. 14(a) the 2σ region in the $(m_\chi, \sigma_p^{\text{SI}})$ plane of the pMSSM, emerging from the profile likelihood of the global constraints. The neutralino composition of the points in green is 90% or more bino-like; points in red are for more than 90% higgsino-like; and points in blue are at least 90% wino-like. Bino/higgsino admixtures are shown in gold, wino/higgsino in magenta, and wino/bino in cyan. Figure 14(a) updates the equivalent plot of Ref. [209], but a similar picture emerges in pMSSM global analyses by other groups, which can feature slightly different choices for the set of constraints or in the number of input parameters (see, e.g., [540, 552, 553]). Note that the constraints from the 2016 LUX results [171] are implemented in the likelihood function, so that the region marked by gray points, which was belonging to the 2σ region in [209], is now shown as excluded at the 95% C.L. We also show with a solid red line the recent 90% C.L. bound from XENON1T [169], not included in the likelihood function. One can see that there are countless possibilities for a neutralino DM in agreement with all the relevant constraints.

In addition, it is possible to have accidental cancellations in the neutralino couplings to the Z and h bosons, as well as cancellations between the heavy and light Higgs diagrams, which result in the suppression of direct detection cross section in so-called blind spot regions of the parameter space [554–557] (see [558] for a recent study). Several points characterized by bino/higgsino admixtures, shown in gold color in Fig. 14(a), must belong to blind spots to evade the most recent DD bounds. It has been shown, e.g., in [559], that LHC searches for heavy Higgs bosons in the $\tau^+\tau^-$ channel are currently extensively probing much of the parameter space giving rise to these special regions.

The strongest indirect limits on the spin-dependent scattering cross section for neutralino DM with mass exceeding the ~ 100 GeV range are given by IceCube/DeepCore [560–562] and ANTARES [404, 563], from observation of neutrinos from the Sun. In Fig. 14(b) we show the bounds as presented in Ref. [209]. The color code highlights the main annihilation final state of the scan points. The plot shows that, while a measurement of σ_p^{SD} remains a very important complementary test, the parameter space of the MSSM is likely to be probed more deeply by other means.

In Fig. 14(c) we show the reach of several γ -ray indirect detection searches in the $(m_\chi, \sigma v)$ plane of the pMSSM with $\Omega_\chi h^2 \approx 0.12$, as a function of the branching fraction $\text{BR}(\chi\chi \rightarrow W^+W^-)$. The figure is taken from Ref. [564]. The points with $m_\chi \approx 2 - 3$ TeV and large branching ratio to W^+W^- are those characterized by a large wino composition (cf. Fig. 14(a)). As these points are subject to the Sommerfeld enhancement [565, 566], a non-perturbative effect that can give a significant boost to the annihilation cross section,

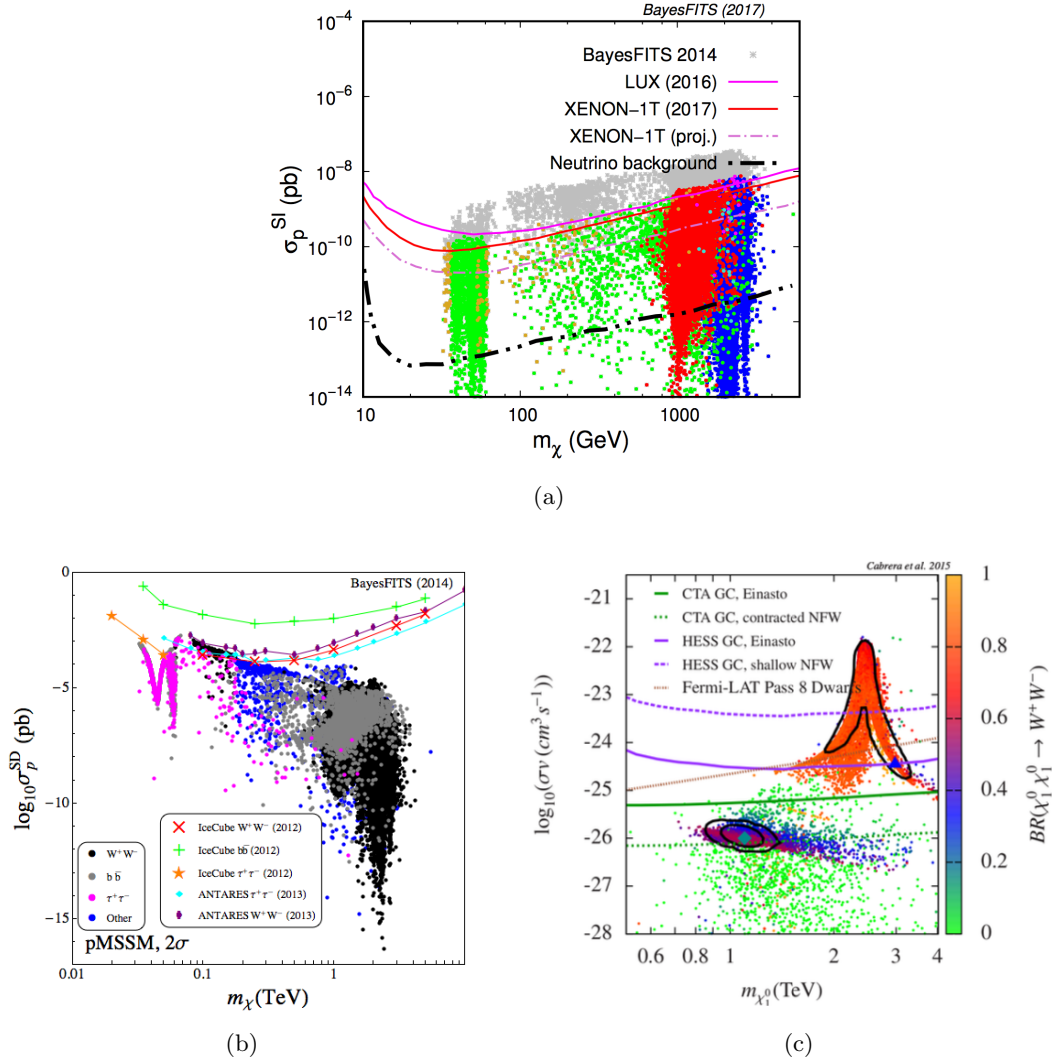


Figure 14: (a) The parameter space of the pMSSM with $\Omega_\chi h^2 \approx 0.12$ in the (m_χ, σ_p^{SI}) plane. Points in green are characterized by a 90% or more bino composition of the neutralino; points in red are $> 90\%$ higgsino; and points in blue are $> 90\%$ wino. Bino/higgsino admixtures are shown in gold, wino/higgsino in magenta, and wino/bino in cyan. The plot updates the equivalent figure in Ref. [209] by including in the likelihood function the DD constraint from [171], which we also show explicitly as a magenta solid line. We have also added the most recent XENON1T bound [169], as a red solid line. (b) A plot of the bounds on σ_p^{SD} from neutrinos from the Sun at IceCube [560–562] and ANTARES [404, 563], for different final states of annihilation, taken from Ref. [209]. The limits are presented for the W^+W^- , $b\bar{b}$, and $\tau^+\tau^-$ final states. (c) The sensitivity of several ID searches to the large mass region of the MSSM in the $(m_\chi, \sigma v)$ plane, as a function of the branching ratio $BR(\chi\chi \rightarrow W^+W^-)$. The figure is taken from [564].

they appear to be in tension with observations from the Galactic Center at the Cherenkov telescope H.E.S.S. [567]. The extent of the tension depends of course on the choice of halo profile. This was observed first in [568–570]. The ~ 1 TeV higgsino region can also be seen in Fig. 14(c), for slightly lower σv , and characterized by $BR(\chi\chi \rightarrow W^+W^-) \approx 0.5$, as the remaining 50% is dominated by the Zh final state.

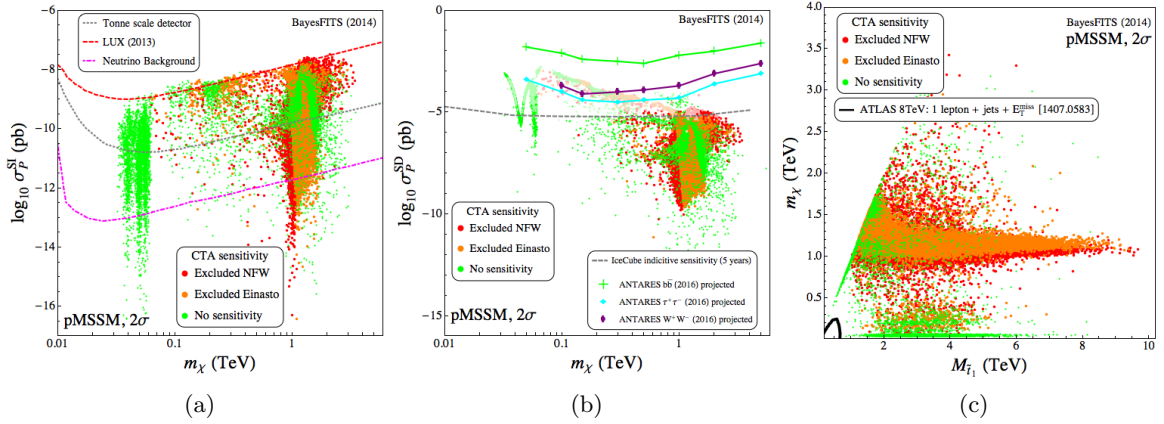


Figure 15: (a) The sensitivity of CTA 500 h Galactic Center observation in the $(m_\chi, \sigma_p^{\text{SI}})$ plane of the pMSSM, for two choices of halo profile: NFW (red points), or Einasto (red+orange points). The approximate projected sensitivity of 1-tonne detectors is shown as a dotted gray line. The onset of the atmospheric and diffuse supernova neutrino background is shown with a dot-dashed magenta line. (b) The sensitivity of CTA to the pMSSM in the $(m_\chi, \sigma_p^{\text{SD}})$ plane. Lighter shaded points are within the projected sensitivity of IceCube/DeepCore. The dashed gray line is indicative of IceCube’s future sensitivity. (c) Sensitivity of CTA in the $(m_{\tilde{t}_1}, m_\chi)$ plane. The thick black line shows the approximate LHC lower bound on stop/neutralino masses. All figures are taken from [209].

One can see in Fig. 14(c) that the Cherenkov Telescope Array (CTA), with ~ 500 h of observation of the Galactic Center, will probe most of the pMSSM parameter space with DM mass in the TeV range. We make the point again that in the majority of SUSY models with parameters defined at some high scale this is the region emerging as favored after the discovery of the Higgs boson at 125 GeV. Thus, CTA will prove to be an indispensable instrument to probe ranges of SUSY-model parameters that would otherwise be entirely out of reach by other direct means.

To highlight the idea of complementarity, we show in Fig. 15(a) the reach of CTA with 500 h of observation of the Galactic Center, compared to the reach of 1-tonne detectors in the $(m_\chi, \sigma_p^{\text{SI}})$ plane. The color code is explained in the caption. In Fig. 15(b) we present the equivalent picture in the $(m_\chi, \sigma_p^{\text{SD}})$ plane, compared to the estimated IceCube reach. And finally, we show in Fig. 15(c) the reach of CTA compared to the present limits on stop mass obtained in simplified models at the LHC. Figure 15 is taken from [209]. Improvements in the LHC limits are not expected to have any effect on the sensitivity of CTA. Indeed, CTA remains sensitive to spectra where the gluinos and squarks lie well beyond the reach of present and future colliders.

4.5 Going beyond standard assumptions

In this topical review we have focused on reasonable but simplest underlying assumptions about DM that are usually made in phenomenological studies of the subject. One is that the DM in the Universe comprises (or is dominated by) just one species. This translates into insisting that its relic density saturates the measured value of about 0.12. However, as

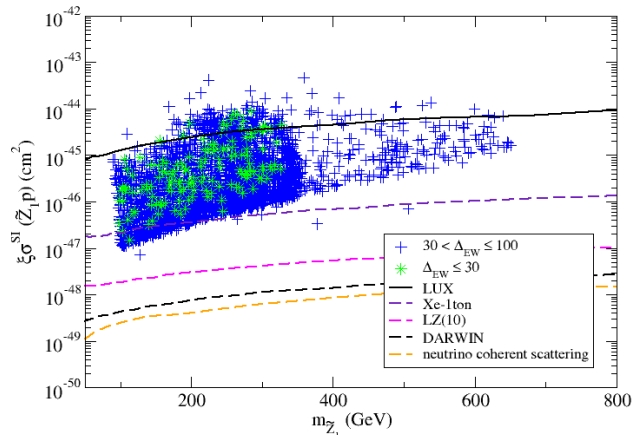


Figure 16: Reach of the spin-independent direct detection searches for neutralino DM in the scenario with two-component DM (neutralino and axino). The plot is taken from Ref. [575].

we already mentioned in Section 2.2.2, the correct WIMP DM relic density can be obtained even if the relevant annihilation rate varies from the canonical thermal value.

Another usually made assumption, or actually set of assumptions, is that, in the early Universe DM particles were generated only (or mostly) through their freeze-out out of thermal equilibrium. Although these assumptions are certainly sensible, neither of them is necessarily correct. It is therefore interesting to see how various results and conclusions derived in the literature can be affected by going beyond the standard freeze-out paradigm. In this section we will briefly illustrate this with a few examples in the context of neutralino DM. For a more comprehensive review see, e.g., [10].

4.5.1 Multi-component DM

There is really no reason, other than simplicity, to insist that the whole of DM is made up of just one species of particles. There exist several scenarios, in SUSY or not, where this is not necessarily the case. In fact, the idea that, for instance, the neutralino and the axion – arguably the two DM candidates most strongly motivated by particle physics – could easily co-exist in the Universe in basically any proportion has been around for decades. As was mentioned in Sec. 4.2, this can be motivated by insisting on keeping the scale of SUSY breaking as low as possible, in order to reduce the level of fine tuning among SUSY parameters. In such regions of the parameter space where the neutralino is close to a pure higgsino (or a pure wino), the relic density of DM is too low as DM mass is not large enough. This can also be consistently realized in specific, well motivated models [571–573]. Other possibilities include employing an additional, non-thermal component [574].

We illustrate this in Fig. 16. We can see that prospects for WIMP detection remain good, despite lower number density. For earlier works reaching similar conclusions, see, e.g., [576].

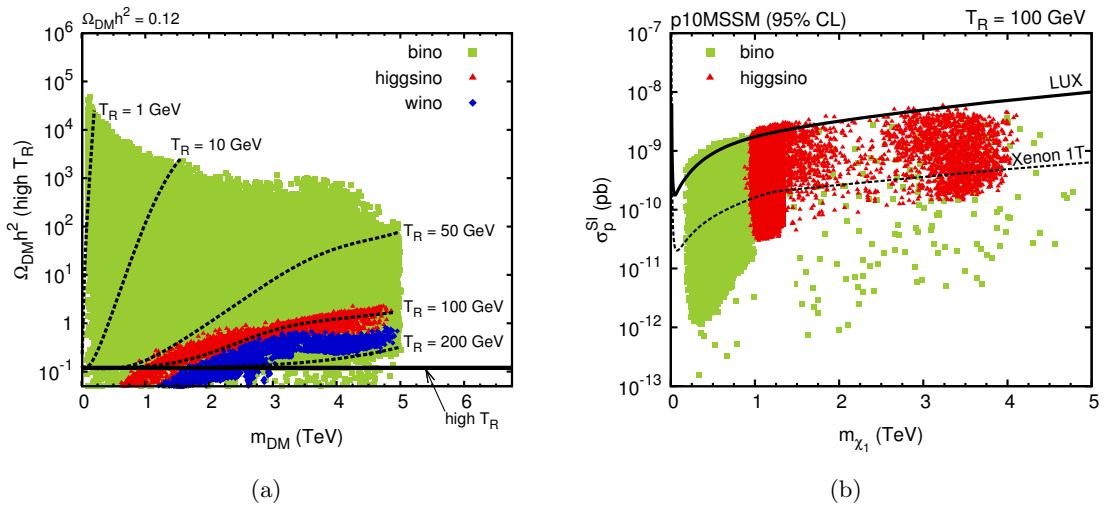


Figure 17: (a) Contours (black dotted) of constant $\Omega_{\text{DM}} h^2 = 0.12$ for different values of the reheating temperature, T_R , in the MSSM, in the $(m_{\text{DM}}, \Omega_{\text{DM}} h^2(\text{high } T_R))$ plane, where $\Omega_{\text{DM}} h^2(\text{high } T_R)$ corresponds to the standard cosmological scenario for which the correct value of the neutralino relic density is obtained along the the solid black horizontal line. Green squares correspond to bino DM, red triangles to higgsino DM and blue diamonds to the wino DM case. Negligible direct and/or cascade decays of the inflaton field are assumed. (b) Direct detection cross section, σ_p^{SI} , as a function of m_{χ} in the ten-parameter subset of the MSSM (p10MSSM) for which 95% C.L. region (including the relic density constraint) for $T_R = 100 \text{ GeV}$ is shown. The solid (dashed) black lines correspond to LUX (projected XENON1T) limit on σ_p^{SI} . Color coding as in the left panel. Taken from Ref. [77].

4.5.2 Low reheating temperature

It is usually assumed that, when WIMPs freeze out the thermal plasma, the Universe has already reached radiation dominated (RD) thermal equilibrium. In other words, the value of the reheating temperature T_R , which marks the onset of the RD epoch, is assumed to be much larger than the freeze-out temperature. This does not have to be the case and can strongly alter our conclusions about WIMP DM properties.

Low T_R can result from an extended reheating period in the evolution of the Universe after an inflationary epoch. In addition to modifying the DM population from freeze-out, it can also be changed by an additional entropy production from decays of some heavy species that took place after the DM freeze-out. As a result one can either reduce or increase the DM relic density depending on whether the additional entropy production is accompanied by efficient direct and/or cascade decays of the heavy field to the DM particles.

From the phenomenological point of view, this mechanism allows one to fit the relic density constraint for almost any scenario with neutralino DM [577, 578] (for a recent discussion, see [77]). We illustrate this in Fig. 17(a) where the lines of constant $\Omega_{\chi} h^2 = 0.12$ are shown for several values of the reheating temperatures, $T_R = 1, 10, 50, 100, 200 \text{ GeV}$ as a function of the neutralino DM mass and $\Omega_{\chi} h^2$ (high T_R), i.e., the value of the DM relic density corresponding to the standard cosmological scenario with high T_R . In particular one can see that for $T_R \approx 100 \text{ GeV}$ the correct value of $\Omega_{\chi} h^2$ for higgsino DM can be obtained for

masses significantly larger than 1 TeV. Such a heavy higgsino can still be within the reach of one-tonne detectors, as can be seen in Fig. 17(b), where we show the direct detection spin-independent cross section, σ_p^{SI} , as a function of m_χ , for phenomenologically favored points in the p10MSSM obtained assuming $T_R = 100$ GeV [77].

5 Summary and conclusions

It is not easy to look for the invisible but, in the case of DM, it is certainly worth the effort. A detection of a DM signal is likely not only to confirm the common belief that most of the dark mass in the Universe is made up of WIMPs but to hopefully shed some light on the particle physics framework that it is part of. In this topical review we have provided an overview of the current experimental situation, paying particular attention to current bounds and recent claims and hints of a possible signal in a wide range of experiments. On the particle physics side, we reviewed several candidates for explaining the DM, concentrating mostly on the class of WIMPs that could be produced mostly through the freeze-out mechanism. We have paid attention to the neutralino of SUSY since it remains the most strongly motivated candidate that additionally shows excellent detection prospects. We have emphasized that the currently most interesting – in our opinion – case of ~ 1 TeV higgsino-like neutralino in unified SUSY models will nearly fully be tested in the new tonne-scale underground detectors which are coming online. However, one should remember that, even if eventually a genuine DM signal is detected, then it is likely that several measurements will have to be made in both direct and indirect detection experiments – and this will likely be possible only under rather favorable conditions – in order to shed some light on the actual nature of the WIMP.

Acknowledgements

We are indebted to Andrew J. Williams for profusely contributing to the early stages of this work. We would also like to thank Kamila Kowalska for her input on the recasting of the recent LHC bounds and for discussions. ST would like to thank Kevork Abazajian, Jonathan L. Feng, Dan Hooper, Manoj Kaplinghat, Christopher Karwin, Simona Murgia and Timothy M.P. Tait for helpful discussions and comments. LR is supported in part by the National Science Centre (NCN) research grant No. 2015-18-A-ST2-00748 and by the Lancaster-Manchester-Sheffield Consortium for Fundamental Physics under STFC Grant No. ST/L000520/1. The work of EMS is supported by the Alexander von Humboldt Foundation. ST is partly supported by the Polish Ministry of Science and Higher Education under research grant 1309/MOB/IV/2015/0 and by NSF Grant No. PHY-1620638.

References

- [1] E. W. Kolb and M. S. Turner, *The Early Universe*, *Front. Phys.* **69** (1990) 1–547.
- [2] K. Griest and M. Kamionkowski, *Unitarity Limits on the Mass and Radius of Dark Matter Particles*, *Phys. Rev. Lett.* **64** (1990) 615.

- [3] G. D’Amico, M. Kamionkowski, and K. Sigurdson, *Dark Matter Astrophysics*, [arXiv:0907.1912](#).
- [4] A. Del Popolo, *Nonbaryonic Dark Matter in Cosmology*, *Int. J. Mod. Phys. D* **23** (2014) 1430005, [[arXiv:1305.0456](#)].
- [5] G. Jungman, M. Kamionkowski, and K. Griest, *Supersymmetric dark matter*, *Phys.Rept.* **267** (1996) 195–373, [[hep-ph/9506380](#)].
- [6] G. Bertone, D. Hooper, and J. Silk, *Particle dark matter: Evidence, candidates and constraints*, *Phys. Rept.* **405** (2005) 279–390, [[hep-ph/0404175](#)].
- [7] J. L. Feng, *Dark Matter Candidates from Particle Physics and Methods of Detection*, *Ann. Rev. Astron. Astrophys.* **48** (2010) 495–545, [[arXiv:1003.0904](#)].
- [8] V. A. Bednyakov, *Is it possible to discover a dark matter particle with an accelerator?*, *Phys. Part. Nucl.* **47** (2016), no. 5 711–774, [[arXiv:1505.04380](#)].
- [9] G. Arcadi, M. Dutra, P. Ghosh, M. Lindner, Y. Mambrini, M. Pierre, S. Profumo, and F. S. Queiroz, *The waning of the WIMP? A review of models, searches, and constraints*, *Eur. Phys. J. C* **78** (2018), no. 3 203, [[arXiv:1703.07364](#)].
- [10] H. Baer, K.-Y. Choi, J. E. Kim, and L. Roszkowski, *Dark matter production in the early Universe: beyond the thermal WIMP paradigm*, *Phys. Rept.* **555** (2014) 1–60, [[arXiv:1407.0017](#)].
- [11] J. Conrad, J. Cohen-Tanugi, and L. E. Strigari, *WIMP searches with gamma rays in the Fermi era: challenges, methods and results*, *J. Exp. Theor. Phys.* **121** (2015), no. 6 1104–1135, [[arXiv:1503.06348](#)]. [*Zh. Eksp. Teor. Fiz.*148,no.6,1257(2015)].
- [12] J. M. Gaskins, *A review of indirect searches for particle dark matter*, *Contemp. Phys.* **57** (2016), no. 4 496–525, [[arXiv:1604.00014](#)].
- [13] F. Zwicky, *Die Rotverschiebung von extragalaktischen Nebeln*, *Helv. Phys. Acta* **6** (1933) 110–127.
- [14] J. C. Kapteyn, *First Attempt at a Theory of the Arrangement and Motion of the Sidereal System*, *Astrophysical Journal* **55** (1922) 302.
- [15] J. H. Oort, *The force exerted by the stellar system in the direction perpendicular to the galactic plane and some related problems*, *Bull. Astron. Inst. Netherlands* **6** (1932) 249.
- [16] J. H. Jeans, *The Motions of Stars in a Kapteyn-Universe*, *Mon Not R Astron Soc* **82(3)** (1922) 122–132.
- [17] G. Bertone and D. Hooper, *A History of Dark Matter*, *Submitted to: Rev. Mod. Phys.* (2016) [[arXiv:1605.04909](#)].
- [18] H. W. Babcock, *Rotation of the Andromeda Nebula*, *Lick Obs. Bull.* **19** (1939) 1.
- [19] V. C. Rubin and W. K. Ford, Jr., *Rotation of the Andromeda Nebula from a Spectroscopic Survey of Emission Regions*, *Astrophys. J.* **159** (1970) 379–403.
- [20] M. S. Roberts and R. N. Whitehurst, *The Rotation Curve and Geometry of M31 at Large Galactocentric Distances*, *Astrophys. J.* **201** (1975) 327.
- [21] V. C. Rubin, N. Thonnard, and W. K. Ford, Jr., *Rotational properties of 21 SC galaxies with a large range of luminosities and radii, from NGC 4605 /R = 4kpc/ to UGC 2885 /R = 122 kpc/*, *Astrophys. J.* **238** (1980) 471.

- [22] R. Massey, T. Kitching, and J. Richard, *The dark matter of gravitational lensing*, *Rept. Prog. Phys.* **73** (2010) 086901, [[arXiv:1001.1739](#)].
- [23] D. Clowe, M. Bradac, A. H. Gonzalez, M. Markevitch, S. W. Randall, C. Jones, and D. Zaritsky, *A direct empirical proof of the existence of dark matter*, *Astrophys. J.* **648** (2006) L109–L113, [[astro-ph/0608407](#)].
- [24] M. Petrou, *Dynamical models of spheroidal systems*. PhD thesis, Univ. Cambridge, 1981.
- [25] B. Paczynski, *Gravitational microlensing by the galactic halo*, *Astrophys. J.* **304** (1986) 1–5.
- [26] **EROS-2** Collaboration, P. Tisserand et al., *Limits on the Macho Content of the Galactic Halo from the EROS-2 Survey of the Magellanic Clouds*, *Astron. Astrophys.* **469** (2007) 387–404, [[astro-ph/0607207](#)].
- [27] L. Fu et al., *CFHTLenS: Cosmological constraints from a combination of cosmic shear two-point and three-point correlations*, *Mon. Not. Roy. Astron. Soc.* **441** (2014) 2725–2743, [[arXiv:1404.5469](#)].
- [28] **Planck** Collaboration, P. A. R. Ade et al., *Planck 2015 results. XIII. Cosmological parameters*, *Astron. Astrophys.* **594** (2016) A13, [[arXiv:1502.01589](#)].
- [29] **Planck** Collaboration, P. A. R. Ade et al., *Planck 2013 results. XVI. Cosmological parameters*, *Astron. Astrophys.* **571** (2014) A16, [[arXiv:1303.5076](#)].
- [30] M. Li, X.-D. Li, S. Wang, and Y. Wang, *Dark Energy*, *Commun. Theor. Phys.* **56** (2011) 525–604, [[arXiv:1103.5870](#)].
- [31] D. H. Weinberg, M. J. Mortonson, D. J. Eisenstein, C. Hirata, A. G. Riess, and E. Rozo, *Observational Probes of Cosmic Acceleration*, *Phys. Rept.* **530** (2013) 87–255, [[arXiv:1201.2434](#)].
- [32] M. Milgrom, *A Modification of the Newtonian dynamics as a possible alternative to the hidden mass hypothesis*, *Astrophys. J.* **270** (1983) 365–370.
- [33] G. W. Angus, B. Famaey, and D. A. Buote, *X-ray Group and cluster mass profiles in MOND: Unexplained mass on the group scale*, *Mon. Not. Roy. Astron. Soc.* **387** (2008) 1470, [[arXiv:0709.0108](#)].
- [34] S. Bharadwaj and S. Kar, *Modeling galaxy halos using dark matter with pressure*, *Phys. Rev.* **D68** (2003) 023516, [[astro-ph/0304504](#)].
- [35] H. Velten and D. Schwarz, *Dissipation of dark matter*, *Phys. Rev.* **D86** (2012) 083501, [[arXiv:1206.0986](#)].
- [36] S. W. Randall, M. Markevitch, D. Clowe, A. H. Gonzalez, and M. Bradac, *Constraints on the Self-Interaction Cross-Section of Dark Matter from Numerical Simulations of the Merging Galaxy Cluster 1E 0657-56*, *Astrophys. J.* **679** (2008) 1173–1180, [[arXiv:0704.0261](#)].
- [37] Y. Hochberg, E. Kuflik, T. Volansky, and J. G. Wacker, *Mechanism for Thermal Relic Dark Matter of Strongly Interacting Massive Particles*, *Phys. Rev. Lett.* **113** (2014) 171301, [[arXiv:1402.5143](#)].
- [38] B. J. Carr and S. W. Hawking, *Black holes in the early Universe*, *Mon. Not. Roy. Astron. Soc.* **168** (1974) 399–415.
- [39] **Virgo, LIGO Scientific** Collaboration, B. P. Abbott et al., *Observation of Gravitational*

- Waves from a Binary Black Hole Merger*, *Phys. Rev. Lett.* **116** (2016), no. 6 061102, [[arXiv:1602.03837](#)].
- [40] S. Bird, I. Cholis, J. B. Muoz, Y. Ali-Hamoud, M. Kamionkowski, E. D. Kovetz, A. Raccanelli, and A. G. Riess, *Did LIGO detect dark matter?*, *Phys. Rev. Lett.* **116** (2016), no. 20 201301, [[arXiv:1603.00464](#)].
- [41] B. Carr, F. Kuhnel, and M. Sandstad, *Primordial Black Holes as Dark Matter*, *Phys. Rev. D* **94** (2016), no. 8 083504, [[arXiv:1607.06077](#)].
- [42] D. Gaggero, G. Bertone, F. Calore, R. M. T. Connors, M. Lovell, S. Markoff, and E. Storm, *Searching for Primordial Black Holes in the radio and X-ray sky*, *Phys. Rev. Lett.* **118** (2017), no. 24 241101, [[arXiv:1612.00457](#)].
- [43] C. S. Frenk and S. D. M. White, *Dark matter and cosmic structure*, *Annalen Phys.* **524** (2012) 507–534, [[arXiv:1210.0544](#)].
- [44] K. Abazajian, *Linear cosmological structure limits on warm dark matter*, *Phys. Rev. D* **73** (2006) 063513, [[astro-ph/0512631](#)].
- [45] R. de Putter et al., *New Neutrino Mass Bounds from Sloan Digital Sky Survey III Data Release 8 Photometric Luminous Galaxies*, *Astrophys. J.* **761** (2012) 12, [[arXiv:1201.1909](#)].
- [46] V. N. Lukash, E. V. Mikheeva, and A. M. Malinovsky, *Formation of the large-scale structure of the Universe*, *Phys. Usp.* **54** (2011) 983–1005, [[arXiv:1209.0371](#)].
- [47] S. Tremaine and J. E. Gunn, *Dynamical Role of Light Neutral Leptons in Cosmology*, *Phys. Rev. Lett.* **42** (1979) 407–410.
- [48] S. D. M. White, C. S. Frenk, and M. Davis, *Clustering in a Neutrino Dominated Universe*, *Astrophys. J.* **274** (1983) L1–L5.
- [49] B. Moore, S. Ghigna, F. Governato, G. Lake, T. R. Quinn, J. Stadel, and P. Tozzi, *Dark matter substructure within galactic halos*, *Astrophys. J.* **524** (1999) L19–L22, [[astro-ph/9907411](#)].
- [50] A. A. Klypin, A. V. Kravtsov, O. Valenzuela, and F. Prada, *Where are the missing Galactic satellites?*, *Astrophys. J.* **522** (1999) 82–92, [[astro-ph/9901240](#)].
- [51] M. Boylan-Kolchin, J. S. Bullock, and M. Kaplinghat, *Too big to fail? The puzzling darkness of massive Milky Way subhaloes*, *Mon. Not. Roy. Astron. Soc.* **415** (2011) L40, [[arXiv:1103.0007](#)].
- [52] M. Boylan-Kolchin, J. S. Bullock, and M. Kaplinghat, *The Milky Way’s bright satellites as an apparent failure of LCDM*, *Mon. Not. Roy. Astron. Soc.* **422** (2012) 1203–1218, [[arXiv:1111.2048](#)].
- [53] A. Del Popolo and M. Le Delliou, *Small scale problems of the Λ CDM model: a short review*, *Galaxies* **5** (2017), no. 1 17, [[arXiv:1606.07790](#)].
- [54] M. R. Lovell, V. Eke, C. S. Frenk, L. Gao, A. Jenkins, T. Theuns, J. Wang, D. M. White, A. Boyarsky, and O. Ruchayskiy, *The Haloes of Bright Satellite Galaxies in a Warm Dark Matter Universe*, *Mon. Not. Roy. Astron. Soc.* **420** (2012) 2318–2324, [[arXiv:1104.2929](#)].
- [55] M. Viel, G. D. Becker, J. S. Bolton, and M. G. Haehnelt, *Warm dark matter as a solution to the small scale crisis: New constraints from high redshift Lyman- α forest data*, *Phys. Rev. D* **88** (2013) 043502, [[arXiv:1306.2314](#)].

- [56] K. N. Abazajian, *Sterile neutrinos in cosmology*, *Phys. Rept.* **711-712** (2017) 1–28, [[arXiv:1705.01837](#)].
- [57] B. Audren, J. Lesgourgues, G. Mangano, P. D. Serpico, and T. Tram, *Strongest model-independent bound on the lifetime of dark matter*, *JCAP* **1412** (2014) 028, [[arXiv:1407.2418](#)].
- [58] T. Moroi, H. Murayama, and M. Yamaguchi, *Cosmological constraints on the light stable gravitino*, *Phys. Lett.* **B303** (1993) 289–294.
- [59] M. Bolz, A. Brandenburg, and W. Buchmuller, *Thermal production of gravitinos*, *Nucl. Phys.* **B606** (2001) 518–544, [[hep-ph/0012052](#)]. [Erratum: *Nucl. Phys.*B790,336(2008)].
- [60] J. L. Feng, A. Rajaraman, and F. Takayama, *Superweakly interacting massive particles*, *Phys. Rev. Lett.* **91** (2003) 011302, [[hep-ph/0302215](#)].
- [61] J. L. Feng, A. Rajaraman, and F. Takayama, *SuperWIMP dark matter signals from the early universe*, *Phys. Rev.* **D68** (2003) 063504, [[hep-ph/0306024](#)].
- [62] J. Pradler and F. D. Steffen, *Thermal gravitino production and collider tests of leptogenesis*, *Phys. Rev.* **D75** (2007) 023509, [[hep-ph/0608344](#)].
- [63] V. S. Rychkov and A. Strumia, *Thermal production of gravitinos*, *Phys. Rev.* **D75** (2007) 075011, [[hep-ph/0701104](#)].
- [64] L. Covi, J. E. Kim, and L. Roszkowski, *Axinos as cold dark matter*, *Phys. Rev. Lett.* **82** (1999) 4180–4183, [[hep-ph/9905212](#)].
- [65] L. Covi, H.-B. Kim, J. E. Kim, and L. Roszkowski, *Axinos as dark matter*, *JHEP* **05** (2001) 033, [[hep-ph/0101009](#)].
- [66] M. Kawasaki, K. Kohri, and T. Moroi, *Hadronic decay of late - decaying particles and Big-Bang Nucleosynthesis*, *Phys. Lett.* **B625** (2005) 7–12, [[astro-ph/0402490](#)].
- [67] M. Kawasaki, K. Kohri, and T. Moroi, *Big-Bang nucleosynthesis and hadronic decay of long-lived massive particles*, *Phys. Rev.* **D71** (2005) 083502, [[astro-ph/0408426](#)].
- [68] K. Jedamzik, *Big bang nucleosynthesis constraints on hadronically and electromagnetically decaying relic neutral particles*, *Phys. Rev.* **D74** (2006) 103509, [[hep-ph/0604251](#)].
- [69] P. Gondolo and G. Gelmini, *Cosmic abundances of stable particles: Improved analysis*, *Nucl. Phys.* **B360** (1991) 145–179.
- [70] **Particle Data Group** Collaboration, C. Patrignani et al., *Review of Particle Physics*, *Chin. Phys.* **C40** (2016), no. 10 100001.
- [71] T. Nihei, L. Roszkowski, and R. Ruiz de Austri, *Towards an accurate calculation of the neutralino relic density*, *JHEP* **05** (2001) 063, [[hep-ph/0102308](#)].
- [72] G. Steigman, B. Dasgupta, and J. F. Beacom, *Precise Relic WIMP Abundance and its Impact on Searches for Dark Matter Annihilation*, *Phys. Rev.* **D86** (2012) 023506, [[arXiv:1204.3622](#)].
- [73] J. L. Feng and J. Kumar, *The WIMPless Miracle: Dark-Matter Particles without Weak-Scale Masses or Weak Interactions*, *Phys. Rev. Lett.* **101** (2008) 231301, [[arXiv:0803.4196](#)].
- [74] A. L. Erickcek, *The Dark Matter Annihilation Boost from Low-Temperature Reheating*, *Phys. Rev.* **D92** (2015), no. 10 103505, [[arXiv:1504.03335](#)].

- [75] K. Griest and D. Seckel, *Three exceptions in the calculation of relic abundances*, *Phys. Rev.* **D43** (1991) 3191–3203.
- [76] G. F. Giudice, E. W. Kolb, and A. Riotto, *Largest temperature of the radiation era and its cosmological implications*, *Phys. Rev.* **D64** (2001) 023508, [[hep-ph/0005123](#)].
- [77] L. Roszkowski, S. Trojanowski, and K. Turzyski, *Neutralino and gravitino dark matter with low reheating temperature*, *JHEP* **11** (2014) 146, [[arXiv:1406.0012](#)].
- [78] L. J. Hall, K. Jedamzik, J. March-Russell, and S. M. West, *Freeze-In Production of FIMP Dark Matter*, *JHEP* **1003** (2010) 080, [[arXiv:0911.1120](#)].
- [79] N. Bernal, M. Heikinheimo, T. Tenkanen, K. Tuominen, and V. Vaskonen, *The Dawn of FIMP Dark Matter: A Review of Models and Constraints*, *Int. J. Mod. Phys.* **A32** (2017), no. 27 1730023, [[arXiv:1706.07442](#)].
- [80] K.-Y. Choi, L. Covi, J. E. Kim, and L. Roszkowski, *Axino Cold Dark Matter Revisited*, *JHEP* **04** (2012) 106, [[arXiv:1108.2282](#)].
- [81] K.-Y. Choi, J. E. Kim, and L. Roszkowski, *Review of axino dark matter*, *J. Korean Phys. Soc.* **63** (2013) 1685–1695, [[arXiv:1307.3330](#)].
- [82] T. Moroi and L. Randall, *Wino cold dark matter from anomaly mediated SUSY breaking*, *Nucl. Phys.* **B570** (2000) 455–472, [[hep-ph/9906527](#)].
- [83] B. S. Acharya, P. Kumar, K. Bobkov, G. Kane, J. Shao, and S. Watson, *Non-thermal Dark Matter and the Moduli Problem in String Frameworks*, *JHEP* **06** (2008) 064, [[arXiv:0804.0863](#)].
- [84] M. Fujii and K. Hamaguchi, *Nonthermal dark matter via Affleck-Dine baryogenesis and its detection possibility*, *Phys. Rev.* **D66** (2002) 083501, [[hep-ph/0205044](#)].
- [85] D. H. Lyth and E. D. Stewart, *Thermal inflation and the moduli problem*, *Phys. Rev.* **D53** (1996) 1784–1798, [[hep-ph/9510204](#)].
- [86] R. Jeannerot, X. Zhang, and R. H. Brandenberger, *Non-thermal production of neutralino cold dark matter from cosmic string decays*, *JHEP* **12** (1999) 003, [[hep-ph/9901357](#)].
- [87] M. L. Graesser, I. M. Shoemaker, and L. Vecchi, *Asymmetric WIMP dark matter*, *JHEP* **10** (2011) 110, [[arXiv:1103.2771](#)].
- [88] H. Iminiyaz, M. Drees, and X. Chen, *Relic Abundance of Asymmetric Dark Matter*, *JCAP* **1107** (2011) 003, [[arXiv:1104.5548](#)].
- [89] K. Petraki and R. R. Volkas, *Review of asymmetric dark matter*, *Int. J. Mod. Phys.* **A28** (2013) 1330028, [[arXiv:1305.4939](#)].
- [90] P. Salati, *Quintessence and the relic density of neutralinos*, *Phys. Lett.* **B571** (2003) 121–131, [[astro-ph/0207396](#)].
- [91] L. Roszkowski, *Particle dark matter: A Theorist’s perspective*, *Pramana* **62** (2004) 389–401, [[hep-ph/0404052](#)].
- [92] G. B. Gelmini, *Light weakly interacting massive particles*, *Rept. Prog. Phys.* **80** (2017), no. 8 082201, [[arXiv:1612.09137](#)].
- [93] H. Goldberg, *Constraint on the Photino Mass from Cosmology*, *Phys. Rev. Lett.* **50** (1983) 1419. [Erratum: *Phys. Rev. Lett.*103,099905(2009)].

- [94] J. R. Ellis, J. S. Hagelin, D. V. Nanopoulos, K. A. Olive, and M. Srednicki, *Supersymmetric Relics from the Big Bang*, *Nucl. Phys.* **B238** (1984) 453–476.
- [95] N. G. Deshpande and E. Ma, *Pattern of Symmetry Breaking with Two Higgs Doublets*, *Phys. Rev.* **D18** (1978) 2574.
- [96] G. C. Branco, P. M. Ferreira, L. Lavoura, M. N. Rebelo, M. Sher, and J. P. Silva, *Theory and phenomenology of two-Higgs-doublet models*, *Phys. Rept.* **516** (2012) 1–102, [[arXiv:1106.0034](#)].
- [97] R. Barbieri, L. J. Hall, and V. S. Rychkov, *Improved naturalness with a heavy Higgs: An Alternative road to LHC physics*, *Phys. Rev.* **D74** (2006) 015007, [[hep-ph/0603188](#)].
- [98] E. Ma, *Verifiable radiative seesaw mechanism of neutrino mass and dark matter*, *Phys. Rev.* **D73** (2006) 077301, [[hep-ph/0601225](#)].
- [99] A. Goudelis, B. Herrmann, and O. Stål, *Dark matter in the Inert Doublet Model after the discovery of a Higgs-like boson at the LHC*, *JHEP* **09** (2013) 106, [[arXiv:1303.3010](#)].
- [100] H.-S. Goh, L. J. Hall, and P. Kumar, *The Leptonic Higgs as a Messenger of Dark Matter*, *JHEP* **05** (2009) 097, [[arXiv:0902.0814](#)].
- [101] M. Aoki, S. Kanemura, and O. Seto, *Neutrino mass, Dark Matter and Baryon Asymmetry via TeV-Scale Physics without Fine-Tuning*, *Phys. Rev. Lett.* **102** (2009) 051805, [[arXiv:0807.0361](#)].
- [102] M. S. Boucenna and S. Profumo, *Direct and Indirect Singlet Scalar Dark Matter Detection in the Lepton-Specific two-Higgs-doublet Model*, *Phys. Rev.* **D84** (2011) 055011, [[arXiv:1106.3368](#)].
- [103] N. Arkani-Hamed, A. G. Cohen, and H. Georgi, *Electroweak symmetry breaking from dimensional deconstruction*, *Phys. Lett.* **B513** (2001) 232–240, [[hep-ph/0105239](#)].
- [104] N. Arkani-Hamed, A. G. Cohen, T. Gregoire, and J. G. Wacker, *Phenomenology of electroweak symmetry breaking from theory space*, *JHEP* **08** (2002) 020, [[hep-ph/0202089](#)].
- [105] N. Arkani-Hamed, A. G. Cohen, E. Katz, A. E. Nelson, T. Gregoire, and J. G. Wacker, *The Minimal moose for a little Higgs*, *JHEP* **08** (2002) 021, [[hep-ph/0206020](#)].
- [106] N. Arkani-Hamed, A. G. Cohen, E. Katz, and A. E. Nelson, *The Littlest Higgs*, *JHEP* **07** (2002) 034, [[hep-ph/0206021](#)].
- [107] D. E. Kaplan and M. Schmaltz, *The Little Higgs from a simple group*, *JHEP* **10** (2003) 039, [[hep-ph/0302049](#)].
- [108] M. Schmaltz, *Physics beyond the standard model (theory): Introducing the little Higgs*, *Nucl. Phys. Proc. Suppl.* **117** (2003) 40–49, [[hep-ph/0210415](#)].
- [109] S. Chang and J. G. Wacker, *Little Higgs and custodial SU(2)*, *Phys. Rev.* **D69** (2004) 035002, [[hep-ph/0303001](#)].
- [110] M. Schmaltz and D. Tucker-Smith, *Little Higgs review*, *Ann. Rev. Nucl. Part. Sci.* **55** (2005) 229–270, [[hep-ph/0502182](#)].
- [111] I. Low, *T parity and the littlest Higgs*, *JHEP* **10** (2004) 067, [[hep-ph/0409025](#)].
- [112] J. Hubisz and P. Meade, *Phenomenology of the littlest Higgs with T-parity*, *Phys. Rev.* **D71** (2005) 035016, [[hep-ph/0411264](#)].

- [113] J. Hubisz, P. Meade, A. Noble, and M. Perelstein, *Electroweak precision constraints on the lightest Higgs model with T parity*, *JHEP* **01** (2006) 135, [[hep-ph/0506042](#)].
- [114] A. Birkedal-Hansen and J. G. Wacker, *Scalar dark matter from theory space*, *Phys. Rev.* **D69** (2004) 065022, [[hep-ph/0306161](#)].
- [115] A. Martin, *Dark matter in the simplest little Higgs model*, [[hep-ph/0602206](#)].
- [116] A. Freitas, P. Schwaller, and D. Wyler, *A Little Higgs Model with Exact Dark Matter Parity*, *JHEP* **12** (2009) 027, [[arXiv:0906.1816](#)].
- [117] L. Wang, J. M. Yang, and J. Zhu, *Dark matter in the little Higgs model under current experimental constraints from the LHC, Planck, and Xenon data*, *Phys. Rev.* **D88** (2013), no. 7 075018, [[arXiv:1307.7780](#)].
- [118] Z. Chacko, H.-S. Goh, and R. Harnik, *The Twin Higgs: Natural electroweak breaking from mirror symmetry*, *Phys. Rev. Lett.* **96** (2006) 231802, [[hep-ph/0506256](#)].
- [119] Z. Chacko, H.-S. Goh, and R. Harnik, *A Twin Higgs model from left-right symmetry*, *JHEP* **01** (2006) 108, [[hep-ph/0512088](#)].
- [120] R. Barbieri, T. Gregoire, and L. J. Hall, *Mirror world at the large hadron collider*, [[hep-ph/0509242](#)].
- [121] N. Craig and K. Howe, *Doubling down on naturalness with a supersymmetric twin Higgs*, *JHEP* **03** (2014) 140, [[arXiv:1312.1341](#)].
- [122] I. Garcia Garcia, R. Lasenby, and J. March-Russell, *Twin Higgs WIMP Dark Matter*, *Phys. Rev.* **D92** (2015), no. 5 055034, [[arXiv:1505.07109](#)].
- [123] S. El Hedri and A. Hook, *Minimal Signatures of Naturalness*, *JHEP* **10** (2013) 105, [[arXiv:1305.6608](#)].
- [124] D. Poland and J. Thaler, *The Dark Top*, *JHEP* **11** (2008) 083, [[arXiv:0808.1290](#)].
- [125] E. M. Dolle and S. Su, *Dark Matter in the Left Right Twin Higgs Model*, *Phys. Rev.* **D77** (2008) 075013, [[arXiv:0712.1234](#)].
- [126] J. S. Hagelin, G. L. Kane, and S. Raby, *Perhaps Scalar Neutrinos Are the Lightest Supersymmetric Partners*, *Nucl. Phys.* **B241** (1984) 638–652.
- [127] L. E. Ibanez, *The Scalar Neutrinos as the Lightest Supersymmetric Particles and Cosmology*, *Phys. Lett.* **B137** (1984) 160–164.
- [128] T. Falk, K. A. Olive, and M. Srednicki, *Heavy sneutrinos as dark matter*, *Phys. Lett.* **B339** (1994) 248–251, [[hep-ph/9409270](#)].
- [129] L. J. Hall, T. Moroi, and H. Murayama, *Sneutrino cold dark matter with lepton number violation*, *Phys. Lett.* **B424** (1998) 305–312, [[hep-ph/9712515](#)].
- [130] C. Arina and N. Fornengo, *Sneutrino cold dark matter, a new analysis: Relic abundance and detection rates*, *JHEP* **11** (2007) 029, [[arXiv:0709.4477](#)].
- [131] N. Arkani-Hamed, L. J. Hall, H. Murayama, D. Tucker-Smith, and N. Weiner, *Small neutrino masses from supersymmetry breaking*, *Phys. Rev.* **D64** (2001) 115011, [[hep-ph/0006312](#)].
- [132] G. Belanger, M. Kakizaki, E. K. Park, S. Kraml, and A. Pukhov, *Light mixed sneutrinos as thermal dark matter*, *JCAP* **1011** (2010) 017, [[arXiv:1008.0580](#)].

- [133] B. Dumont, G. Belanger, S. Fichet, S. Kraml, and T. Schwetz, *Mixed sneutrino dark matter in light of the 2011 XENON and LHC results*, *JCAP* **1209** (2012) 013, [[arXiv:1206.1521](#)].
- [134] M. Kakizaki, E.-K. Park, J.-h. Park, and A. Santa, *Phenomenological constraints on light mixed sneutrino dark matter scenarios*, *Phys. Lett.* **B749** (2015) 44–49, [[arXiv:1503.06783](#)].
- [135] H. V. Klapdor-Kleingrothaus, S. Kolb, and V. A. Kuzmin, *Light lepton number violating sneutrinos and the baryon number of the universe*, *Phys. Rev.* **D62** (2000) 035014, [[hep-ph/9909546](#)].
- [136] S. Kolb, M. Hirsch, H. V. Klapdor-Kleingrothaus, and O. Panella, *Collider signatures of sneutrino cold dark matter*, *Phys. Lett.* **B478** (2000) 262–268, [[hep-ph/9910542](#)].
- [137] T. Asaka, K. Ishiwata, and T. Moroi, *Right-handed sneutrino as cold dark matter*, *Phys. Rev.* **D73** (2006) 051301, [[hep-ph/0512118](#)].
- [138] S. Banerjee, G. Blanger, B. Mukhopadhyaya, and P. D. Serpico, *Signatures of sneutrino dark matter in an extension of the CMSSM*, *JHEP* **07** (2016) 095, [[arXiv:1603.08834](#)].
- [139] T. Appelquist, H.-C. Cheng, and B. A. Dobrescu, *Bounds on universal extra dimensions*, *Phys. Rev.* **D64** (2001) 035002, [[hep-ph/0012100](#)].
- [140] H.-C. Cheng, J. L. Feng, and K. T. Matchev, *Kaluza-Klein dark matter*, *Phys. Rev. Lett.* **89** (2002) 211301, [[hep-ph/0207125](#)].
- [141] G. Servant and T. M. P. Tait, *Is the lightest Kaluza-Klein particle a viable dark matter candidate?*, *Nucl. Phys.* **B650** (2003) 391–419, [[hep-ph/0206071](#)].
- [142] M. Kakizaki, S. Matsumoto, and M. Senami, *Relic abundance of dark matter in the minimal universal extra dimension model*, *Phys. Rev.* **D74** (2006) 023504, [[hep-ph/0605280](#)].
- [143] D. Hooper and S. Profumo, *Dark matter and collider phenomenology of universal extra dimensions*, *Phys. Rept.* **453** (2007) 29–115, [[hep-ph/0701197](#)].
- [144] J. M. Cornell, S. Profumo, and W. Shepherd, *Dark matter in minimal universal extra dimensions with a stable vacuum and the “right” Higgs boson*, *Phys. Rev.* **D89** (2014), no. 5 056005, [[arXiv:1401.7050](#)].
- [145] G. Servant, *Status Report on Universal Extra Dimensions After LHC8*, *Mod. Phys. Lett.* **A30** (2015), no. 15 1540011, [[arXiv:1401.4176](#)].
- [146] A. Karam and K. Tamvakis, *Dark matter and neutrino masses from a scale-invariant multi-Higgs portal*, *Phys. Rev.* **D92** (2015), no. 7 075010, [[arXiv:1508.03031](#)].
- [147] A. Karam and K. Tamvakis, *Dark Matter from a Classically Scale-Invariant $SU(3)_X$* , *Phys. Rev.* **D94** (2016), no. 5 055004, [[arXiv:1607.01001](#)].
- [148] M. W. Goodman and E. Witten, *Detectability of Certain Dark Matter Candidates*, *Phys. Rev.* **D31** (1985) 3059.
- [149] J. D. Lewin and P. F. Smith, *Review of mathematics, numerical factors, and corrections for dark matter experiments based on elastic nuclear recoil*, *Astropart. Phys.* **6** (1996) 87–112.
- [150] R. J. Gaitskell, *Direct detection of dark matter*, *Ann. Rev. Nucl. Part. Sci.* **54** (2004) 315–359.
- [151] A. H. G. Peter, V. Gluscevic, A. M. Green, B. J. Kavanagh, and S. K. Lee, *WIMP physics with ensembles of direct-detection experiments*, *Phys. Dark Univ.* **5-6** (2014) 45–74, [[arXiv:1310.7039](#)].

- [152] T. Marrodán Undagoitia and L. Rauch, *Dark matter direct-detection experiments*, *J. Phys.* **G43** (2016), no. 1 013001, [[arXiv:1509.08767](#)].
- [153] A. K. Drukier, K. Freese, and D. N. Spergel, *Detecting Cold Dark Matter Candidates*, *Phys. Rev.* **D33** (1986) 3495–3508.
- [154] K. Freese, M. Lisanti, and C. Savage, *Colloquium: Annual modulation of dark matter*, *Rev. Mod. Phys.* **85** (2013) 1561–1581, [[arXiv:1209.3339](#)].
- [155] D. N. Spergel, *The Motion of the Earth and the Detection of Wimps*, *Phys. Rev.* **D37** (1988) 1353.
- [156] F. Mayet et al., *A review of the discovery reach of directional Dark Matter detection*, *Phys. Rept.* **627** (2016) 1–49, [[arXiv:1602.03781](#)].
- [157] V. Cirigliano, M. L. Graesser, and G. Ovanessian, *WIMP-nucleus scattering in chiral effective theory*, *JHEP* **10** (2012) 025, [[arXiv:1205.2695](#)].
- [158] J. Fan, M. Reece, and L.-T. Wang, *Non-relativistic effective theory of dark matter direct detection*, *JCAP* **1011** (2010) 042, [[arXiv:1008.1591](#)].
- [159] A. L. Fitzpatrick, W. Haxton, E. Katz, N. Lubbers, and Y. Xu, *The Effective Field Theory of Dark Matter Direct Detection*, *JCAP* **1302** (2013) 004, [[arXiv:1203.3542](#)].
- [160] M. Hoferichter, P. Klos, and A. Schwenk, *Chiral power counting of one- and two-body currents in direct detection of dark matter*, *Phys. Lett.* **B746** (2015) 410–416, [[arXiv:1503.04811](#)].
- [161] P. Klos, J. Menndez, D. Gazit, and A. Schwenk, *Large-scale nuclear structure calculations for spin-dependent WIMP scattering with chiral effective field theory currents*, *Phys. Rev.* **D88** (2013), no. 8 083516, [[arXiv:1304.7684](#)]. [Erratum: *Phys. Rev.* **D89**, no. 2, 029901 (2014)].
- [162] A. Crivellin, M. Hoferichter, and M. Procura, *Accurate evaluation of hadronic uncertainties in spin-independent WIMP-nucleon scattering: Disentangling two- and three-flavor effects*, *Phys. Rev.* **D89** (2014) 054021, [[arXiv:1312.4951](#)].
- [163] D. Z. Freedman, *Coherent neutrino nucleus scattering as a probe of the weak neutral current*, *Phys. Rev.* **D9** (1974) 1389–1392.
- [164] B. Cabrera, L. M. Krauss, and F. Wilczek, *Bolometric Detection of Neutrinos*, *Phys.Rev.Lett.* **55** (1985) 25.
- [165] J. Billard, L. Strigari, and E. Figueroa-Feliciano, *Implication of neutrino backgrounds on the reach of next generation dark matter direct detection experiments*, *Phys.Rev.* **D89** (2014) 023524, [[arXiv:1307.5458](#)].
- [166] V. Chepel and H. Araújo, *Liquid noble gas detectors for low energy particle physics*, *Journal of Instrumentation* **8** (Apr., 2013) R04001, [[arXiv:1207.2292](#)].
- [167] DAMA Collaboration, R. Bernabei et al., *The DAMA/LIBRA apparatus*, *Nucl. Instrum. Meth.* **A592** (2008) 297–315, [[arXiv:0804.2738](#)].
- [168] R. Bernabei et al., *Final model independent result of DAMA/LIBRA-phase1*, *Eur. Phys. J.* **C73** (2013) 2648, [[arXiv:1308.5109](#)].
- [169] XENON Collaboration, E. Aprile et al., *First Dark Matter Search Results from the XENON1T Experiment*, *Phys. Rev. Lett.* **119** (2017), no. 18 181301, [[arXiv:1705.06655](#)].

- [170] E. Aprile et al., *Dark Matter Search Results from a One Tonne \times Year Exposure of XENON1T*, [arXiv:1805.12562](#).
- [171] **LUX** Collaboration, D. S. Akerib et al., *Results from a search for dark matter in the complete LUX exposure*, *Phys. Rev. Lett.* **118** (2017), no. 2 021303, [[arXiv:1608.07648](#)].
- [172] **PandaX-II** Collaboration, A. Tan et al., *Dark Matter Results from First 98.7 Days of Data from the PandaX-II Experiment*, *Phys. Rev. Lett.* **117** (2016), no. 12 121303, [[arXiv:1607.07400](#)].
- [173] **SuperCDMS** Collaboration, R. Agnese et al., *New Results from the Search for Low-Mass Weakly Interacting Massive Particles with the CDMS Low Ionization Threshold Experiment*, *Phys. Rev. Lett.* **116** (2016), no. 7 071301, [[arXiv:1509.02448](#)].
- [174] **XMASS** Collaboration, K. Abe et al., *Direct dark matter search by annual modulation in XMASS-I*, *Phys. Lett.* **B759** (2016) 272–276, [[arXiv:1511.04807](#)].
- [175] J. H. Davis, *The Past and Future of Light Dark Matter Direct Detection*, *Int. J. Mod. Phys.* **A30** (2015), no. 15 1530038, [[arXiv:1506.03924](#)].
- [176] S. C. Kim et al., *New Limits on Interactions between Weakly Interacting Massive Particles and Nucleons Obtained with CsI(Tl) Crystal Detectors*, *Phys. Rev. Lett.* **108** (2012) 181301, [[arXiv:1204.2646](#)].
- [177] **XENON** Collaboration, E. Aprile et al., *Search for magnetic inelastic dark matter with XENON100*, *JCAP* **1710** (2017), no. 10 039, [[arXiv:1704.05804](#)].
- [178] G. Barelo, S. Chang, and C. A. Newby, *A Model Independent Approach to Inelastic Dark Matter Scattering*, *Phys. Rev.* **D90** (2014), no. 9 094027, [[arXiv:1409.0536](#)].
- [179] E. Del Nobile, G. B. Gelmini, A. Georgescu, and J.-H. Huh, *Reevaluation of spin-dependent WIMP-proton interactions as an explanation of the DAMA data*, *JCAP* **1508** (2015), no. 08 046, [[arXiv:1502.07682](#)].
- [180] E. Aprile et al., *Search for WIMP Inelastic Scattering off Xenon Nuclei with XENON100*, [arXiv:1705.05830](#).
- [181] J. Kopp, V. Niro, T. Schwetz, and J. Zupan, *DAMA/LIBRA and leptonically interacting Dark Matter*, *Phys. Rev.* **D80** (2009) 083502, [[arXiv:0907.3159](#)].
- [182] **XENON** Collaboration, E. Aprile et al., *Search for Electronic Recoil Event Rate Modulation with 4 Years of XENON100 Data*, *Phys. Rev. Lett.* **118** (2017), no. 10 101101, [[arXiv:1701.00769](#)].
- [183] S. P. Ahlen, F. T. Avignone, R. L. Brodzinski, A. K. Drukier, G. Gelmini, and D. N. Spergel, *Limits on Cold Dark Matter Candidates from an Ultralow Background Germanium Spectrometer*, *Phys. Lett.* **B195** (1987) 603–608.
- [184] **CoGeNT** Collaboration, C. Aalseth et al., *CoGeNT: A Search for Low-Mass Dark Matter using p-type Point Contact Germanium Detectors*, *Phys.Rev.* **D88** (2013), no. 1 012002, [[arXiv:1208.5737](#)].
- [185] C. E. Aalseth et al., *Maximum Likelihood Signal Extraction Method Applied to 3.4 years of CoGeNT Data*, [arXiv:1401.6234](#).
- [186] J. H. Davis, C. McCabe, and C. Boehm, *Quantifying the evidence for Dark Matter in CoGeNT data*, *JCAP* **1408** (2014) 014, [[arXiv:1405.0495](#)].

- [187] **CDEX** Collaboration, Q. Yue et al., *Limits on light WIMPs from the CDEX-1 experiment with a p-type point-contact germanium detector at the China Jingping Underground Laboratory*, *Phys. Rev.* **D90** (2014) 091701, [[arXiv:1404.4946](#)].
- [188] **Majorana** Collaboration, G. K. Giovanetti et al., *A Dark Matter Search with MALBEK*, *Phys. Procedia* **61** (2015) 77–84, [[arXiv:1407.2238](#)].
- [189] E. Del Nobile, G. B. Gelmini, P. Gondolo, and J.-H. Huh, *Halo-independent analysis of direct detection data for light WIMPs*, *JCAP* **1310** (2013) 026, [[arXiv:1304.6183](#)].
- [190] **CDMS** Collaboration, R. Agnese et al., *Silicon Detector Dark Matter Results from the Final Exposure of CDMS II*, *Phys.Rev.Lett.* **111** (2013) 251301, [[arXiv:1304.4279](#)].
- [191] **SuperCDMS** Collaboration, R. Agnese et al., *Maximum Likelihood Analysis of Low Energy CDMS II Germanium Data*, *Phys. Rev. D* (2014) [[arXiv:1410.1003](#)]. [*Phys. Rev.*D91,052021(2015)].
- [192] **SuperCDMS** Collaboration, R. Agnese et al., *Search for Low-Mass Weakly Interacting Massive Particles Using Voltage-Assisted Calorimetric Ionization Detection in the SuperCDMS Experiment*, *Phys. Rev. Lett.* **112** (2014), no. 4 041302, [[arXiv:1309.3259](#)].
- [193] G. B. Gelmini, J.-H. Huh, and S. J. Witte, *Assessing Compatibility of Direct Detection Data: Halo-Independent Global Likelihood Analyses*, *JCAP* **1610** (2016), no. 10 029, [[arXiv:1607.02445](#)].
- [194] G. Angloher et al., *Results from 730 kg days of the CRESST-II Dark Matter Search*, *Eur. Phys. J.* **C72** (2012) 1971, [[arXiv:1109.0702](#)].
- [195] M. Kuźniak, M. G. Boulay, and T. Pollmann, *Surface roughness interpretation of 730 kg days CRESST-II results*, *Astropart. Phys.* **36** (2012) 77–82, [[arXiv:1203.1576](#)].
- [196] **CRESST-II** Collaboration, G. Angloher et al., *Results on low mass WIMPs using an upgraded CRESST-II detector*, *Eur. Phys. J.* **C74** (2014), no. 12 3184, [[arXiv:1407.3146](#)].
- [197] **XENON100** Collaboration, E. Aprile et al., *XENON100 Dark Matter Results from a Combination of 477 Live Days*, *Phys. Rev.* **D94** (2016), no. 12 122001, [[arXiv:1609.06154](#)].
- [198] **PICO** Collaboration, C. Amole et al., *Dark matter search results from the PICO-60 CF₃I bubble chamber*, *Phys. Rev.* **D93** (2016), no. 5 052014, [[arXiv:1510.07754](#)].
- [199] **PICO** Collaboration, C. Amole et al., *Improved dark matter search results from PICO-2L Run 2*, *Phys. Rev.* **D93** (2016), no. 6 061101, [[arXiv:1601.03729](#)].
- [200] **LUX** Collaboration, D. S. Akerib et al., *Results on the Spin-Dependent Scattering of Weakly Interacting Massive Particles on Nucleons from the Run 3 Data of the LUX Experiment*, *Phys. Rev. Lett.* **116** (2016), no. 16 161302, [[arXiv:1602.03489](#)].
- [201] **XENON** Collaboration, E. Aprile et al., *Physics reach of the XENON1T dark matter experiment*, *JCAP* **1604** (2016), no. 04 027, [[arXiv:1512.07501](#)].
- [202] **LUX, LZ** Collaboration, M. Szydagis, *The Present and Future of Searching for Dark Matter with LUX and LZ*, in *38th International Conference on High Energy Physics (ICHEP 2016) Chicago, IL, USA, August 03-10, 2016*, 2016. [[arXiv:1611.05525](#)].
- [203] **DARWIN** Collaboration, J. Aalbers et al., *DARWIN: towards the ultimate dark matter detector*, *JCAP* **1611** (2016) 017, [[arXiv:1606.07001](#)].
- [204] **DEAP** Collaboration, P. A. Amaudruz et al., *DEAP-3600 Dark Matter Search*, *Nucl. Part. Phys. Proc.* **273-275** (2016) 340–346, [[arXiv:1410.7673](#)].

- [205] **ArDM** Collaboration, J. Calvo et al., *Status of ArDM-1t: First observations from operation with a full ton-scale liquid argon target*, [arXiv:1505.02443](#).
- [206] C. E. Aalseth et al., *The DarkSide Multiton Detector for the Direct Dark Matter Search*, *Adv. High Energy Phys.* **2015** (2015) 541362.
- [207] **SuperCDMS** Collaboration, R. Agnese et al., *Projected Sensitivity of the SuperCDMS SNOLAB experiment*, *Phys. Rev.* **D95** (2017), no. 8 082002, [[arXiv:1610.00006](#)].
- [208] R. Strauss et al., *The CRESST-III low-mass WIMP detector*, *J. Phys. Conf. Ser.* **718** (2016), no. 4 042048.
- [209] L. Roszkowski, E. M. Sessolo, and A. J. Williams, *Prospects for dark matter searches in the pMSSM*, *JHEP* **02** (2015) 014, [[arXiv:1411.5214](#)].
- [210] L. Roszkowski, E. M. Sessolo, and A. J. Williams, *What next for the CMSSM and the NUHM: Improved prospects for superpartner and dark matter detection*, *JHEP* **1408** (2014) 067, [[arXiv:1405.4289](#)].
- [211] A. M. Green, *Astrophysical uncertainties on direct detection experiments*, *Mod. Phys. Lett.* **A27** (2012) 1230004, [[arXiv:1112.0524](#)].
- [212] M. Kamionkowski and A. Kinkhabwala, *Galactic halo models and particle dark matter detection*, *Phys. Rev.* **D57** (1998) 3256–3263, [[hep-ph/9710337](#)].
- [213] C. McCabe, *The Astrophysical Uncertainties Of Dark Matter Direct Detection Experiments*, *Phys. Rev.* **D82** (2010) 023530, [[arXiv:1005.0579](#)].
- [214] M. Drees and C.-L. Shan, *Model-Independent Determination of the WIMP Mass from Direct Dark Matter Detection Data*, *JCAP* **0806** (2008) 012, [[arXiv:0803.4477](#)].
- [215] E. Del Nobile, G. B. Gelmini, P. Gondolo, and J.-H. Huh, *Update on the Halo-Independent Comparison of Direct Dark Matter Detection Data*, *Phys. Procedia* **61** (2015) 45–54, [[arXiv:1405.5582](#)].
- [216] M. Beck et al., *Searching for dark matter with the enriched detectors of the Heidelberg - Moscow Double Beta Decay Experiment*, *Phys. Lett.* **B336** (1994) 141–146.
- [217] S. Liem, G. Bertone, F. Calore, R. Ruiz de Austri, T. M. P. Tait, R. Trotta, and C. Weniger, *Effective field theory of dark matter: a global analysis*, *JHEP* **09** (2016) 077, [[arXiv:1603.05994](#)].
- [218] A. DiFranzo, K. I. Nagao, A. Rajaraman, and T. M. P. Tait, *Simplified Models for Dark Matter Interacting with Quarks*, *JHEP* **11** (2013) 014, [[arXiv:1308.2679](#)]. [Erratum: *JHEP*01,162(2014)].
- [219] A. Alves, S. Profumo, and F. S. Queiroz, *The dark Z' portal: direct, indirect and collider searches*, *JHEP* **04** (2014) 063, [[arXiv:1312.5281](#)].
- [220] M. R. Buckley, D. Feld, and D. Goncalves, *Scalar Simplified Models for Dark Matter*, *Phys. Rev.* **D91** (2015) 015017, [[arXiv:1410.6497](#)].
- [221] A. Choudhury, K. Kowalska, L. Roszkowski, E. M. Sessolo, and A. J. Williams, *Less-simplified models of dark matter for direct detection and the LHC*, *JHEP* **04** (2016) 182, [[arXiv:1509.05771](#)].
- [222] S. Matsumoto, S. Mukhopadhyay, and Y.-L. S. Tsai, *Effective Theory of WIMP Dark Matter supplemented by Simplified Models: Singlet-like Majorana fermion case*, *Phys. Rev.* **D94** (2016), no. 6 065034, [[arXiv:1604.02230](#)].

- [223] N. F. Bell, Y. Cai, J. B. Dent, R. K. Leane, and T. J. Weiler, *Dark matter at the LHC: Effective field theories and gauge invariance*, *Phys. Rev.* **D92** (2015), no. 5 053008, [[arXiv:1503.07874](#)].
- [224] F. Kahlhoefer, K. Schmidt-Hoberg, T. Schwetz, and S. Vogl, *Implications of unitarity and gauge invariance for simplified dark matter models*, *JHEP* **02** (2016) 016, [[arXiv:1510.02110](#)].
- [225] A. De Simone and T. Jacques, *Simplified Models vs. Effective Field Theory Approaches in Dark Matter Searches*, *Eur. Phys. J.* **C76** (2016), no. 7 367, [[arXiv:1603.08002](#)].
- [226] M. Cirelli, G. Corcella, A. Hektor, G. Hutsi, M. Kadastik, P. Panci, M. Raidal, F. Sala, and A. Strumia, *PPPC 4 DM ID: A Poor Particle Physicist Cookbook for Dark Matter Indirect Detection*, *JCAP* **1103** (2011) 051, [[arXiv:1012.4515](#)].
- [227] S. Ando and E. Komatsu, *Anisotropy of the cosmic gamma-ray background from dark matter annihilation*, *Phys. Rev.* **D73** (2006) 023521, [[astro-ph/0512217](#)].
- [228] M. Bahr et al., *Herwig++ Physics and Manual*, *Eur. Phys. J.* **C58** (2008) 639–707, [[arXiv:0803.0883](#)].
- [229] T. Gleisberg, S. Hoeche, F. Krauss, M. Schonherr, S. Schumann, F. Siegert, and J. Winter, *Event generation with SHERPA 1.1*, *JHEP* **02** (2009) 007, [[arXiv:0811.4622](#)].
- [230] T. Sjostrand, S. Mrenna, and P. Z. Skands, *A Brief Introduction to PYTHIA 8.1*, *Comput.Phys.Commun.* **178** (2008) 852–867, [[arXiv:0710.3820](#)].
- [231] P. Ciafaloni, D. Comelli, A. Riotto, F. Sala, A. Strumia, and A. Urbano, *Weak Corrections are Relevant for Dark Matter Indirect Detection*, *JCAP* **1103** (2011) 019, [[arXiv:1009.0224](#)].
- [232] L. Bergstrom, P. Ullio, and J. H. Buckley, *Observability of gamma-rays from dark matter neutralino annihilations in the Milky Way halo*, *Astropart. Phys.* **9** (1998) 137–162, [[astro-ph/9712318](#)].
- [233] T. Bringmann, L. Bergstrom, and J. Edsjo, *New Gamma-Ray Contributions to Supersymmetric Dark Matter Annihilation*, *JHEP* **01** (2008) 049, [[arXiv:0710.3169](#)].
- [234] P. Gondolo and J. Silk, *Dark matter annihilation at the galactic center*, *Phys. Rev. Lett.* **83** (1999) 1719–1722, [[astro-ph/9906391](#)].
- [235] J. F. Navarro, A. Ludlow, V. Springel, J. Wang, M. Vogelsberger, S. D. M. White, A. Jenkins, C. S. Frenk, and A. Helmi, *The Diversity and Similarity of Cold Dark Matter Halos*, *Mon. Not. Roy. Astron. Soc.* **402** (2010) 21, [[arXiv:0810.1522](#)].
- [236] F. Iocco, M. Pato, G. Bertone, and P. Jetzer, *Dark Matter distribution in the Milky Way: microlensing and dynamical constraints*, *JCAP* **1111** (2011) 029, [[arXiv:1107.5810](#)].
- [237] R. Catena and P. Ullio, *A novel determination of the local dark matter density*, *JCAP* **1008** (2010) 004, [[arXiv:0907.0018](#)].
- [238] F. Nesti and P. Salucci, *The Dark Matter halo of the Milky Way, AD 2013*, *JCAP* **1307** (2013) 016, [[arXiv:1304.5127](#)].
- [239] **Fermi-LAT** Collaboration, M. Ackermann et al., *Constraints on the Galactic Halo Dark Matter from Fermi-LAT Diffuse Measurements*, *Astrophys. J.* **761** (2012) 91, [[arXiv:1205.6474](#)].

- [240] M. Mateo, *Dwarf galaxies of the Local Group*, *Ann. Rev. Astron. Astrophys.* **36** (1998) 435–506, [[astro-ph/9810070](#)].
- [241] A. W. McConnachie, *The observed properties of dwarf galaxies in and around the Local Group*, *Astron. J.* **144** (2012) 4, [[arXiv:1204.1562](#)].
- [242] G. D. Martinez, J. S. Bullock, M. Kaplinghat, L. E. Strigari, and R. Trotta, *Indirect Dark Matter Detection from Dwarf Satellites: Joint Expectations from Astrophysics and Supersymmetry*, *JCAP* **0906** (2009) 014, [[arXiv:0902.4715](#)].
- [243] M. G. Walker, M. Mateo, E. W. Olszewski, J. Penarrubia, N. W. Evans, and G. Gilmore, *A Universal Mass Profile for Dwarf Spheroidal Galaxies*, *Astrophys. J.* **704** (2009) 1274–1287, [[arXiv:0906.0341](#)]. [Erratum: *Astrophys. J.* 710,886(2010)].
- [244] J. Wolf, G. D. Martinez, J. S. Bullock, M. Kaplinghat, M. Geha, R. R. Munoz, J. D. Simon, and F. F. Avedo, *Accurate Masses for Dispersion-supported Galaxies*, *Mon. Not. Roy. Astron. Soc.* **406** (2010) 1220, [[arXiv:0908.2995](#)].
- [245] T. E. Jeltema, J. Kehayias, and S. Profumo, *Gamma Rays from Clusters and Groups of Galaxies: Cosmic Rays versus Dark Matter*, *Phys. Rev.* **D80** (2009) 023005, [[arXiv:0812.0597](#)].
- [246] A. Pinzke and C. Pfrommer, *Simulating the gamma-ray emission from galaxy clusters: a universal cosmic ray spectrum and spatial distribution*, *Mon. Not. Roy. Astron. Soc.* **409** (2010) 449, [[arXiv:1001.5023](#)].
- [247] **Fermi-LAT** Collaboration, A. A. Abdo et al., *Constraints on Cosmological Dark Matter Annihilation from the Fermi-LAT Isotropic Diffuse Gamma-Ray Measurement*, *JCAP* **1004** (2010) 014, [[arXiv:1002.4415](#)].
- [248] M. Taoso, S. Ando, G. Bertone, and S. Profumo, *Angular correlations in the cosmic gamma-ray background from dark matter annihilation around intermediate-mass black holes*, *Phys. Rev.* **D79** (2009) 043521, [[arXiv:0811.4493](#)].
- [249] J.-Q. Xia, A. Cuoco, E. Branchini, and M. Viel, *Tomography of the Fermi-lat γ -ray Diffuse Extragalactic Signal via Cross Correlations With Galaxy Catalogs*, *Astrophys. J. Suppl.* **217** (2015), no. 1 15, [[arXiv:1503.05918](#)].
- [250] J. Conrad, *Indirect Detection of WIMP Dark Matter: a compact review*, in *Interplay between Particle and Astroparticle physics London, United Kingdom, August 18-22, 2014*, 2014. [[arXiv:1411.1925](#)].
- [251] D. J. Thompson et al., *Calibration of the Energetic Gamma-Ray Experiment Telescope (EGRET) for the Compton Gamma-Ray Observatory*, *Astrophys. J. Suppl.* **86** (1993) 629–656.
- [252] **Fermi-LAT** Collaboration, W. B. Atwood et al., *The Large Area Telescope on the Fermi Gamma-ray Space Telescope Mission*, *Astrophys. J.* **697** (2009) 1071–1102, [[arXiv:0902.1089](#)].
- [253] D. Heck, G. Schatz, T. Thouw, J. Knapp, and J. N. Capdevielle, *CORSIKA: A Monte Carlo code to simulate extensive air showers*, .
- [254] **MAGIC** Collaboration, J. Aleksic et al., *Performance of the MAGIC stereo system obtained with Crab Nebula data*, *Astropart. Phys.* **35** (2012) 435–448, [[arXiv:1108.1477](#)].
- [255] J. Holder et al., *Status of the VERITAS Observatory*, *AIP Conf. Proc.* **1085** (2009) 657–660, [[arXiv:0810.0474](#)].

- [256] **HESS** Collaboration, F. Aharonian et al., *Observations of the Crab Nebula with H.E.S.S.*, *Astron. Astrophys.* **457** (2006) 899–915, [[astro-ph/0607333](#)].
- [257] **CTA Consortium** Collaboration, M. Actis et al., *Design concepts for the Cherenkov Telescope Array CTA: An advanced facility for ground-based high-energy gamma-ray astronomy*, *Exper. Astron.* **32** (2011) 193–316, [[arXiv:1008.3703](#)].
- [258] **DES, Fermi-LAT** Collaboration, A. Albert et al., *Searching for Dark Matter Annihilation in Recently Discovered Milky Way Satellites with Fermi-LAT*, *Astrophys. J.* **834** (2017), no. 2 110, [[arXiv:1611.03184](#)].
- [259] **Fermi-LAT, MAGIC** Collaboration, M. L. Ahnen et al., *Limits to dark matter annihilation cross-section from a combined analysis of MAGIC and Fermi-LAT observations of dwarf satellite galaxies*, *JCAP* **1602** (2016), no. 02 039, [[arXiv:1601.06590](#)].
- [260] **HESS** Collaboration, H. Abdallah et al., *Search for dark matter annihilations towards the inner Galactic halo from 10 years of observations with H.E.S.S.*, *Phys. Rev. Lett.* **117** (2016), no. 11 111301, [[arXiv:1607.08142](#)].
- [261] G. A. Gómez-Vargas, M. A. Sánchez-Conde, J.-H. Huh, M. Peiró, F. Prada, A. Morselli, A. Klypin, D. G. Cerdeño, Y. Mambrini, and C. Muñoz, *Constraints on WIMP annihilation for contracted dark matter in the inner Galaxy with the Fermi-LAT*, *JCAP* **1310** (2013) 029, [[arXiv:1308.3515](#)].
- [262] **Fermi-LAT** Collaboration, E. Charles et al., *Sensitivity Projections for Dark Matter Searches with the Fermi Large Area Telescope*, *Phys. Rept.* **636** (2016) 1–46, [[arXiv:1605.02016](#)].
- [263] **CTA** Collaboration, J. Carr et al., *Prospects for Indirect Dark Matter Searches with the Cherenkov Telescope Array (CTA)*, *PoS ICRC2015* (2016) 1203, [[arXiv:1508.06128](#)].
- [264] D. Hooper, C. Kelso, and F. S. Queiroz, *Stringent and Robust Constraints on the Dark Matter Annihilation Cross Section From the Region of the Galactic Center*, *Astropart. Phys.* **46** (2013) 55–70, [[arXiv:1209.3015](#)].
- [265] **Fermi-LAT** Collaboration, S. Zimmer, *Galaxy Clusters with the Fermi-LAT: Status and Implications for Cosmic Rays and Dark Matter Physics*, in *Fifth International Fermi Symposium Nagoya, Japan, October 20-24, 2014*, vol. C141020.1, 2015. [[arXiv:1502.02653](#)].
- [266] **Fermi-LAT** Collaboration, M. Ackermann et al., *Limits on Dark Matter Annihilation Signals from the Fermi LAT 4-year Measurement of the Isotropic Gamma-Ray Background*, *JCAP* **1509** (2015), no. 09 008, [[arXiv:1501.05464](#)].
- [267] M. Fornasa et al., *Angular power spectrum of the diffuse gamma-ray emission as measured by the Fermi Large Area Telescope and constraints on its dark matter interpretation*, *Phys. Rev.* **D94** (2016), no. 12 123005, [[arXiv:1608.07289](#)].
- [268] **MAGIC** Collaboration, J. Aleksic et al., *Searches for Dark Matter annihilation signatures in the Segue 1 satellite galaxy with the MAGIC-I telescope*, *JCAP* **1106** (2011) 035, [[arXiv:1103.0477](#)].
- [269] **H.E.S.S.** Collaboration, A. Abramowski et al., *Search for dark matter annihilation signatures in H.E.S.S. observations of Dwarf Spheroidal Galaxies*, *Phys. Rev.* **D90** (2014) 112012, [[arXiv:1410.2589](#)].
- [270] **VERITAS** Collaboration, B. Zitzer, *The VERITAS Dark Matter Program*, in *Fifth*

International Fermi Symposium Nagoya, Japan, October 20-24, 2014, 2015.
[arXiv:1503.00743](#).

- [271] **VERITAS** Collaboration, S. Archambault et al., *Dark Matter Constraints from a Joint Analysis of Dwarf Spheroidal Galaxy Observations with VERITAS*, *Phys. Rev.* **D95** (2017), no. 8 082001, [[arXiv:1703.04937](#)].
- [272] **Fermi-LAT** Collaboration, M. Ackermann et al., *Updated search for spectral lines from Galactic dark matter interactions with pass 8 data from the Fermi Large Area Telescope*, *Phys. Rev.* **D91** (2015), no. 12 122002, [[arXiv:1506.00013](#)].
- [273] **HESS** Collaboration, H. Abdalla et al., *H.E.S.S. Limits on Linelike Dark Matter Signatures in the 100 GeV to 2 TeV Energy Range Close to the Galactic Center*, *Phys. Rev. Lett.* **117** (2016), no. 15 151302, [[arXiv:1609.08091](#)].
- [274] D. Q. Adams, L. Bergstrom, and D. Spolyar, *Improved Constraints on Dark Matter Annihilation to a Line using Fermi-LAT observations of Galaxy Clusters*, [arXiv:1606.09642](#).
- [275] N. Padmanabhan and D. P. Finkbeiner, *Detecting dark matter annihilation with CMB polarization: Signatures and experimental prospects*, *Phys. Rev.* **D72** (2005) 023508, [[astro-ph/0503486](#)].
- [276] K. Bernlöhner, A. Barnacka, Y. Becherini, O. Blanch Bigas, E. Carmona, et al., *Monte Carlo design studies for the Cherenkov Telescope Array*, *Astropart.Phys.* **43** (2013) 171–188, [[arXiv:1210.3503](#)].
- [277] O. Adriani et al., *The CALorimetric Electron Telescope (CALET) for high-energy astroparticle physics on the International Space Station*, *EPJ Web Conf.* **95** (2015) 04056.
- [278] N. P. Topchiev et al., *GAMMA-400 gamma-ray observatory*, in *Proceedings, 34th International Cosmic Ray Conference (ICRC 2015)*, 2015. [arXiv:1507.06246](#).
- [279] X. Huang et al., *Perspective of monochromatic gamma-ray line detection with the High Energy cosmic-Radiation Detection (HERD) facility onboard China's space station*, *Astropart. Phys.* **78** (2016) 35–42, [[arXiv:1509.02672](#)].
- [280] L. Goodenough and D. Hooper, *Possible Evidence For Dark Matter Annihilation In The Inner Milky Way From The Fermi Gamma Ray Space Telescope*, [arXiv:0910.2998](#).
- [281] D. Hooper and L. Goodenough, *Dark Matter Annihilation in The Galactic Center As Seen by the Fermi Gamma Ray Space Telescope*, *Phys. Lett.* **B697** (2014) 412–428, [[arXiv:1010.2752](#)].
- [282] D. Hooper and T. Linden, *On The Origin Of The Gamma Rays From The Galactic Center*, *Phys. Rev.* **D84** (2011) 123005, [[arXiv:1110.0006](#)].
- [283] K. N. Abazajian and M. Kaplinghat, *Detection of a Gamma-Ray Source in the Galactic Center Consistent with Extended Emission from Dark Matter Annihilation and Concentrated Astrophysical Emission*, *Phys. Rev.* **D86** (2012) 083511, [[arXiv:1207.6047](#)]. [Erratum: *Phys. Rev.* D87,129902(2013)].
- [284] C. Gordon and O. Macias, *Dark Matter and Pulsar Model Constraints from Galactic Center Fermi-LAT Gamma Ray Observations*, *Phys. Rev.* **D88** (2013), no. 8 083521, [[arXiv:1306.5725](#)]. [Erratum: *Phys. Rev.* D89,no.4,049901(2014)].
- [285] K. N. Abazajian, N. Canac, S. Horiuchi, and M. Kaplinghat, *Astrophysical and Dark*

- Matter Interpretations of Extended Gamma-Ray Emission from the Galactic Center*, *Phys. Rev.* **D90** (2014), no. 2 023526, [[arXiv:1402.4090](#)].
- [286] T. Daylan, D. P. Finkbeiner, D. Hooper, T. Linden, S. K. N. Portillo, N. L. Rodd, and T. R. Slatyer, *The characterization of the gamma-ray signal from the central Milky Way: A case for annihilating dark matter*, *Phys. Dark Univ.* **12** (2016) 1–23, [[arXiv:1402.6703](#)].
- [287] F. Calore, I. Cholis, and C. Weniger, *Background model systematics for the Fermi GeV excess*, *JCAP* **1503** (2015) 038, [[arXiv:1409.0042](#)].
- [288] C. Karwin, S. Murgia, T. M. P. Tait, T. A. Porter, and P. Tanedo, *Dark Matter Interpretation of the Fermi-LAT Observation Toward the Galactic Center*, *Phys. Rev.* **D95** (2017), no. 10 103005, [[arXiv:1612.05687](#)].
- [289] **Fermi-LAT** Collaboration, M. Ajello et al., *Fermi-LAT Observations of High-Energy γ -Ray Emission Toward the Galactic Center*, *Astrophys. J.* **819** (2016), no. 1 44, [[arXiv:1511.02938](#)].
- [290] B. Zhou, Y.-F. Liang, X. Huang, X. Li, Y.-Z. Fan, L. Feng, and J. Chang, *GeV excess in the Milky Way: The role of diffuse galactic gamma-ray emission templates*, *Phys. Rev.* **D91** (2015), no. 12 123010, [[arXiv:1406.6948](#)].
- [291] X. Huang, T. Enlin, and M. Selig, *Galactic dark matter search via phenomenological astrophysics modeling*, *JCAP* **1604** (2016), no. 04 030, [[arXiv:1511.02621](#)].
- [292] R. Bartels, S. Krishnamurthy, and C. Weniger, *Strong support for the millisecond pulsar origin of the Galactic center GeV excess*, *Phys. Rev. Lett.* **116** (2016), no. 5 051102, [[arXiv:1506.05104](#)].
- [293] S. K. Lee, M. Lisanti, B. R. Safdi, T. R. Slatyer, and W. Xue, *Evidence for Unresolved γ -Ray Point Sources in the Inner Galaxy*, *Phys. Rev. Lett.* **116** (2016), no. 5 051103, [[arXiv:1506.05124](#)].
- [294] H. A. Clark, P. Scott, R. Trotta, and G. F. Lewis, *Substructure considerations rule out dark matter interpretation of Fermi Galactic Center excess*, [[arXiv:1612.01539](#)].
- [295] **Fermi-LAT** Collaboration, M. Ajello et al., *Characterizing the population of pulsars in the Galactic bulge with the Fermi Large Area Telescope*, *Submitted to: Astrophys. J.* (2017) [[arXiv:1705.00009](#)].
- [296] S. Horiuchi, M. Kaplinghat, and A. Kwa, *Investigating the Uniformity of the Excess Gamma rays towards the Galactic Center Region*, *JCAP* **1611** (2016), no. 11 053, [[arXiv:1604.01402](#)].
- [297] **Fermi-LAT** Collaboration, M. Ackermann et al., *The Fermi Galactic Center GeV Excess and Implications for Dark Matter*, *Astrophys. J.* **840** (2017), no. 1 43, [[arXiv:1704.03910](#)].
- [298] **Fermi-LAT** Collaboration, M. Ackermann et al., *Observations of M31 and M33 with the Fermi Large Area Telescope: A Galactic Center Excess in Andromeda?*, *Astrophys. J.* **836** (2017), no. 2 208, [[arXiv:1702.08602](#)].
- [299] I. Cholis, D. Hooper, and T. Linden, *A New Determination of the Spectra and Luminosity Function of Gamma-Ray Millisecond Pulsars*, [[arXiv:1407.5583](#)].
- [300] K. N. Abazajian, *The Consistency of Fermi-LAT Observations of the Galactic Center with a Millisecond Pulsar Population in the Central Stellar Cluster*, *JCAP* **1103** (2011) 010, [[arXiv:1011.4275](#)].

- [301] I. Cholis, D. Hooper, and T. Linden, *Challenges in Explaining the Galactic Center Gamma-Ray Excess with Millisecond Pulsars*, *JCAP* **1506** (2015), no. 06 043, [[arXiv:1407.5625](#)].
- [302] D. Haggard, C. Heinke, D. Hooper, and T. Linden, *Low Mass X-Ray Binaries in the Inner Galaxy: Implications for Millisecond Pulsars and the GeV Excess*, *JCAP* **1705** (2017) 056, [[arXiv:1701.02726](#)].
- [303] D. Hooper, I. Cholis, T. Linden, J. Siegal-Gaskins, and T. Slatyer, *Pulsars Cannot Account for the Inner Galaxy's GeV Excess*, *Phys. Rev.* **D88** (2013) 083009, [[arXiv:1305.0830](#)].
- [304] D. Hooper and T. Linden, *The Gamma-Ray Pulsar Population of Globular Clusters: Implications for the GeV Excess*, *JCAP* **1608** (2016), no. 08 018, [[arXiv:1606.09250](#)].
- [305] O. Macias and C. Gordon, *Contribution of cosmic rays interacting with molecular clouds to the Galactic Center gamma-ray excess*, *Phys. Rev.* **D89** (2014), no. 6 063515, [[arXiv:1312.6671](#)].
- [306] E. Carlson and S. Profumo, *Cosmic Ray Protons in the Inner Galaxy and the Galactic Center Gamma-Ray Excess*, *Phys. Rev.* **D90** (2014), no. 2 023015, [[arXiv:1405.7685](#)].
- [307] I. Cholis, C. Evoli, F. Calore, T. Linden, C. Weniger, and D. Hooper, *The Galactic Center GeV Excess from a Series of Leptonic Cosmic-Ray Outbursts*, *JCAP* **1512** (2015), no. 12 005, [[arXiv:1506.05119](#)].
- [308] O. Macias, C. Gordon, R. M. Crocker, B. Coleman, D. Paterson, S. Horiuchi, and M. Pohl, *X-Shaped Bulge Preferred Over Dark Matter for the Galactic Center Gamma-Ray Excess*, *Nature Astronomy* (2016) [[arXiv:1611.06644](#)].
- [309] **DES** Collaboration, K. Bechtol et al., *Eight New Milky Way Companions Discovered in First-Year Dark Energy Survey Data*, *Astrophys. J.* **807** (2015), no. 1 50, [[arXiv:1503.02584](#)].
- [310] A. Geringer-Sameth, M. G. Walker, S. M. Koushiappas, S. E. Koposov, V. Belokurov, G. Torrealba, and N. W. Evans, *Indication of Gamma-ray Emission from the Newly Discovered Dwarf Galaxy Reticulum II*, *Phys. Rev. Lett.* **115** (2015), no. 8 081101, [[arXiv:1503.02320](#)].
- [311] D. Hooper and T. Linden, *On The Gamma-Ray Emission From Reticulum II and Other Dwarf Galaxies*, *JCAP* **1509** (2015), no. 09 016, [[arXiv:1503.06209](#)].
- [312] S. Li, Y.-F. Liang, K.-K. Duan, Z.-Q. Shen, X. Huang, X. Li, Y.-Z. Fan, N.-H. Liao, L. Feng, and J. Chang, *Search for gamma-ray emission from eight dwarf spheroidal galaxy candidates discovered in Year Two of Dark Energy Survey with Fermi-LAT data*, *Phys. Rev.* **D93** (2016), no. 4 043518, [[arXiv:1511.09252](#)].
- [313] **DES, Fermi-LAT** Collaboration, A. Drlica-Wagner et al., *Search for Gamma-Ray Emission from DES Dwarf Spheroidal Galaxy Candidates with Fermi-LAT Data*, *Astrophys. J.* **809** (2015), no. 1 L4, [[arXiv:1503.02632](#)].
- [314] Y.-F. Liang, Z.-Q. Shen, X. Li, Y.-Z. Fan, X. Huang, S.-J. Lei, L. Feng, E.-W. Liang, and J. Chang, *Search for a gamma-ray line feature from a group of nearby galaxy clusters with Fermi LAT Pass 8 data*, *Phys. Rev.* **D93** (2016), no. 10 103525, [[arXiv:1602.06527](#)].
- [315] T. Bringmann, M. Vollmann, and C. Weniger, *Updated cosmic-ray and radio constraints on light dark matter: Implications for the GeV gamma-ray excess at the Galactic center*, *Phys. Rev.* **D90** (2014), no. 12 123001, [[arXiv:1406.6027](#)].

- [316] M. Cirelli, D. Gaggero, G. Giesen, M. Taoso, and A. Urbano, *Antiproton constraints on the GeV gamma-ray excess: a comprehensive analysis*, *JCAP* **1412** (2014), no. 12 045, [[arXiv:1407.2173](#)].
- [317] A. Cuoco, J. Heisig, M. Korsmeier, and M. Krmer, *Probing dark matter annihilation in the Galaxy with antiprotons and gamma rays*, *JCAP* **1710** (2017), no. 10 053, [[arXiv:1704.08258](#)].
- [318] A. Butter, S. Murgia, T. Plehn, and T. M. P. Tait, *Saving the MSSM from the Galactic Center Excess*, *Phys. Rev.* **D96** (2017), no. 3 035036, [[arXiv:1612.07115](#)].
- [319] P. Agrawal, B. Batell, P. J. Fox, and R. Harnik, *WIMPs at the Galactic Center*, *JCAP* **1505** (2015) 011, [[arXiv:1411.2592](#)].
- [320] C. Cheung, M. Papucci, D. Sanford, N. R. Shah, and K. M. Zurek, *NMSSM Interpretation of the Galactic Center Excess*, *Phys. Rev.* **D90** (2014), no. 7 075011, [[arXiv:1406.6372](#)].
- [321] M. Cahill-Rowley, J. Gainer, J. Hewett, and T. Rizzo, *Towards a Supersymmetric Description of the Fermi Galactic Center Excess*, *JHEP* **02** (2015) 057, [[arXiv:1409.1573](#)].
- [322] F. Calore, I. Cholis, C. McCabe, and C. Weniger, *A Tale of Tails: Dark Matter Interpretations of the Fermi GeV Excess in Light of Background Model Systematics*, *Phys. Rev.* **D91** (2015), no. 6 063003, [[arXiv:1411.4647](#)].
- [323] A. Achterberg, S. Amoroso, S. Caron, L. Hendriks, R. Ruiz de Austri, and C. Weniger, *A description of the Galactic Center excess in the Minimal Supersymmetric Standard Model*, *JCAP* **1508** (2015), no. 08 006, [[arXiv:1502.05703](#)].
- [324] T. Gherghetta, B. von Harling, A. D. Medina, M. A. Schmidt, and T. Trott, *SUSY implications from WIMP annihilation into scalars at the Galactic Center*, *Phys. Rev.* **D91** (2015) 105004, [[arXiv:1502.07173](#)].
- [325] G. Bertone, F. Calore, S. Caron, R. Ruiz, J. S. Kim, R. Trotta, and C. Weniger, *Global analysis of the pMSSM in light of the Fermi GeV excess: prospects for the LHC Run-II and astroparticle experiments*, *JCAP* **1604** (2016), no. 04 037, [[arXiv:1507.07008](#)].
- [326] M. Abdullah, A. DiFranzo, A. Rajaraman, T. M. P. Tait, P. Tanedo, and A. M. Wijangco, *Hidden on-shell mediators for the Galactic Center γ -ray excess*, *Phys. Rev.* **D90** (2014), no. 3 035004, [[arXiv:1404.6528](#)].
- [327] A. Martin, J. Shelton, and J. Unwin, *Fitting the Galactic Center Gamma-Ray Excess with Cascade Annihilations*, *Phys. Rev.* **D90** (2014), no. 10 103513, [[arXiv:1405.0272](#)].
- [328] C. Boehm, M. J. Dolan, and C. McCabe, *A weighty interpretation of the Galactic Centre excess*, *Phys. Rev.* **D90** (2014), no. 2 023531, [[arXiv:1404.4977](#)].
- [329] A. Alves, S. Profumo, F. S. Queiroz, and W. Shepherd, *Effective field theory approach to the Galactic Center gamma-ray excess*, *Phys. Rev.* **D90** (2014), no. 11 115003, [[arXiv:1403.5027](#)].
- [330] C. Balz and T. Li, *Simplified Dark Matter Models Confront the Gamma Ray Excess*, *Phys. Rev.* **D90** (2014), no. 5 055026, [[arXiv:1407.0174](#)].
- [331] S. Ipek, D. McKeen, and A. E. Nelson, *A Renormalizable Model for the Galactic Center Gamma Ray Excess from Dark Matter Annihilation*, *Phys. Rev.* **D90** (2014), no. 5 055021, [[arXiv:1404.3716](#)].

- [332] A. Cuoco, B. Eiteneuer, J. Heisig, and M. Krmer, *A global fit of the γ -ray galactic center excess within the scalar singlet Higgs portal model*, *JCAP* **1606** (2016), no. 06 050, [[arXiv:1603.08228](#)].
- [333] L. Wang and X.-F. Han, *A simplified 2HDM with a scalar dark matter and the galactic center gamma-ray excess*, *Phys. Lett.* **B739** (2014) 416–420, [[arXiv:1406.3598](#)].
- [334] B. Eiteneuer, A. Goudelis, and J. Heisig, *The inert doublet model in the light of Fermi-LAT gamma-ray data: a global fit analysis*, *Eur. Phys. J.* **C77** (2017), no. 9 624, [[arXiv:1705.01458](#)].
- [335] D. Hooper, *Z' mediated dark matter models for the Galactic Center gamma-ray excess*, *Phys. Rev.* **D91** (2015) 035025, [[arXiv:1411.4079](#)].
- [336] P. Ko, W.-I. Park, and Y. Tang, *Higgs portal vector dark matter for GeV scale γ -ray excess from galactic center*, *JCAP* **1409** (2014) 013, [[arXiv:1404.5257](#)].
- [337] T. Lacroix, C. Boehm, and J. Silk, *Fitting the Fermi-LAT GeV excess: On the importance of including the propagation of electrons from dark matter*, *Phys. Rev.* **D90** (2014), no. 4 043508, [[arXiv:1403.1987](#)].
- [338] T. Bringmann, X. Huang, A. Ibarra, S. Vogl, and C. Weniger, *Fermi LAT Search for Internal Bremsstrahlung Signatures from Dark Matter Annihilation*, *JCAP* **1207** (2012) 054, [[arXiv:1203.1312](#)].
- [339] C. Weniger, *A Tentative Gamma-Ray Line from Dark Matter Annihilation at the Fermi Large Area Telescope*, *JCAP* **1208** (2012) 007, [[arXiv:1204.2797](#)].
- [340] T. Cohen, M. Lisanti, T. R. Slatyer, and J. G. Wacker, *Illuminating the 130 GeV Gamma Line with Continuum Photons*, *JHEP* **10** (2012) 134, [[arXiv:1207.0800](#)].
- [341] W. Buchmuller and M. Garny, *Decaying vs Annihilating Dark Matter in Light of a Tentative Gamma-Ray Line*, *JCAP* **1208** (2012) 035, [[arXiv:1206.7056](#)].
- [342] D. P. Finkbeiner, *Microwave ISM emission observed by wmap*, *Astrophys. J.* **614** (2004) 186–193, [[astro-ph/0311547](#)].
- [343] G. Dobler, D. P. Finkbeiner, I. Cholis, T. R. Slatyer, and N. Weiner, *The Fermi Haze: A Gamma-Ray Counterpart to the Microwave Haze*, *Astrophys. J.* **717** (2010) 825–842, [[arXiv:0910.4583](#)].
- [344] M. Su, T. R. Slatyer, and D. P. Finkbeiner, *Giant Gamma-ray Bubbles from Fermi-LAT: AGN Activity or Bipolar Galactic Wind?*, *Astrophys. J.* **724** (2010) 1044–1082, [[arXiv:1005.5480](#)].
- [345] **Planck** Collaboration, P. A. R. Ade et al., *Planck Intermediate Results. IX. Detection of the Galactic haze with Planck*, *Astron. Astrophys.* **554** (2013) A139, [[arXiv:1208.5483](#)].
- [346] A. E. Egorov, J. M. Gaskins, E. Pierpaoli, and D. Pietrobon, *Dark matter implications of the WMAP-Planck Haze*, *JCAP* **1603** (2016), no. 03 060, [[arXiv:1509.05135](#)].
- [347] J. Knodlseder et al., *Early SPI / INTEGRAL constraints on the morphology of the 511 keV line emission in the 4th galactic quadrant*, *Astron. Astrophys.* **411** (2003) L457–L460, [[astro-ph/0309442](#)].
- [348] P. Jean et al., *Early SPI / INTEGRAL measurements of 511 keV line emission from the 4th quadrant of the Galaxy*, *Astron. Astrophys.* **407** (2003) L55, [[astro-ph/0309484](#)].

- [349] C. Boehm, D. Hooper, J. Silk, M. Casse, and J. Paul, *MeV dark matter: Has it been detected?*, *Phys. Rev. Lett.* **92** (2004) 101301, [[astro-ph/0309686](#)].
- [350] T. Siegert, R. Diehl, A. C. Vincent, F. Guglielmetti, M. G. H. Krause, and C. Boehm, *Search for 511 keV Emission in Satellite Galaxies of the Milky Way with INTEGRAL/SPI*, *Astron. Astrophys.* **595** (2016) A25, [[arXiv:1608.00393](#)].
- [351] D. J. Fixsen et al., *ARCADE 2 Measurement of the Extra-Galactic Sky Temperature at 3-90 GHz*, *Astrophys. J.* **734** (2009) 11, [[arXiv:0901.0555](#)].
- [352] M. Seiffert et al., *Interpretation of the Extragalactic Radio Background*, [[arXiv:0901.0559](#)].
- [353] N. Fornengo, R. Lineros, M. Regis, and M. Taoso, *Possibility of a Dark Matter Interpretation for the Excess in Isotropic Radio Emission Reported by ARCADE*, *Phys. Rev. Lett.* **107** (2011) 271302, [[arXiv:1108.0569](#)].
- [354] D. Hooper, A. V. Belikov, T. E. Jeltema, T. Linden, S. Profumo, and T. R. Slatyer, *The Isotropic Radio Background and Annihilating Dark Matter*, *Phys. Rev.* **D86** (2012) 103003, [[arXiv:1203.3547](#)].
- [355] M. Fairbairn and P. Grothaus, *Note on the dark matter explanation of the ARCADE excess and AMS data*, *Phys. Rev.* **D90** (2014), no. 12 127302, [[arXiv:1407.4849](#)].
- [356] J. Singal, L. Stawarz, A. Lawrence, and V. Petrosian, *Sources of the Radio Background Considered*, *Mon. Not. Roy. Astron. Soc.* **409** (2010) 1172, [[arXiv:0909.1997](#)].
- [357] K. Fang and T. Linden, *Cluster Mergers and the Origin of the ARCADE-2 Excess*, *JCAP* **1610** (2016), no. 10 004, [[arXiv:1506.05807](#)].
- [358] N. Bernal, A. Goudelis, Y. Mambrini, and C. Munoz, *Determining the WIMP mass using the complementarity between direct and indirect searches and the ILC*, *JCAP* **0901** (2009) 046, [[arXiv:0804.1976](#)].
- [359] C. Arina, G. Bertone, and H. Silverwood, *Complementarity of direct and indirect Dark Matter detection experiments*, *Phys. Rev.* **D88** (2013), no. 1 013002, [[arXiv:1304.5119](#)].
- [360] B. J. Kavanagh, M. Fornasa, and A. M. Green, *Probing WIMP particle physics and astrophysics with direct detection and neutrino telescope data*, *Phys. Rev.* **D91** (2015), no. 10 103533, [[arXiv:1410.8051](#)].
- [361] L. Roszkowski, E. M. Sessolo, S. Trojanowski, and A. J. Williams, *Reconstructing WIMP properties through an interplay of signal measurements in direct detection, Fermi-LAT, and CTA searches for dark matter*, *JCAP* **1608** (2016), no. 08 033, [[arXiv:1603.06519](#)].
- [362] L. Roszkowski, S. Trojanowski, and K. Turzynski, *Towards understanding thermal history of the Universe through direct and indirect detection of dark matter*, *JCAP* **1710** (2017), no. 10 005, [[arXiv:1703.00841](#)].
- [363] J. Silk and M. Srednicki, *Cosmic Ray anti-Protons as a Probe of a Photino Dominated Universe*, *Phys. Rev. Lett.* **53** (1984) 624.
- [364] P. Blasi, *The Origin of Galactic Cosmic Rays*, *Astron. Astrophys. Rev.* **21** (2013) 70, [[arXiv:1311.7346](#)].
- [365] N. Fornengo, L. Maccione, and A. Vittino, *Dark matter searches with cosmic antideuterons: status and perspectives*, *JCAP* **1309** (2013) 031, [[arXiv:1306.4171](#)].
- [366] E. Carlson, A. Coogan, T. Linden, S. Profumo, A. Ibarra, and S. Wild, *Antihelium from Dark Matter*, *Phys. Rev.* **D89** (2014), no. 7 076005, [[arXiv:1401.2461](#)].

- [367] M. Cirelli, N. Fornengo, M. Taoso, and A. Vittino, *Anti-helium from Dark Matter annihilations*, *JHEP* **08** (2014) 009, [[arXiv:1401.4017](#)].
- [368] A. W. Strong, I. V. Moskalenko, and V. S. Ptuskin, *Cosmic-ray propagation and interactions in the Galaxy*, *Ann. Rev. Nucl. Part. Sci.* **57** (2007) 285–327, [[astro-ph/0701517](#)].
- [369] L. J. Gleeson and W. I. Axford, *Solar Modulation of Galactic Cosmic Rays*, *Astrophys. J.* **154** (1968) 1011.
- [370] D. Maurin, F. Donato, R. Taillet, and P. Salati, *Cosmic rays below $z=30$ in a diffusion model: new constraints on propagation parameters*, *Astrophys. J.* **555** (2001) 585–596, [[astro-ph/0101231](#)].
- [371] F. Donato, D. Maurin, P. Salati, A. Barrau, G. Boudoul, and R. Taillet, *Anti-protons from spallations of cosmic rays on interstellar matter*, *Astrophys. J.* **563** (2001) 172–184, [[astro-ph/0103150](#)].
- [372] **HEAT** Collaboration, S. W. Barwick et al., *Cosmic ray positrons at high-energies: A New measurement*, *Phys. Rev. Lett.* **75** (1995) 390–393, [[astro-ph/9505141](#)].
- [373] J. Chang et al., *An excess of cosmic ray electrons at energies of 300-800 GeV*, *Nature* **456** (2008) 362–365.
- [374] **Pierre Auger** Collaboration, J. Abraham et al., *Properties and performance of the prototype instrument for the Pierre Auger Observatory*, *Nucl. Instrum. Meth.* **A523** (2004) 50–95.
- [375] **Telescope Array** Collaboration, H. Kawai et al., *Telescope array experiment*, *Nucl. Phys. Proc. Suppl.* **175-176** (2008) 221–226.
- [376] P. Picozza et al., *PAMELA: A Payload for Antimatter Matter Exploration and Light-nuclei Astrophysics*, *Astropart. Phys.* **27** (2007) 296–315, [[astro-ph/0608697](#)].
- [377] **AMS** Collaboration, M. Aguilar et al., *First Result from the Alpha Magnetic Spectrometer on the International Space Station: Precision Measurement of the Positron Fraction in Primary Cosmic Rays of 0.5350 GeV*, *Phys.Rev.Lett.* **110** (2013) 141102.
- [378] **PAMELA** Collaboration, O. Adriani et al., *An anomalous positron abundance in cosmic rays with energies 1.5-100 GeV*, *Nature* **458** (2009) 607–609, [[arXiv:0810.4995](#)].
- [379] **Fermi-LAT** Collaboration, M. Ackermann et al., *Measurement of separate cosmic-ray electron and positron spectra with the Fermi Large Area Telescope*, *Phys. Rev. Lett.* **108** (2012) 011103, [[arXiv:1109.0521](#)].
- [380] **AMS** Collaboration, L. Accardo et al., *High Statistics Measurement of the Positron Fraction in Primary Cosmic Rays of 0.5-500 GeV with the Alpha Magnetic Spectrometer on the International Space Station*, *Phys. Rev. Lett.* **113** (2014) 121101.
- [381] O. Adriani et al., *Search for Anisotropies in Cosmic-ray Positrons Detected by the PAMELA Experiment*, *Astrophys. J.* **811** (2015), no. 1 21, [[arXiv:1509.06249](#)].
- [382] M. Cirelli, M. Kadastik, M. Raidal, and A. Strumia, *Model-independent implications of the e^+ , anti-proton cosmic ray spectra on properties of Dark Matter*, *Nucl.Phys.* **B813** (2009) 1–21, [[arXiv:0809.2409](#)].
- [383] L. Bergstrom, T. Bringmann, and J. Edsjo, *New Positron Spectral Features from*

- Supersymmetric Dark Matter - a Way to Explain the PAMELA Data?*, *Phys. Rev.* **D78** (2008) 103520, [[arXiv:0808.3725](#)].
- [384] D. Hooper and K. M. Zurek, *The PAMELA and ATIC Signals From Kaluza-Klein Dark Matter*, *Phys. Rev.* **D79** (2009) 103529, [[arXiv:0902.0593](#)].
- [385] E. Nezri, M. H. G. Tytgat, and G. Vertongen, *e^+ and anti- p from inert doublet model dark matter*, *JCAP* **0904** (2009) 014, [[arXiv:0901.2556](#)].
- [386] K. M. Zurek, *Multi-Component Dark Matter*, *Phys. Rev.* **D79** (2009) 115002, [[arXiv:0811.4429](#)].
- [387] C.-R. Chen, M. M. Nojiri, F. Takahashi, and T. T. Yanagida, *Decaying Hidden Gauge Boson and the PAMELA and ATIC/PPB-BETS Anomalies*, *Prog. Theor. Phys.* **122** (2009) 553–559, [[arXiv:0811.3357](#)].
- [388] C.-R. Chen and F. Takahashi, *Cosmic rays from Leptonic Dark Matter*, *JCAP* **0902** (2009) 004, [[arXiv:0810.4110](#)].
- [389] F. Donato, D. Maurin, P. Brun, T. Delahaye, and P. Salati, *Constraints on WIMP Dark Matter from the High Energy PAMELA \bar{p}/p data*, *Phys. Rev. Lett.* **102** (2009) 071301, [[arXiv:0810.5292](#)].
- [390] O. Adriani et al., *A new measurement of the antiproton-to-proton flux ratio up to 100 GeV in the cosmic radiation*, *Phys. Rev. Lett.* **102** (2009) 051101, [[arXiv:0810.4994](#)].
- [391] S. Profumo and T. E. Jeltema, *Extragalactic Inverse Compton Light from Dark Matter Annihilation and the Pamela Positron Excess*, *JCAP* **0907** (2009) 020, [[arXiv:0906.0001](#)].
- [392] M. Cirelli, P. Panci, and P. D. Serpico, *Diffuse gamma ray constraints on annihilating or decaying Dark Matter after Fermi*, *Nucl. Phys.* **B840** (2010) 284–303, [[arXiv:0912.0663](#)].
- [393] G. Huetsi, A. Hektor, and M. Raidal, *Constraints on leptonically annihilating Dark Matter from reionization and extragalactic gamma background*, *Astron. Astrophys.* **505** (2009) 999–1005, [[arXiv:0906.4550](#)].
- [394] M. Cirelli, F. Iocco, and P. Panci, *Constraints on Dark Matter annihilations from reionization and heating of the intergalactic gas*, *JCAP* **0910** (2009) 009, [[arXiv:0907.0719](#)].
- [395] G. Bertone, M. Cirelli, A. Strumia, and M. Taoso, *Gamma-ray and radio tests of the e^+e^- excess from DM annihilations*, *JCAP* **0903** (2009) 009, [[arXiv:0811.3744](#)].
- [396] S. Profumo, *Dissecting cosmic-ray electron-positron data with Occam’s Razor: the role of known Pulsars*, *Central Eur. J. Phys.* **10** (2011) 1–31, [[arXiv:0812.4457](#)].
- [397] **AMS** Collaboration, M. Aguilar et al., *Antiproton Flux, Antiproton-to-Proton Flux Ratio, and Properties of Elementary Particle Fluxes in Primary Cosmic Rays Measured with the Alpha Magnetic Spectrometer on the International Space Station*, *Phys. Rev. Lett.* **117** (2016), no. 9 091103.
- [398] G. Giesen, M. Boudaud, Y. Gnolini, V. Poulin, M. Cirelli, P. Salati, and P. D. Serpico, *AMS-02 antiprotons, at last! Secondary astrophysical component and immediate implications for Dark Matter*, *JCAP* **1509** (2015), no. 09 023, [[arXiv:1504.04276](#)].
- [399] A. Cuoco, M. Krmer, and M. Korsmeier, *Novel Dark Matter Constraints from Antiprotons in Light of AMS-02*, *Phys. Rev. Lett.* **118** (2017), no. 19 191102, [[arXiv:1610.03071](#)].

- [400] M.-Y. Cui, Q. Yuan, Y.-L. S. Tsai, and Y.-Z. Fan, *Possible dark matter annihilation signal in the AMS-02 antiproton data*, *Phys. Rev. Lett.* **118** (2017), no. 19 191101, [[arXiv:1610.03840](#)].
- [401] **CALET** Collaboration, S. Torii, *The CALorimetric Electron Telescope (CALET): a High-Energy Astroparticle Physics Observatory on the International Space Station*, *PoS ICRC2015* (2016) 581.
- [402] **DAMPE** Collaboration, F. Gargano, *DAMPE space mission: first data*, in *25th European Cosmic Ray Symposium (ECRS 2016) Turin, Italy, September 04-09, 2016*, 2017. [[arXiv:1701.05046](#)].
- [403] H. Fuke et al., *Current status and future plans for the general antiparticle spectrometer (GAPS)*, *Adv. Space Res.* **41** (2008) 2056–2060.
- [404] **ANTARES** Collaboration, S. Adrian-Martinez et al., *Limits on Dark Matter Annihilation in the Sun using the ANTARES Neutrino Telescope*, *Phys. Lett.* **B759** (2016) 69–74, [[arXiv:1603.02228](#)].
- [405] **IceCube** Collaboration, M. G. Aartsen et al., *Search for annihilating dark matter in the Sun with 3 years of IceCube data*, *Eur. Phys. J.* **C77** (2017), no. 3 146, [[arXiv:1612.05949](#)].
- [406] **Super-Kamiokande** Collaboration, K. Choi et al., *Search for neutrinos from annihilation of captured low-mass dark matter particles in the Sun by Super-Kamiokande*, *Phys. Rev. Lett.* **114** (2015), no. 14 141301, [[arXiv:1503.04858](#)].
- [407] L. M. Krauss, M. Srednicki, and F. Wilczek, *Solar System Constraints and Signatures for Dark Matter Candidates*, *Phys. Rev.* **D33** (1986) 2079–2083.
- [408] W. H. Press and D. N. Spergel, *Capture by the sun of a galactic population of weakly interacting massive particles*, *Astrophys. J.* **296** (1985) 679–684.
- [409] A. Gould, *Resonant Enhancements in WIMP Capture by the Earth*, *Astrophys. J.* **321** (1987) 571.
- [410] G. Busoni, A. De Simone, and W.-C. Huang, *On the Minimum Dark Matter Mass Testable by Neutrinos from the Sun*, *JCAP* **1307** (2013) 010, [[arXiv:1305.1817](#)].
- [411] P. Baratella, M. Cirelli, A. Hektor, J. Pata, M. Piibeleht, and A. Strumia, *PPPC 4 DM ν : a Poor Particle Physicist Cookbook for Neutrinos from Dark Matter annihilations in the Sun*, *JCAP* **1403** (2014) 053, [[arXiv:1312.6408](#)].
- [412] M. Danninger and C. Rott, *Solar WIMPs unravelled: Experiments, astrophysical uncertainties, and interactive tools*, *Phys. Dark Univ.* **5-6** (2014) 35–44, [[arXiv:1509.08230](#)].
- [413] M. M. Boliev, S. V. Demidov, S. P. Mikheyev, and O. V. Suvorova, *Search for muon signal from dark matter annihilations in the Sun with the Baksan Underground Scintillator Telescope for 24.12 years*, *JCAP* **1309** (2013) 019, [[arXiv:1301.1138](#)].
- [414] W.-L. Guo, *Detecting electron neutrinos from solar dark matter annihilation by JUNO*, *JCAP* **1601** (2016), no. 01 039, [[arXiv:1511.04888](#)].
- [415] J. Kumar and P. Sandick, *Searching for Dark Matter Annihilation to Monoenergetic Neutrinos with Liquid Scintillation Detectors*, *JCAP* **1506** (2015), no. 06 035, [[arXiv:1502.02091](#)].

- [416] A. V. Avrorin et al., *Current status of the BAIKAL-GVD project*, *Nucl. Instrum. Meth.* **A725** (2013) 23–26.
- [417] **IceCube** Collaboration, M. G. Aartsen et al., *PINGU: A Vision for Neutrino and Particle Physics at the South Pole*, *J. Phys.* **G44** (2017), no. 5 054006, [[arXiv:1607.02671](#)].
- [418] **Hyper-Kamiokande Working Group** Collaboration, K. Abe et al., *A Long Baseline Neutrino Oscillation Experiment Using J-PARC Neutrino Beam and Hyper-Kamiokande*, 2014. [[arXiv:1412.4673](#)].
- [419] **KM3Net** Collaboration, S. Adrian-Martinez et al., *Letter of intent for KM3NeT 2.0*, *J. Phys.* **G43** (2016), no. 8 084001, [[arXiv:1601.07459](#)].
- [420] T. K. Gaisser and M. Honda, *Flux of atmospheric neutrinos*, *Ann. Rev. Nucl. Part. Sci.* **52** (2002) 153–199, [[hep-ph/0203272](#)].
- [421] G. Ingelman and M. Thunman, *High-energy neutrino production by cosmic ray interactions in the sun*, *Phys. Rev.* **D54** (1996) 4385–4392, [[hep-ph/9604288](#)].
- [422] **IceCube** Collaboration, M. G. Aartsen et al., *First observation of PeV-energy neutrinos with IceCube*, *Phys. Rev. Lett.* **111** (2013) 021103, [[arXiv:1304.5356](#)].
- [423] **IceCube** Collaboration, M. G. Aartsen et al., *Evidence for High-Energy Extraterrestrial Neutrinos at the IceCube Detector*, *Science* **342** (2013) 1242856, [[arXiv:1311.5238](#)].
- [424] **IceCube** Collaboration, M. G. Aartsen et al., *Observation of High-Energy Astrophysical Neutrinos in Three Years of IceCube Data*, *Phys. Rev. Lett.* **113** (2014) 101101, [[arXiv:1405.5303](#)].
- [425] J. Zavala, *Galactic PeV neutrinos from dark matter annihilation*, *Phys. Rev.* **D89** (2014), no. 12 123516, [[arXiv:1404.2932](#)].
- [426] B. Feldstein, A. Kusenko, S. Matsumoto, and T. T. Yanagida, *Neutrinos at IceCube from Heavy Decaying Dark Matter*, *Phys. Rev.* **D88** (2013), no. 1 015004, [[arXiv:1303.7320](#)].
- [427] E. Waxman and J. N. Bahcall, *High-energy neutrinos from astrophysical sources: An Upper bound*, *Phys. Rev.* **D59** (1999) 023002, [[hep-ph/9807282](#)].
- [428] K. Murase and E. Waxman, *Constraining High-Energy Cosmic Neutrino Sources: Implications and Prospects*, *Phys. Rev.* **D94** (2016), no. 10 103006, [[arXiv:1607.01601](#)].
- [429] E. Bulbul, M. Markevitch, A. Foster, R. K. Smith, M. Loewenstein, and S. W. Randall, *Detection of An Unidentified Emission Line in the Stacked X-ray spectrum of Galaxy Clusters*, *Astrophys. J.* **789** (2014) 13, [[arXiv:1402.2301](#)].
- [430] A. Boyarsky, O. Ruchayskiy, D. Iakubovskiy, and J. Franse, *Unidentified Line in X-Ray Spectra of the Andromeda Galaxy and Perseus Galaxy Cluster*, *Phys. Rev. Lett.* **113** (2014) 251301, [[arXiv:1402.4119](#)].
- [431] H. Ishida, K. S. Jeong, and F. Takahashi, *7 keV sterile neutrino dark matter from split flavor mechanism*, *Phys. Lett.* **B732** (2014) 196–200, [[arXiv:1402.5837](#)].
- [432] K. N. Abazajian, *Resonantly Produced 7 keV Sterile Neutrino Dark Matter Models and the Properties of Milky Way Satellites*, *Phys. Rev. Lett.* **112** (2014), no. 16 161303, [[arXiv:1403.0954](#)].
- [433] O. Urban, N. Werner, S. W. Allen, A. Simionescu, J. S. Kaastra, and L. E. Strigari, *A Suzaku Search for Dark Matter Emission Lines in the X-ray Brightest Galaxy Clusters*, *Mon. Not. Roy. Astron. Soc.* **451** (2015), no. 3 2447–2461, [[arXiv:1411.0050](#)].

- [434] A. Boyarsky, J. Franse, D. Iakubovskiy, and O. Ruchayskiy, *Checking the Dark Matter Origin of a 3.53 keV Line with the Milky Way Center*, *Phys. Rev. Lett.* **115** (2015) 161301, [[arXiv:1408.2503](#)].
- [435] A. Neronov, D. Malyshev, and D. Eckert, *Decaying dark matter search with NuSTAR deep sky observations*, *Phys. Rev.* **D94** (2016), no. 12 123504, [[arXiv:1607.07328](#)].
- [436] N. Cappelluti, E. Bulbul, A. Foster, P. Natarajan, M. C. Urry, M. W. Bautz, F. Civano, E. Miller, and R. K. Smith, *Searching for the 3.5 keV Line in the Deep Fields with Chandra: the 10 Ms observations*, *Astrophys. J.* **854** (2018), no. 2 179, [[arXiv:1701.07932](#)].
- [437] K. Abazajian, G. M. Fuller, and W. H. Tucker, *Direct detection of warm dark matter in the X-ray*, *Astrophys. J.* **562** (2001) 593–604, [[astro-ph/0106002](#)].
- [438] T. Higaki, K. S. Jeong, and F. Takahashi, *The 7 keV axion dark matter and the X-ray line signal*, *Phys. Lett.* **B733** (2014) 25–31, [[arXiv:1402.6965](#)].
- [439] J. Jaeckel, J. Redondo, and A. Ringwald, *3.55 keV hint for decaying axionlike particle dark matter*, *Phys. Rev.* **D89** (2014) 103511, [[arXiv:1402.7335](#)].
- [440] J.-C. Park, S. C. Park, and K. Kong, *X-ray line signal from 7 keV axino dark matter decay*, *Phys. Lett.* **B733** (2014) 217–220, [[arXiv:1403.1536](#)].
- [441] K.-Y. Choi and O. Seto, *X-ray line signal from decaying axino warm dark matter*, *Phys. Lett.* **B735** (2014) 92–94, [[arXiv:1403.1782](#)].
- [442] N. E. Bomark and L. Roszkowski, *3.5 keV x-ray line from decaying gravitino dark matter*, *Phys. Rev.* **D90** (2014) 011701, [[arXiv:1403.6503](#)].
- [443] T. E. Jeltema and S. Profumo, *Discovery of a 3.5 keV line in the Galactic Centre and a critical look at the origin of the line across astronomical targets*, *Mon. Not. Roy. Astron. Soc.* **450** (2015), no. 2 2143–2152, [[arXiv:1408.1699](#)].
- [444] T. E. Jeltema and S. Profumo, *Deep XMM Observations of Draco rule out at the 99% Confidence Level a Dark Matter Decay Origin for the 3.5 keV Line*, *Mon. Not. Roy. Astron. Soc.* **458** (2016) 3592, [[arXiv:1512.01239](#)].
- [445] O. Ruchayskiy, A. Boyarsky, D. Iakubovskiy, E. Bulbul, D. Eckert, J. Franse, D. Malyshev, M. Markevitch, and A. Neronov, *Searching for decaying dark matter in deep XMM-Newton observation of the Draco dwarf spheroidal*, *Mon. Not. Roy. Astron. Soc.* **460** (2016), no. 2 1390–1398, [[arXiv:1512.07217](#)].
- [446] **Hitomi** Collaboration, F. A. Aharonian et al., *Hitomi constraints on the 3.5 keV line in the Perseus galaxy cluster*, *Astrophys. J.* **837** (2017), no. 1 L15, [[arXiv:1607.07420](#)].
- [447] E. Bulbul, M. Markevitch, A. R. Foster, R. K. Smith, M. Loewenstein, and S. W. Randall, *Comment on "Dark matter searches going bananas: the contribution of Potassium (and Chlorine) to the 3.5 keV line"*, [[arXiv:1409.4143](#)].
- [448] L. Gu, J. Kaastra, A. J. J. Raassen, P. D. Mullen, R. S. Cumbee, D. Lyons, and P. C. Stancil, *A novel scenario for the possible X-ray line feature at 3.5 keV: Charge exchange with bare sulfur ions*, *Astron. Astrophys.* **584** (2015) L11, [[arXiv:1511.06557](#)].
- [449] C. Shah, S. Dobrodey, S. Bernitt, R. Steinbrgge, J. R. C. Lpez-Urrutia, L. Gu, and J. Kaastra, *Laboratory measurements compellingly support charge-exchange mechanism for the 'dark matter' ~ 3.5 keV X-ray line*, *Astrophys. J.* **833** (2016), no. 1 52, [[arXiv:1608.04751](#)].

- [450] Q.-H. Cao, C.-R. Chen, C. S. Li, and H. Zhang, *Effective Dark Matter Model: Relic density, CDMS II, Fermi LAT and LHC*, *JHEP* **08** (2011) 018, [[arXiv:0912.4511](#)].
- [451] M. Beltran, D. Hooper, E. W. Kolb, Z. A. C. Krusberg, and T. M. P. Tait, *Maverick dark matter at colliders*, *JHEP* **09** (2010) 037, [[arXiv:1002.4137](#)].
- [452] J. Goodman, M. Ibe, A. Rajaraman, W. Shepherd, T. M. P. Tait, and H.-B. Yu, *Constraints on Light Majorana dark Matter from Colliders*, *Phys. Lett.* **B695** (2011) 185–188, [[arXiv:1005.1286](#)].
- [453] Y. Bai, P. J. Fox, and R. Harnik, *The Tevatron at the Frontier of Dark Matter Direct Detection*, *JHEP* **12** (2010) 048, [[arXiv:1005.3797](#)].
- [454] J. Goodman, M. Ibe, A. Rajaraman, W. Shepherd, T. M. P. Tait, and H.-B. Yu, *Gamma Ray Line Constraints on Effective Theories of Dark Matter*, *Nucl. Phys.* **B844** (2011) 55–68, [[arXiv:1009.0008](#)].
- [455] A. Rajaraman, W. Shepherd, T. M. P. Tait, and A. M. Wijangco, *LHC Bounds on Interactions of Dark Matter*, *Phys. Rev.* **D84** (2011) 095013, [[arXiv:1108.1196](#)].
- [456] P. J. Fox, R. Harnik, J. Kopp, and Y. Tsai, *Missing Energy Signatures of Dark Matter at the LHC*, *Phys.Rev.* **D85** (2012) 056011, [[arXiv:1109.4398](#)].
- [457] K. Cheung, P.-Y. Tseng, Y.-L. S. Tsai, and T.-C. Yuan, *Global Constraints on Effective Dark Matter Interactions: Relic Density, Direct Detection, Indirect Detection, and Collider*, *JCAP* **1205** (2012) 001, [[arXiv:1201.3402](#)].
- [458] S. Matsumoto, S. Mukhopadhyay, and Y.-L. S. Tsai, *Singlet Majorana fermion dark matter: a comprehensive analysis in effective field theory*, *JHEP* **10** (2014) 155, [[arXiv:1407.1859](#)].
- [459] **ATLAS** Collaboration, G. Aad et al., *Search for dark matter in events with a hadronically decaying W or Z boson and missing transverse momentum in pp collisions at $\sqrt{s} = 8$ TeV with the ATLAS detector*, *Phys.Rev.Lett.* **112** (2014), no. 4 041802, [[arXiv:1309.4017](#)].
- [460] **ATLAS** Collaboration, G. Aad et al., *Search for dark matter in events with a Z boson and missing transverse momentum in pp collisions at $\sqrt{s}=8$ TeV with the ATLAS detector*, *Phys.Rev.* **D90** (2014) 012004, [[arXiv:1404.0051](#)].
- [461] **ATLAS** Collaboration, G. Aad et al., *Search for new phenomena in events with a photon and missing transverse momentum in pp collisions at $\sqrt{s} = 8$ TeV with the ATLAS detector*, *Phys. Rev.* **D91** (2015), no. 1 012008, [[arXiv:1411.1559](#)]. [Erratum: *Phys. Rev.D92,no.5,059903(2015)*].
- [462] **ATLAS** Collaboration, G. Aad et al., *Search for new phenomena in final states with an energetic jet and large missing transverse momentum in pp collisions at $\sqrt{s} = 8$ TeV with the ATLAS detector*, *Eur. Phys. J.* **C75** (2015), no. 7 299, [[arXiv:1502.01518](#)]. [Erratum: *Eur. Phys. J.C75,no.9,408(2015)*].
- [463] **CMS** Collaboration, V. Khachatryan et al., *Search for dark matter, extra dimensions, and unparticles in monojet events in proton-proton collisions at $\sqrt{s} = 8$ TeV*, *Eur. Phys. J.* **C75** (2015), no. 5 235, [[arXiv:1408.3583](#)].
- [464] **CMS** Collaboration, V. Khachatryan et al., *Search for new phenomena in monophoton final states in proton-proton collisions at $\sqrt{s} = 8$ TeV*, *Phys. Lett.* **B755** (2016) 102–124, [[arXiv:1410.8812](#)].
- [465] R. J. Hill and M. P. Solon, *Universal behavior in the scattering of heavy, weakly interacting dark matter on nuclear targets*, *Phys. Lett.* **B707** (2012) 539–545, [[arXiv:1111.0016](#)].

- [466] R. J. Hill and M. P. Solon, *WIMP-nucleon scattering with heavy WIMP effective theory*, *Phys. Rev. Lett.* **112** (2014) 211602, [[arXiv:1309.4092](#)].
- [467] L. Vecchi, *WIMPs and Un-Naturalness*, [arXiv:1312.5695](#).
- [468] A. Crivellin, F. D’Eramo, and M. Procura, *New Constraints on Dark Matter Effective Theories from Standard Model Loops*, *Phys. Rev. Lett.* **112** (2014) 191304, [[arXiv:1402.1173](#)].
- [469] R. J. Hill and M. P. Solon, *Standard Model anatomy of WIMP dark matter direct detection II: QCD analysis and hadronic matrix elements*, *Phys. Rev.* **D91** (2015) 043505, [[arXiv:1409.8290](#)].
- [470] F. D’Eramo and M. Procura, *Connecting Dark Matter UV Complete Models to Direct Detection Rates via Effective Field Theory*, *JHEP* **04** (2015) 054, [[arXiv:1411.3342](#)].
- [471] P. J. Fox, R. Harnik, J. Kopp, and Y. Tsai, *LEP Shines Light on Dark Matter*, *Phys. Rev.* **D84** (2011) 014028, [[arXiv:1103.0240](#)].
- [472] I. M. Shoemaker and L. Vecchi, *Unitarity and Monojet Bounds on Models for DAMA, CoGeNT, and CRESST-II*, *Phys. Rev.* **D86** (2012) 015023, [[arXiv:1112.5457](#)].
- [473] G. Busoni, A. De Simone, E. Morgante, and A. Riotto, *On the Validity of the Effective Field Theory for Dark Matter Searches at the LHC*, *Phys. Lett.* **B728** (2014) 412–421, [[arXiv:1307.2253](#)].
- [474] G. Busoni, A. De Simone, J. Gramling, E. Morgante, and A. Riotto, *On the Validity of the Effective Field Theory for Dark Matter Searches at the LHC, Part II: Complete Analysis for the s-channel*, *JCAP* **1406** (2014) 060, [[arXiv:1402.1275](#)].
- [475] G. Busoni, A. De Simone, T. Jacques, E. Morgante, and A. Riotto, *On the Validity of the Effective Field Theory for Dark Matter Searches at the LHC Part III: Analysis for the t-channel*, *JCAP* **1409** (2014) 022, [[arXiv:1405.3101](#)].
- [476] D. Racco, A. Wulzer, and F. Zwirner, *Robust collider limits on heavy-mediator Dark Matter*, *JHEP* **05** (2015) 009, [[arXiv:1502.04701](#)].
- [477] Q.-F. Xiang, X.-J. Bi, P.-F. Yin, and Z.-H. Yu, *Searches for dark matter signals in simplified models at future hadron colliders*, *Phys. Rev.* **D91** (2015) 095020, [[arXiv:1503.02931](#)].
- [478] CMS Collaboration, A. M. Sirunyan et al., *Search for dark matter produced with an energetic jet or a hadronically decaying W or Z boson at $\sqrt{s} = 13$ TeV*, *JHEP* **07** (2017) 014, [[arXiv:1703.01651](#)].
- [479] ATLAS Collaboration, M. Aaboud et al., *Search for new phenomena in final states with an energetic jet and large missing transverse momentum in pp collisions at $\sqrt{s} = 13$ TeV using the ATLAS detector*, *Phys. Rev.* **D94** (2016), no. 3 032005, [[arXiv:1604.07773](#)].
- [480] S. P. Martin, *A Supersymmetry primer*, [hep-ph/9709356](#). [Adv. Ser. Direct. High Energy Phys.18,1(1998)].
- [481] M. Drees, R. Godbole, and P. Roy, *Theory and phenomenology of sparticles: An account of four-dimensional N=1 supersymmetry in high energy physics*. Hackensack, USA: World Scientific 555 p (2004).
- [482] H. Baer and X. Tata, *Weak scale supersymmetry: From superfields to scattering events*. Cambridge University Press, 2006.

- [483] M. T. Grisaru, W. Siegel, and M. Rocek, *Improved Methods for Supergraphs*, *Nucl. Phys.* **B159** (1979) 429.
- [484] N. Seiberg, *Naturalness versus supersymmetric nonrenormalization theorems*, *Phys. Lett.* **B318** (1993) 469–475, [[hep-ph/9309335](#)].
- [485] U. Ellwanger, C. Hugonie, and A. M. Teixeira, *The Next-to-Minimal Supersymmetric Standard Model*, *Phys. Rept.* **496** (2010) 1–77, [[arXiv:0910.1785](#)].
- [486] L. Roszkowski, *Light neutralino as dark matter*, *Phys. Lett.* **B262** (1991) 59–67.
- [487] J. Hisano, S. Matsumoto, M. Nagai, O. Saito, and M. Senami, *Non-perturbative effect on thermal relic abundance of dark matter*, *Phys.Lett.* **B646** (2007) 34–38, [[hep-ph/0610249](#)].
- [488] A. Hryczuk, R. Iengo, and P. Ullio, *Relic densities including Sommerfeld enhancements in the MSSM*, *JHEP* **1103** (2011) 069, [[arXiv:1010.2172](#)].
- [489] M. Beneke, C. Hellmann, and P. Ruiz-Femenia, *Heavy neutralino relic abundance with Sommerfeld enhancements - a study of pMSSM scenarios*, *JHEP* **03** (2015) 162, [[arXiv:1411.6930](#)].
- [490] J. Bramante, N. Desai, P. Fox, A. Martin, B. Ostdiek, and T. Plehn, *Towards the Final Word on Neutralino Dark Matter*, *Phys. Rev.* **D93** (2016), no. 6 063525, [[arXiv:1510.03460](#)].
- [491] S. Mizuta and M. Yamaguchi, *Coannihilation effects and relic abundance of Higgsino dominant LSP(s)*, *Phys. Lett.* **B298** (1993) 120–126, [[hep-ph/9208251](#)].
- [492] J. R. Ellis, T. Falk, and K. A. Olive, *Neutralino - Stau coannihilation and the cosmological upper limit on the mass of the lightest supersymmetric particle*, *Phys.Lett.* **B444** (1998) 367–372, [[hep-ph/9810360](#)].
- [493] T. Nihei, L. Roszkowski, and R. Ruiz de Austri, *Exact cross-sections for the neutralino slepton coannihilation*, *JHEP* **07** (2002) 024, [[hep-ph/0206266](#)].
- [494] L. Roszkowski, R. Ruiz de Austri, and T. Nihei, *New cosmological and experimental constraints on the CMSSM*, *JHEP* **08** (2001) 024, [[hep-ph/0106334](#)].
- [495] S. Profumo and A. Provenza, *Increasing the neutralino relic abundance with slepton coannihilations: Consequences for indirect dark matter detection*, *JCAP* **0612** (2006) 019, [[hep-ph/0609290](#)].
- [496] C. Boehm, A. Djouadi, and M. Drees, *Light scalar top quarks and supersymmetric dark matter*, *Phys. Rev.* **D62** (2000) 035012, [[hep-ph/9911496](#)].
- [497] R. L. Arnowitt, B. Dutta, and Y. Santoso, *Coannihilation effects in supergravity and D-brane models*, *Nucl. Phys.* **B606** (2001) 59–83, [[hep-ph/0102181](#)].
- [498] S. Profumo and C. E. Yaguna, *Gluino coannihilations and heavy bino dark matter*, *Phys. Rev.* **D69** (2004) 115009, [[hep-ph/0402208](#)].
- [499] J. Ellis, K. A. Olive, and J. Zheng, *The Extent of the Stop Coannihilation Strip*, *Eur. Phys. J.* **C74** (2014) 2947, [[arXiv:1404.5571](#)].
- [500] J. Ellis, F. Luo, and K. A. Olive, *Gluino Coannihilation Revisited*, *JHEP* **09** (2015) 127, [[arXiv:1503.07142](#)].
- [501] G. Belanger, F. Boudjema, C. Hugonie, A. Pukhov, and A. Semenov, *Relic density of dark matter in the NMSSM*, *JCAP* **0509** (2005) 001, [[hep-ph/0505142](#)].

- [502] J. R. Ellis, L. Roszkowski, and Z. Lalak, *Higgs effects on the relic supersymmetric particle density*, *Phys.Lett.* **B245** (1990) 545–555.
- [503] M. Drees and M. M. Nojiri, *The Neutralino relic density in minimal $N = 1$ supergravity*, *Phys.Rev.* **D47** (1993) 376–408, [[hep-ph/9207234](#)].
- [504] K. L. Chan, U. Chattopadhyay, and P. Nath, *Naturalness, weak scale supersymmetry and the prospect for the observation of supersymmetry at the Tevatron and at the CERN LHC*, *Phys.Rev.* **D58** (1998) 096004, [[hep-ph/9710473](#)].
- [505] J. L. Feng, K. T. Matchev, and T. Moroi, *Focus points and naturalness in supersymmetry*, *Phys.Rev.* **D61** (2000) 075005, [[hep-ph/9909334](#)].
- [506] **Michigan Center for Theoretical Physics, U. of Michigan** Collaboration, A. Birkedal-Hansen and B. D. Nelson, *Relic neutralino densities and detection rates with nonuniversal gaugino masses*, *Phys. Rev.* **D67** (2003) 095006, [[hep-ph/0211071](#)].
- [507] H. Baer, T. Krupovnickas, A. Mustafayev, E.-K. Park, S. Profumo, and X. Tata, *Exploring the BWCA (bino-wino co-annihilation) scenario for neutralino dark matter*, *JHEP* **12** (2005) 011, [[hep-ph/0511034](#)].
- [508] N. Arkani-Hamed, A. Delgado, and G. Giudice, *The Well-tempered neutralino*, *Nucl.Phys.* **B741** (2006) 108–130, [[hep-ph/0601041](#)].
- [509] K. J. Bae, R. Dermisek, H. D. Kim, and I.-W. Kim, *Mixed bino-wino-higgsino dark matter in gauge messenger models*, *JCAP* **0708** (2007) 014, [[hep-ph/0702041](#)].
- [510] D. Feldman, Z. Liu, P. Nath, and B. D. Nelson, *Explaining PAMELA and WMAP data through Coannihilations in Extended SUGRA with Collider Implications*, *Phys. Rev.* **D80** (2009) 075001, [[arXiv:0907.5392](#)].
- [511] N. Baro, F. Boudjema, and A. Semenov, *Full one-loop corrections to the relic density in the MSSM: A Few examples*, *Phys. Lett.* **B660** (2008) 550–560, [[arXiv:0710.1821](#)].
- [512] A. Chatterjee, M. Drees, and S. Kulkarni, *Radiative Corrections to the Neutralino Dark Matter Relic Density - an Effective Coupling Approach*, *Phys. Rev.* **D86** (2012) 105025, [[arXiv:1209.2328](#)].
- [513] M. Beneke, F. Dighera, and A. Hryczuk, *Relic density computations at NLO: infrared finiteness and thermal correction*, *JHEP* **10** (2014) 45, [[arXiv:1409.3049](#)].
- [514] J. Harz, B. Herrmann, M. Klasen, and K. Kovarik, *One-loop corrections to neutralino-stop coannihilation revisited*, *Phys. Rev.* **D91** (2015), no. 3 034028, [[arXiv:1409.2898](#)].
- [515] G. L. Kane, C. F. Kolda, L. Roszkowski, and J. D. Wells, *Study of constrained minimal supersymmetry*, *Phys.Rev.* **D49** (1994) 6173–6210, [[hep-ph/9312272](#)].
- [516] D. Matalliotakis and H. P. Nilles, *Implications of nonuniversality of soft terms in supersymmetric grand unified theories*, *Nucl. Phys.* **B435** (1995) 115–128, [[hep-ph/9407251](#)].
- [517] H. E. Haber, R. Hempfling, and A. H. Hoang, *Approximating the radiatively corrected Higgs mass in the minimal supersymmetric model*, *Z. Phys.* **C75** (1997) 539–554, [[hep-ph/9609331](#)].
- [518] J. Pardo Vega and G. Villadoro, *SusyHD: Higgs mass Determination in Supersymmetry*, *JHEP* **07** (2015) 159, [[arXiv:1504.05200](#)].

- [519] K. Kowalska, L. Roszkowski, and E. M. Sessolo, *Two ultimate tests of constrained supersymmetry*, *JHEP* **1306** (2013) 078, [[arXiv:1302.5956](#)].
- [520] K. Kowalska, L. Roszkowski, E. M. Sessolo, S. Trojanowski, and A. J. Williams, *Looking for supersymmetry: 1 TeV WIMP and the power of complementarity in LHC and dark matter searches*, in *Proceedings, 50th Rencontres de Moriond, QCD and high energy interactions: La Thuile, Italy, March 21-28, 2015*, pp. 195–198, 2015. [[arXiv:1507.07446](#)].
- [521] H. Baer, V. Barger, and A. Mustafayev, *Implications of a 125 GeV Higgs scalar for LHC SUSY and neutralino dark matter searches*, *Phys. Rev.* **D85** (2012) 075010, [[arXiv:1112.3017](#)].
- [522] M. Kadastik, K. Kannike, A. Racioppi, and M. Raidal, *Implications of the 125 GeV Higgs boson for scalar dark matter and for the CMSSM phenomenology*, *JHEP* **1205** (2012) 061, [[arXiv:1112.3647](#)].
- [523] J. Cao, Z. Heng, D. Li, and J. M. Yang, *Current experimental constraints on the lightest Higgs boson mass in the constrained MSSM*, *Phys.Lett.* **B710** (2012) 665–670, [[arXiv:1112.4391](#)].
- [524] J. Ellis and K. A. Olive, *Revisiting the Higgs Mass and Dark Matter in the CMSSM*, *Eur.Phys.J.* **C72** (2012) 2005, [[arXiv:1202.3262](#)].
- [525] H. Baer, V. Barger, and A. Mustafayev, *Neutralino dark matter in mSUGRA/CMSSM with a 125 GeV light Higgs scalar*, *JHEP* **1205** (2012) 091, [[arXiv:1202.4038](#)].
- [526] P. Bechtle, T. Bringmann, K. Desch, H. Dreiner, M. Hamer, et al., *Constrained Supersymmetry after two years of LHC data: a global view with Fittino*, *JHEP* **1206** (2012) 098, [[arXiv:1204.4199](#)].
- [527] C. Balazs, A. Buckley, D. Carter, B. Farmer, and M. White, *Should we still believe in constrained supersymmetry?*, *Eur.Phys.J.* **C73** (2013) 2563, [[arXiv:1205.1568](#)].
- [528] A. Fowlie, M. Kazana, K. Kowalska, S. Munir, L. Roszkowski, et al., *The CMSSM Favoring New Territories: The Impact of New LHC Limits and a 125 GeV Higgs*, *Phys.Rev.* **D86** (2012) 075010, [[arXiv:1206.0264](#)].
- [529] S. Akula, P. Nath, and G. Peim, *Implications of the Higgs Boson Discovery for mSUGRA*, *Phys.Lett.* **B717** (2012) 188–192, [[arXiv:1207.1839](#)].
- [530] O. Buchmueller, R. Cavanaugh, M. Citron, A. De Roeck, M. Dolan, et al., *The CMSSM and NUHM1 in Light of 7 TeV LHC, B_s to $\mu+\mu-$ and XENON100 Data*, *Eur.Phys.J.* **C72** (2012) 2243, [[arXiv:1207.7315](#)].
- [531] C. Stenge, G. Bertone, F. Feroz, M. Fornasa, R. Ruiz de Austri, et al., *Global Fits of the cMSSM and NUHM including the LHC Higgs discovery and new XENON100 constraints*, *JCAP* **1304** (2013) 013, [[arXiv:1212.2636](#)].
- [532] M. E. Cabrera, J. A. Casas, and R. R. de Austri, *The health of SUSY after the Higgs discovery and the XENON100 data*, *JHEP* **1307** (2013) 182, [[arXiv:1212.4821](#)].
- [533] A. Dighe, D. Ghosh, K. M. Patel, and S. Raychaudhuri, *Testing Times for Supersymmetry: Looking Under the Lamp Post*, *Int.J.Mod.Phys.* **A28** (2013) 1350134, [[arXiv:1303.0721](#)].
- [534] T. Cohen and J. G. Wacker, *Here be Dragons: The Unexplored Continents of the CMSSM*, *JHEP* **09** (2013) 061, [[arXiv:1305.2914](#)].

- [535] O. Buchmueller et al., *The CMSSM and NUHM1 after LHC Run 1*, *Eur. Phys. J.* **C74** (2014), no. 6 2922, [[arXiv:1312.5250](#)].
- [536] P. Bechtle et al., *Killing the cMSSM softly*, *Eur. Phys. J.* **C76** (2016), no. 2 96, [[arXiv:1508.05951](#)].
- [537] C. Han, K.-i. Hikasa, L. Wu, J. M. Yang, and Y. Zhang, *Status of CMSSM in light of current LHC Run-2 and LUX data*, *Phys. Lett.* **B769** (2017) 470–476, [[arXiv:1612.02296](#)].
- [538] **ATLAS Collaboration** Collaboration, *Further searches for squarks and gluinos in final states with jets and missing transverse momentum at $\sqrt{s} = 13$ TeV with the ATLAS detector*, Tech. Rep. ATLAS-CONF-2016-078, CERN, Geneva, Aug, 2016.
- [539] K. Kowalska, *Phenomenological MSSM in light of new 13 TeV LHC data*, *Eur. Phys. J.* **C76** (2016), no. 12 684, [[arXiv:1608.02489](#)].
- [540] E. A. Bagnaschi et al., *Supersymmetric Dark Matter after LHC Run 1*, *Eur. Phys. J.* **C75** (2015) 500, [[arXiv:1508.01173](#)].
- [541] O. Buchmueller, R. Cavanaugh, M. Citron, A. De Roeck, M. Dolan, et al., *The NUHM2 after LHC Run 1*, *Eur.Phys.J.* **C74** (2014), no. 12 3212, [[arXiv:1408.4060](#)].
- [542] M. I. Gresham and K. M. Zurek, *Light Dark Matter Anomalies After LUX*, *Phys. Rev.* **D89** (2014), no. 1 016017, [[arXiv:1311.2082](#)].
- [543] O. Buchmueller, M. J. Dolan, S. A. Malik, and C. McCabe, *Characterising dark matter searches at colliders and direct detection experiments: Vector mediators*, *JHEP* **01** (2015) 037, [[arXiv:1407.8257](#)].
- [544] C. Savage, A. Scaffidi, M. White, and A. G. Williams, *LUX likelihood and limits on spin-independent and spin-dependent WIMP couplings with LUXCalc*, *Phys. Rev.* **D92** (2015), no. 10 103519, [[arXiv:1502.02667](#)].
- [545] X. Huang, Y.-L. S. Tsai, and Q. Yuan, *LikeDM: likelihood calculator of dark matter detection*, *Comput. Phys. Commun.* **213** (2017) 252–263, [[arXiv:1603.07119](#)].
- [546] H. Baer, V. Barger, and H. Serce, *SUSY under siege from direct and indirect WIMP detection experiments*, *Phys. Rev.* **D94** (2016), no. 11 115019, [[arXiv:1609.06735](#)].
- [547] S. Heinemeyer, W. Hollik, and G. Weiglein, *FeynHiggs: A Program for the calculation of the masses of the neutral CP even Higgs bosons in the MSSM*, *Comput. Phys. Commun.* **124** (2000) 76–89, [[hep-ph/9812320](#)].
- [548] T. Hahn, S. Heinemeyer, W. Hollik, H. Rzehak, and G. Weiglein, *High-Precision Predictions for the Light CP -Even Higgs Boson Mass of the Minimal Supersymmetric Standard Model*, *Phys. Rev. Lett.* **112** (2014), no. 14 141801, [[arXiv:1312.4937](#)].
- [549] **MSSM Working Group** Collaboration, A. Djouadi et al., *The Minimal supersymmetric standard model: Group summary report*, in *GDR (Groupement De Recherche) - Supersymetrie Montpellier, France, April 15-17, 1998*, 1998. [hep-ph/9901246](#).
- [550] G. F. Giudice, M. A. Luty, H. Murayama, and R. Rattazzi, *Gaugino mass without singlets*, *JHEP* **9812** (1998) 027, [[hep-ph/9810442](#)].
- [551] L. Randall and R. Sundrum, *Out of this world supersymmetry breaking*, *Nucl.Phys.* **B557** (1999) 79–118, [[hep-th/9810155](#)].
- [552] M. Cahill-Rowley, R. Cotta, A. Drlica-Wagner, S. Funk, J. Hewett, A. Ismail, T. Rizzo, and

- M. Wood, *Complementarity of dark matter searches in the phenomenological MSSM*, *Phys. Rev.* **D91** (2015), no. 5 055011, [[arXiv:1405.6716](#)].
- [553] **ATLAS** Collaboration, G. Aad et al., *Summary of the ATLAS experiment's sensitivity to supersymmetry after LHC Run 1 ? interpreted in the phenomenological MSSM*, *JHEP* **10** (2015) 134, [[arXiv:1508.06608](#)].
- [554] J. R. Ellis, A. Ferstl, and K. A. Olive, *Reevaluation of the elastic scattering of supersymmetric dark matter*, *Phys. Lett.* **B481** (2000) 304–314, [[hep-ph/0001005](#)].
- [555] H. Baer, A. Mustafayev, E.-K. Park, and X. Tata, *Target dark matter detection rates in models with a well-tempered neutralino*, *JCAP* **0701** (2007) 017, [[hep-ph/0611387](#)].
- [556] C. Cheung, L. J. Hall, D. Pinner, and J. T. Ruderman, *Prospects and Blind Spots for Neutralino Dark Matter*, *JHEP* **05** (2013) 100, [[arXiv:1211.4873](#)].
- [557] P. Huang and C. E. M. Wagner, *Blind Spots for neutralino Dark Matter in the MSSM with an intermediate m_A* , *Phys. Rev.* **D90** (2014), no. 1 015018, [[arXiv:1404.0392](#)].
- [558] T. Han, F. Kling, S. Su, and Y. Wu, *Unblinding the dark matter blind spots*, *JHEP* **02** (2017) 057, [[arXiv:1612.02387](#)].
- [559] M. Badziak, M. Olechowski, and P. Szczerbiak, *Is well-tempered neutralino in MSSM still alive after 2016 LUX results?*, *Phys. Lett.* **B770** (2017) 226–235, [[arXiv:1701.05869](#)].
- [560] **IceCube** Collaboration, R. Abbasi et al., *Multi-year search for dark matter annihilations in the Sun with the AMANDA-II and IceCube detectors*, *Phys.Rev.* **D85** (2012) 042002, [[arXiv:1112.1840](#)].
- [561] **IceCube** Collaboration, M. Aartsen et al., *Search for dark matter annihilations in the Sun with the 79-string IceCube detector*, *Phys.Rev.Lett.* **110** (2013), no. 13 131302, [[arXiv:1212.4097](#)].
- [562] **IceCube** Collaboration, M. G. Aartsen et al., *Improved limits on dark matter annihilation in the Sun with the 79-string IceCube detector and implications for supersymmetry*, *JCAP* **1604** (2016), no. 04 022, [[arXiv:1601.00653](#)].
- [563] **ANTARES** Collaboration, S. Adrian-Martinez et al., *First results on dark matter annihilation in the Sun using the ANTARES neutrino telescope*, *JCAP* **1311** (2013) 032, [[arXiv:1302.6516](#)].
- [564] M. E. Cabrera-Catalan, S. Ando, C. Weniger, and F. Zandanel, *Indirect and direct detection prospect for TeV dark matter in the nine parameter MSSM*, *Phys. Rev.* **D92** (2015), no. 3 035018, [[arXiv:1503.00599](#)].
- [565] J. Hisano, S. Matsumoto, and M. M. Nojiri, *Unitarity and higher order corrections in neutralino dark matter annihilation into two photons*, *Phys.Rev.* **D67** (2003) 075014, [[hep-ph/0212022](#)].
- [566] J. Hisano, S. Matsumoto, M. M. Nojiri, and O. Saito, *Non-perturbative effect on dark matter annihilation and gamma ray signature from galactic center*, *Phys.Rev.* **D71** (2005) 063528, [[hep-ph/0412403](#)].
- [567] **HESS** Collaboration, A. Abramowski et al., *Search for photon line-like signatures from Dark Matter annihilations with H.E.S.S.*, *Phys.Rev.Lett.* **110** (2013) 041301, [[arXiv:1301.1173](#)].

- [568] T. Cohen, M. Lisanti, A. Pierce, and T. R. Slatyer, *Wino Dark Matter Under Siege*, *JCAP* **1310** (2013) 061, [[arXiv:1307.4082](#)].
- [569] J. Fan and M. Reece, *In Wino Veritas? Indirect Searches Shed Light on Neutralino Dark Matter*, *JHEP* **1310** (2013) 124, [[arXiv:1307.4400](#)].
- [570] A. Hryczuk, I. Cholis, R. Iengo, M. Tavakoli, and P. Ullio, *Indirect Detection Analysis: Wino Dark Matter Case Study*, *JCAP* **1407** (2014) 031, [[arXiv:1401.6212](#)].
- [571] H. Baer, A. Lessa, S. Rajagopalan, and W. Sreethawong, *Mixed axion/neutralino cold dark matter in supersymmetric models*, *JCAP* **1106** (2011) 031, [[arXiv:1103.5413](#)].
- [572] H. Baer, A. Lessa, and W. Sreethawong, *Coupled Boltzmann calculation of mixed axion/neutralino cold dark matter production in the early universe*, *JCAP* **1201** (2012) 036, [[arXiv:1110.2491](#)].
- [573] K. J. Bae, H. Baer, A. Lessa, and H. Serce, *Mixed axion-wino dark matter*, *Front.in Phys.* **3** (2015) 49, [[arXiv:1502.07198](#)].
- [574] R. Allahverdi, B. Dutta, and K. Sinha, *Non-thermal Higgsino Dark Matter: Cosmological Motivations and Implications for a 125 GeV Higgs*, *Phys. Rev.* **D86** (2012) 095016, [[arXiv:1208.0115](#)].
- [575] H. Baer, *(Mainly) axion dark matter*, [arXiv:1510.07501](#). [AIP Conf. Proc.1743,050002(2016)].
- [576] G. Duda, G. Gelmini, and P. Gondolo, *Detection of a subdominant density component of cold dark matter*, *Phys. Lett.* **B529** (2002) 187–192, [[hep-ph/0102200](#)].
- [577] G. B. Gelmini and P. Gondolo, *Neutralino with the right cold dark matter abundance in (almost) any supersymmetric model*, *Phys. Rev.* **D74** (2006) 023510, [[hep-ph/0602230](#)].
- [578] G. Gelmini, P. Gondolo, A. Soldatenko, and C. E. Yaguna, *The Effect of a late decaying scalar on the neutralino relic density*, *Phys. Rev.* **D74** (2006) 083514, [[hep-ph/0605016](#)].